Non-Orthogonal Multiple Access with Imperfect Successive Interference Cancellation in Spectrum-Sharing Network under Interference Power Constraints

Prepared by

MALVERN CHAMISA – Student Number: 1909738

A dissertation submitted to the Faculty of Engineering and the Built Environment, University of Witwatersrand, Johannesburg, in fulfilment of the requirements for the degree of Master of Science in Engineering at the University of the Witwatersrand, Johannesburg

Supervisor: Prof Fambirai Takawira

Co-Supervisor: Dr Jules M Moualeu

August 2020

Declaration

I **Malvern Chamisa** declare that this dissertation is my unaided work. It is being submitted to the degree of Master of Science in Engineering to the University of the Witwatersrand, Johannesburg. It has not been submitted before for any degree or examination to any other University.

....

(Signature of Candidate)

……1st………. day of ………SEPTEMBER………… year …2020….

Abstract

In this research, a non-orthogonal multiple access (NOMA) scheme is investigated with successive interference cancellation (SIC) error in an underlay cognitive radio network. This system has an intermediate set of relays in the secondary network to improve network reliability. The research examines the outage probability of a dual-hop NOMA system with SIC error exposed to Rayleigh fading. The secondary network is allowed to access the licensed primary network frequency band if it does not exceed the maximum allowable transmit power. Concurrent transmission of the primary and secondary network will only occur if the secondary network transmissions do not exceed preset interference temperature. The inclusion of relays increases network coverage and the research analyses the effect of the number of relays in the system and makes a comparison of outage probability of the secondary network in decode and forward (DF) and amplify and forward (AF) relaying scheme. Considering interference power constraints, a relay that maximises the received signal-to-interference-and-noise ratio (SINR) is selected among the secondary set of relays. We derive analytical expressions for the asymptotic analysis of the NOMA system and then perform simulations to verify the accuracy of the model.

Dedication

I want to dedicate this work to my family; my wife and most importantly, my daughter Tinevimbo Chamisa.; for all the unwavering support and inspiration they gave to me during my studies. The battle would not have been any easy without their love and comfort.

Special dedication goes to my late father, for I believe wherever he is, this work makes him proud of his son. May his soul rest in peace.

Acknowledgements

I want to acknowledge my supervisor, Professor Fambirai Takawira, for the support and direction he gave during the research period. A very special mention goes to Doctor Jules Moualeu, for his efforts in improving the quality of the project and for always making time to assist whenever I seek help.

Many thanks also go to the Centre for Telecommunication Access Service (CeTAS) and SENTECH group for their invaluable financial contributions to my studies and upkeep. The staff in the school of Electrical and Information Engineering is also acknowledged for the very important roles they played towards the success of this research project.

Publications

- Malvern Chamisa, Fambirai Takawira and Jules Moualeu, "*Non-Orthogonal Multiple Access in Spectrum-Sharing Network under Interference Power Constraints*", in Proc. IEEE AFRICON, Accra, Ghana, 25-27 Sep 2019, pp. 1-6...

- Malvern Chamisa, Fambirai Takawira and Jules Moualeu, "*Underlay Spectrum-Sharing Non-Orthogonal Multiple Access Network with Imperfect SIC*", Submitted to IET Communications, 13 Feb 2020, pp. 1-9…

Table of Contents

Declaration i

Abstract ii

Dedication iii

Acknowledgements iv

Publications v

Table of Contents vi

List of Figures x

Glossary of Terms and Abbreviations xiii

Glossary of Nomenclature xv

Chapter 1 Introduction 1

1.1 Non-Orthogonal Multiple Access 2

1.2 NOMA Principle 2

1.3 Problem Statement and Motivation 3

1.4 Research Question 6

1.4.1 Research Sub-questions 6

1.4.2 Main Contributions 6

1.5 The organisation of the Dissertation 7

Chapter 2 Literature Review 8

2.1 Introduction 8

2.2 Cooperative Communication and Relay Selection 8

2.2.1 Fixed Amplify and Forward Scenario 10

2.2.2 Fixed Decode and Forward Scenario 10

2.2.3 Adaptive Relaying Scenario 10

2.3 Background on Relay Selection 11

2.3.1 Opportunistic Relay Selection Strategy 11

2.3.2 Proactive Relay Selection 12

2.3.3 Reactive Relay Selection 12

2.3.4 Max-min Relay Selection 12

2.3.5 Max-max Relay Selection 13

2.4 Non-Orthogonal Multiple Access (NOMA) 15

2.4.1 NOMA in Uplink Transmission Scenario 15

2.4.2 NOMA in Downlink Transmission Scenario 15

2.5 NOMA and Relay Selection 16

2.5.1 NOMA schemes in partial relay selection 17

2.5.2 Joint user and relay selection for cooperative NOMA networks 18

2.5.3 Underlay cognitive networks with cooperative NOMA 19

2.6 NOMA and Successive Interference Cancellation 21

2.6.1 NOMA with imperfect SIC Implementation 22

2.6.2 Exploiting NOMA in cooperative relay sharing 22

2.6.3 Cooperative NOMA systems with imperfect SIC in cognitive Radio Networks 24

2.7 Spectrum Sharing in Cognitive Radio Networks 24

2.8 Cognitive Radio Network with Relay Selection 26

2.8.1 Cognitive Coded Cooperation in Underlay Spectrum sharing network 26

2.8.2 Underlay Cognitive Multiple relay Networks 27

2.9 Conclusion 28

Chapter 3 NOMA in Spectrum-Sharing Network under Interference Power Constraints 30

3.1 Introduction 30

3.2 System Model 30

3.3 Outage Performance Analysis 34

3.3.1 Outage Probability at D_1 35

3.3.2 Outage Probability at D_2 38

3.4 Numerical Results 44

3.5 Conclusion 48

Chapter 4 Underlay Spectrum Sharing NOMA network with Imperfect SIC 49

4.1 Introduction 49

4.2 System Model 50

4.3 Outage Probability Analysis 54

4.3.1 Outage Probability at U_1 54

4.3.2 Outage Probability at U_2 58

4.4 Asymptotic Performance Analysis 60

4.4.1 Asymptotic Analysis for the scenario with $\gamma_I \rightarrow \infty$ 61

4.4.2 Asymptotic Analysis with $\gamma_o \rightarrow \infty$ 63

4.5 Numerical Results and Discussions 65

4.6 Conclusions 71

Chapter 5 NOMA in Spectrum Sharing with Amplify and Forward Relaying 72

5.1 Introduction 72

5.2 System Model 72

5.2.1 Phase 1 73

5.2.2 Phase 2 74

5.3 Numerical Results 76

5.4 Conclusion 81

Chapter 6 Conclusion 83

6.1 Summary 83

6.2 Contributions 85

6.3 Future Works 86

References 88

Appendix A 97

A.1 Derivation of SINR in first phase 97

A.2 Derivation of SINR in second phase 98

Appendix B 100

B.1 Derivation of CDF $F_{\gamma_{SD_1}}(\gamma_{th})$ 100

Appendix C 103

C.1 Derivation of SINR at U_1 to detect v_1 ($\gamma_{R_jU_1}^{v_1}$ 103

List of Figures

Figure 1.1 A smart city representation in the fifth generation and beyond 1

Figure 1.2 Basic 2 user NOMA downlink scenario 3

Figure 2.1 Common cooperative communication network model 9

Figure 2.2 A model for max-max relay selection scheme with the source – relay link transmission in the 1st time slot and relay – destination transmission in the 2nd time slot. 13

Figure 2.3 System model for NOMA model will PRS 17

Figure 2.4 Two-slot AF cooperative NOMA system model. 19

Figure 2.5 Cognitive radio network with cooperative NOMA 21

Figure 2.6 System model for NOMA-RS. 23

Figure 2.7 System model of an underlay cognitive NOMA network where, $h_{i,j}$ $(i \neq j, i \in \{p, s, r\}, j \in \{p, r, d_1, d_2\})$ is the channel coefficient. 24

Figure 2.8 System model of coded cooperation with relay selection in an underlay spectrum sharing environment. 27

Figure 2.9 Model of an underlay cognitive radio network with multiple relays 28

Figure 3.1 Illustration of a cooperative underlay CR-NOMA wireless system with DF partial relay selection. 31

Figure 3.2 Outage probability of $D_1$and D_2versus γ_P for $\gamma_I = 15, 25$ and 35 dB. 45

Figure 3.3 Outage probability of $D_1$and D_2 versus γ_I for $\gamma_P = 15, 25$ and 35 dB 45

Figure 3.4 Outage probability of $D_1$and D_2 versus γ_P (SNR) with different number of DF relays (K=1, 2 and 3) when $\gamma_I = 25$ dB. 46

Figure 3.5 Outage probability of D_2 versus γ_P (SNR) with and without $R_k \rightarrow D_2$ link, when $\gamma_I = 25$ dB. 47

Figure 3.6 Outage probability of D_1 versus γ_P (after SIC assuming D_2 is a cooperative NOMA user and when D_2 signal is treated as interference) with $\gamma_I = 25$ dB. 48

Figure 4.1 Illustration of an underlay spectrum-sharing network with downlink cooperative NOMA. 50

Figure 4.2 Outage probability versus interference power constraint with, $\xi = 0.01$ and $\frac{I_p}{N_o} = \{15, 25, 35\}$ dB. 66

Figure 4.3 Outage probability versus maximum available transmit power with $\xi = 0.01$ and $\frac{I_p}{N_o} = \{15, 25, 35\}$ dB. 67

Figure 4.4 Outage probability of U_2 versus $\frac{P}{\mathcal{N}_0}$ with different number of relays, J = {1, 2, 3} when $\gamma_I = 25$ dB and $\xi = \{0, 0.05\}$. 68

Figure 4.5 Outage probability of U_2 versus maximum allowable transmit power (SNR) in cases where the h_{U_2} link is includes and excludes, with $\gamma_I = 25$ dB. 69

Figure 4.6 Outage probability versus interference power constraint with, $\xi = 0.05$, and $\frac{P}{\mathcal{N}_0} = 25$ dB. 70

Figure 4.7 Outage probability versus maximum allowable transmit power with, $\xi = 0.05$ and $\gamma_I = 25$ dB. 71

Figure 5.1 System model of a downlink cooperative NOMA system in an underlay cognitive radio network with AF relaying. 73

Figure 5.2 Outage probability against $\frac{P}{\mathcal{N}_0}$ for different interference power values, $\frac{I_p}{N_o} = \{15, 25, 35\}$ dB. 77

Figure 5.3 Outage probability against $\frac{I_p}{N_o}$ with the maximum allowable transmit power taking values, $\{15, 25, 35\}$ dB. 78

Figure 5.4 Outage probability against $\frac{P}{\mathcal{N}_0}$(dB) with different number of relays, $J = \{1, 2, 3\}$ when $\frac{I_p}{N_o} = 25$ dB. 79

Figure 5.5 A comparison of the outage probability against $\frac{P}{\mathcal{N}_0}$ for different interference power values, $\frac{I_p}{N_o} = \{15, 25, 35\}$ dB, using AF relaying vs DF relaying for U_1. 80

Figure 5.6 A comparison of the outage probability against $\frac{P}{\mathcal{N}_0}$ for different interference power values, $\frac{I_p}{N_o} = \{15, 25, 35\}$ dB, using AF relaying vs DF relaying for U_2. 81

Glossary of Terms and Abbreviations

Abbreviation/Term	Description
5G	Fifth Generation
ASI	Activity Side Information
AWGN	Additive White Gaussian Noise
AF	Amplify and Forward
ARQ	Automatic Repeat reQuest
BS	Base Station
BER	Bit Error Rate
CSI	Channel State Information
CCI	Co-Channel Interference
CSI	Codebook Side Information
CR	Cognitive Radio
CRN	Cognitive Radio Network
DF	Decode and Forward
IDF	Incremental Decode and Forward
LTE	Long Term Evolution
MAP	Maximum a Posteriori
ML	Maximum-Likelihood
MRC	Maximum Ratio Combining
MGF	Moment Generating Function
NOMA	Non-Orthogonal Multiple Access
ORS	Opportunistic Relay Selection
OMA	Orthogonal Multiple Access
OTN	Opportunistic Two-Way Relaying Network
OFDMA	Orthogonal Frequency Division Multiple Access
PRS	Partial Relay Selection
PUs	Primary Users
RS	Relay Selection
SUs	Secondary Users

SC	Selection Combining
SINR	Signal to Interference and Noise Ratio
SNR	Signal to Noise Ratio
SIC	Successive Interference Cancellation
TWR	Two-Way Relaying
QoS	Quality of Service

Glossary of Nomenclature

Symbol	Description
$\lvert a_1\rvert,\ \lvert a_2\rvert$	Power allocation ratios
$\lvert d_1\rvert,\ \lvert d_2\rvert$	Power allocation ratios
$\lvert \delta_1\rvert,\ \lvert \delta_2\rvert$	Power allocation ratios
D_1	NOMA user 1
D_2	NOMA user 2
P_S	Source transmit power
P_{R_k} , P_{R_j}	k^{th} and j^{th} relay transmit power
R_k	The k^{th} relay
R_j	The j^{th} relay
U_1	NOMA user 1
U_2	NOMA user 2
$\lvert h_1\rvert^2$	Source to user 1 channel gain
$\lvert h_2\rvert^2$	Source to user 2 channel gain
$\lvert h_{SV}\rvert^2$	Secondary source to primary receiver channel gain
$\lvert h_{R_kV}\rvert^2$	k^{th} relay to primary receiver channel gain
$k*$	Selected relay in a set of 1 to K relays
$\gamma_{SR\,k}$	Instantaneous SNR between the source and the k^{th} relay
γ_{R_kD}	Instantaneous SNR between the kth relay and the destination
γ_{U_1}	Instantaneous SINR received at user 1
γ_{U_2}	Instantaneous SINR received at user 2
$h_{SR\,1}$	Fading amplitude between source and 1^{st} relay
$t_{R\,j}$	Fading amplitude between source and j^{th} relay
$h_{SR\,k}$	Fading amplitude between source and k^{th} relay
h_{R_1D}	Fading amplitude between 1^{st} relay and destination
$h_{UR\,k}$	Fading amplitude between primary source and k^{th} relay
$h_{UD\,1}$	Fading amplitude between primary source and destination 1

h_{UD_2}	Fading amplitude between primary source and destination 2
h_{SD_1}	Fading amplitude between secondary source and destination 1
t_{U_1}	Fading amplitude between secondary source and user 1
h_{SD_2}	Fading amplitude between secondary source and destination 2
t_{U_2}	Fading amplitude between secondary source and user 2
t_{s_p}	Fading amplitude between secondary source and primary receiver
P_P	Transmit power of the primary transmitter
$\mathcal{N}_0$	Power spectral density of the AWGN
P_t	Maximum allowable transmit power
I_p	Interference temperature limit
h_{R_kD}	Fading amplitude between k^{th} relay and destination
h_{SR}	Fading amplitude between source and relay
h_{SD}	Fading amplitude between source and destination
h_{RD}	Fading amplitude between relay and destination
η_{SD}	Additive white Gaussian noise
η_{SR} , η_{RD}	Additive white Gaussian noise
n_{R_j} , n_{R_k}	Additive white Gaussian noise
n_{U_1} , n_{U_2}	Additive white Gaussian noise
y_{SR}	Received signal at the relay from the source
y_{D_1}	Received signal at the destination 1 from the source
y_{D_2}	Received signal at the destination 2 from the source
y_{SD}	Received signal at the destination from the source
y_{RD}	Received signal at the destination from the relay
x'	Signal transmitted from the primary transmitter
x_{R_k}	Transmitted signal from the selected relay node
x''	Transmitted signal from the primary transmitter in the second phase
x_S	Transmitted signal from secondary source
σ^2	Variance
U_i	Refers to the i^{th} NOMA user

U_N	Refers to the Nth NOMA user
y_i	Received signal at U_i
PU-Tx (U)	Primary transmitter
PU-Rx (V)	Primary receiver
g_{U_1}	Fading amplitude between primary source and user1
g_{U_2}	Fading amplitude between primary source and user 2
g_{R_j}	Fading amplitude between primary source and jth relay
v	Transmitted information symbol from secondary source
v'	Signal transmitted from the primary transmitter
v_{R_j}	Transmitted signal from the selected relay node
v''	Transmitted signal from the primary transmitter in the second phase
ζ_{2_1}	Residual interference from imperfect SIC

Chapter 1 Introduction

There has been a general increase in the demand for high-speed internet connectivity with the advancement of technology. Human interaction with devices has been on the rise, and the future is shifting to a smart world [1] as shown in Figure 1.1 adopted from [2], in which intelligent devices do most of the day to day work. It is clear that to have confidence in these devices there is a need for a trusted connection and most of the gadgets will require high data volumes. Traffic demand will increase for both uplink and downlink.

Figure 1.1 A smart city representation in the fifth generation and beyond [2]

The high demand in bandwidth, in turn, results in the need for high spectrum utilization which at present is a challenge to the telecommunications industry. The wireless spectrum is strained and existing wireless solutions are not able to meet the demands of the increase in the traffic using existing resources [3]. It is expected that the fifth-generation (5G) mobile networks will have a latency as low as 1 ms and throughput as high as 10 Gbps which is more than 100x the LTE capabilities

[4]. There is a need to research and develop new technologies to optimize spectrum usage, the channel capacity performance and power usage of the system.

1.1 Non-Orthogonal Multiple Access

Recently a lot of research has been conducted on the possibility of using Non-orthogonal Multiple Access (NOMA) to improve spectral efficiency and throughput [5]. NOMA has been proposed as a multiple access scheme that will play a great part in the future of radio access [6-9]. The rate of conducted research has significantly increased because of the rapid growth in wireless communication systems putting pressure on the dem n and for high-speed connectivity.

Wireless multiple access systems can be categorized in two ways, the orthogonal multiple access such as (OMA) [10] and non-orthogonal multiple access (NOMA) [11]. In Orthogonal Frequency Division Multiple Access (OFDMA) wireless systems, throughput is optimized by utilization of diversity gain [12] based on the received channel state information (CSI) of all sub-channels. The user with the best channel conditions gets priority on spectrum allocation. OFDMA wireless systems have drawbacks in very high data-rate communications because they do not allow frequency reuse within one cell [11]. A spectrum in OFDMA is dedicated to one user and this limits the overall cell throughput. NOMA, on the contrary, can allocate the same spectrum to multiple users at the same instance within one cell. This results in higher throughput due to spectrum reuse within a cell. NOMA can yield a significant spectral efficiency gain by scheduling multiple users over the same spectrum resources but at different power levels. NOMA has been proposed as a promising technique in future wireless communication systems because it brings a balance between user fairness and system throughput.

1.2 NOMA Principle

NOMA is receiving great attention from the wireless community because it can transmit to multiplexed users using the same spectrum resources but varying power allocation ratios. These spectrum resources range from time, space, frequency and code. Based on each users' channel quality, NOMA superposes the message signals of many users in the power domain at the source (transmitter). Each will perform successive interference cancellation by first decoding the information of the user with stronger interference and subtracting them allowing it to decode its intended information last. [13].

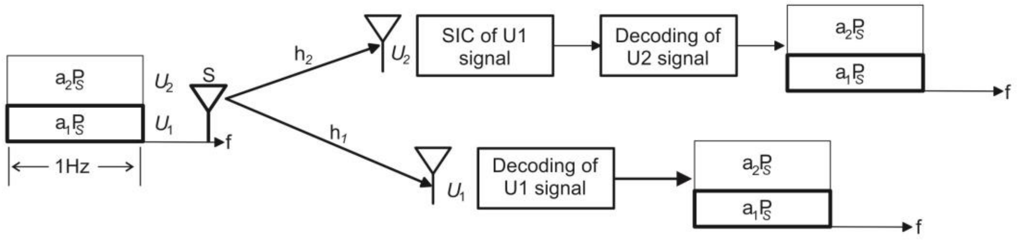

Figure 1.2 Basic 2 user NOMA downlink scenario [13]

In a basic downlink NOMA scenario as shown in Figure 1.2 above the scheme considers a single antenna base station (s) with 2 NOMA users, U_1 and U_2 sharing the same bandwidth (f) of 1 Hz. It is assumed that all links exhibit Rayleigh block fading and additive white Gaussian noise. Complex channel coefficients for $\boldsymbol{U_1}$ and $\boldsymbol{U_2}$ are denoted by h_1 and h_2 respectively such that $0 < h_1 \leq h_2$, which shows that U_2 has at least greater or equal channel gain to U_1. In this scenario multiplexing is performed in the power domain and based on NOMA we assume a power allocation ratio in which $|a_1| > |a_2|$ given $|a_1| + |a_2| = 1$, with $a_1P_S + a_2P_S = P_S$ where a_1 and a_2 are the power allocation coefficients for $\boldsymbol{U_1}$ and $\boldsymbol{U_2}$ respectively and P_S is the source transit power. U_2, will start by decoding the signal meant for U_1 and then subtract it from the received signal to decode its signal. U_1, will decode its signal taking the signal meant for U_2 as interference.

1.3 Problem Statement and Motivation

The concept of NOMA has been researched in various wireless systems. A NOMA design for uplink transmission in which several users could share the same sub-carrier without increasing redundancy was investigated in [14], incorporating cognitive radio (CR) network. CR network comes in as an efficient way to resolve the radio spectrum scarcity. It allows the unlicensed users to utilize the licensed user's spectrum provided the quality of service (QoS) of the licensed users is not affected. A NOMA system performance analysis in CR with randomly deployed users was done in [14] considering different power constraints on the primary transmitter. [14], derived closed-form expressions for outage probability using stochastic geometry. A CR NOMA setup in which a primary user and secondary users could be served simultaneously by a base station such that the primary user is allocated with high power than secondary users to guarantee the high priority of its message was proposed in [15]. To evaluate the performance of the proposed scheme, [16] derived the outage probability and system throughput for the primary and secondary network in closed-form for Nakagami-*m* fading.

Moreover, the performance of NOMA in relay networks has been analysed, since relays have been addressed as a promising solution to improve reliability and extend radio coverage in communication systems. This solution has been applied in cognitive radio networks with relay selection, also a relay system employing NOMA scheme has been studied in [17], through analysis of achievable rate in a Rayleigh fading channel. In addition, [18] provide the asymptotic expressions and used a sub-optimal power allocation scheme at the source. In [19-20], NOMA with partial relay selection was examined, in which the outage probability and the corresponding asymptotic behaviour were analysed. NOMA was applied to a cooperative scenario, where a user with stronger channel gain was used to relay for another user experiencing poorer channel gain.

It is key to note that the performance of NOMA schemes in the context of CR networks remains to be better explored in the technical literature which is the main motivation of my research.

- Literature has not covered a model where NOMA is implemented in CR with a set of AF relays. The closest contribution in literature is [21], where the authors considered a cooperative NOMA system where the users which are closer to the secondary base station would be used to relay data to a single far user. This, in essence, is a Decode and Forward (DF) scenario and this also motivates our work to consider straight NOMA with two users and a set of relays that forward without performing any successive interference cancellation (SIC).

- Another gap exists in the literature in that work that incorporates SIC error in the derivation and analysis of outage probability expressions for a CR NOMA scenario is still open to be explored. In [22] the authors investigated SIC error in which two sources transmit to two corresponding destinations over the same frequency via a single DF relay. Also [23] studied a cooperative NOMA system with imperfect SIC in an underlay CR network with a single DF relay.
- Another gap exists in the literature in that there is a need to also derive asymptotic outage performance for the model that incorporates SIC error in a CR NOMA system with RS.

The thesis focuses on the integration of NOMA in a CR network with a set of relays to maximise spectral efficiency and ensuring minimal outage probability under maximum interference power constraints. The research is mainly guided by the following areas:

- A NOMA system in a CR network setup with an intermediate multiple AF and DF relay system. In this setup, the secondary network transmits in an underlay spectrum sharing mode. The transmit power of the secondary source and the selected relay are constrained by the maximum allowable transmit power without causing interference, determined by the primary receiver.
- The effects of co-channel interferences (CCI) [24] from the simultaneous primary transmission on the secondary network in terms of outage probability is analysed. The exact expressions of the outage probability are derived for the secondary network to establish the relay with the best channel strength and subsequently select the respective relay for transmission.
- In the process of determining the SNR of the received signal, we consider SIC error for the stronger user and investigate the impact this has on the outage performance.

- An analysis of the asymptotic outage performance of a NOMA system in underlay spectrum sharing is analysed as well. Expressions of the asymptotic outage probability are derived and analysed for the secondary network which is in a NOMA setup.

1.4 Research Question

To what extent does the incorporation of Non-Orthogonal Multiple Access in an underlay spectrum-sharing network affect system performance in terms of outage probability considering SIC error?

1.4.1 Research Sub-questions

i. How does an interference power constraint setup in an underlay NOMA cognitive radio network affect the best relay selection in a set of relays?

ii. How does SIC error affect the outage probability of the NOMA underlay cognitive radio system?

iii. What is the impact of asymptotic outage performance in a NOMA underlay cognitive radio network?

1.4.2 Main Contributions

i. We propose a cooperative underlay CR-NOMA wireless system with partial relay selection (AF and DF). We derive outage expressions and the relayed signal is transmitted to the destination

ii. We provide insights on the impact of the number of relays available in the network and the interfering signals from the primary transmissions on the underlying performance metric

iii. The impact of considering SIC error on the outage performance of the stronger NOMA user in an underlay cognitive radio system.

iv. An analytical approach to derive the asymptotic outage performance in a NOMA underlay cognitive radio network.

1.5 The organisation of the Dissertation

In this section we provide the various chapters that make up the remainder of the dissertation:

Chapter 2: This chapter provides a survey of the works that have been carried out to date. It looks at the different concepts that have been investigated in the literature that are used as building blocks of this dissertation. We carry out an exhaustive interference investigation of NOMA systems, cognitive radio networks, relay selection and successive cancellation.

Chapter 3: The chapter proposes NOMA in spectrum sharing network under interference power constraints. A model is developed and we derive closed-form expressions for outage probability assuming perfect SIC and DF relaying scheme. The chapter incorporates simulation results which are used to verify the analytical mathematical formulations for outage performance.

Chapter 4: In this chapter we analyse the model in chapter 3 assuming perfect SIC but implemented with AF relaying.

Chapter 5: We remodel chapter 3 taking into account the impact of SIC error on the outage performance of the system. Moreover, we also derive the asymptotic outage performance of the users. Simulation results are obtained to validate the mathematical analysis proposed.

Chapter 6: This chapter gives a summary of the main work covered in the thesis and a conclusion to the dissertation. We also give recommendations and prospective works that could still be investigated in the future.

Chapter 2 Literature Review

2.1 Introduction

The purpose of this chapter is to provide an extensive survey that helps to understand the significant accomplishments that have been done in the area of NOMA. Several concepts have been integrated with NOMA in a bid to optimize spectral efficiency and also to achieve high throughput.

The rest of the chapter comprises Section 2.2, which gives a review of relay selection and cooperative communication. Section 2.3 highlights some research studies related to NOMA, while Section 2.4 discusses the current research work covering successive interference cancellation error. Section 2.5 elaborates on spectrum sharing in cognitive radio networks, and Section 2.6 reviews some work on NOMA integrated with relay selection.

2.2 Cooperative Communication and Relay Selection

The basic principle of cooperative communication refers to the use of other communication devices to relay transmission. The source will send information to the relay in the first time slot and the destination as well if a direct link exists. The relay will then forward the transmission to the destination in the second time slot. The main advantage of cooperative communication is that it increases capacity performance. If the channel between the source and destination experiences high channel fading, the link will have poor performance, and if a relaying link exists, this will increase the reliability of the system. If the relay used for transmission is closer to the source, then that implies that the source will save power for transmission. The system will need to use lower resource through the selection of the appropriate relay for transmission.

Recent works on wireless communication systems have revealed that incorporating a relaying network in a cognitive radio network (CRN) improves transmission reliability, robustness to channel impairments and system throughput without increasing the transmit power. Research in [25-26] has shown that there are two main relaying protocols, decode and forward (DF) and amplify and forward (AF). In DF, the relay decodes and does re-encoding of the received transmission at the relay while AF multiplies the signal with an amplification factor then forwards to the intended destination. The amplification factor in AF is dependent on the relative strengths of the source-to-relay and relay-to-destination links.

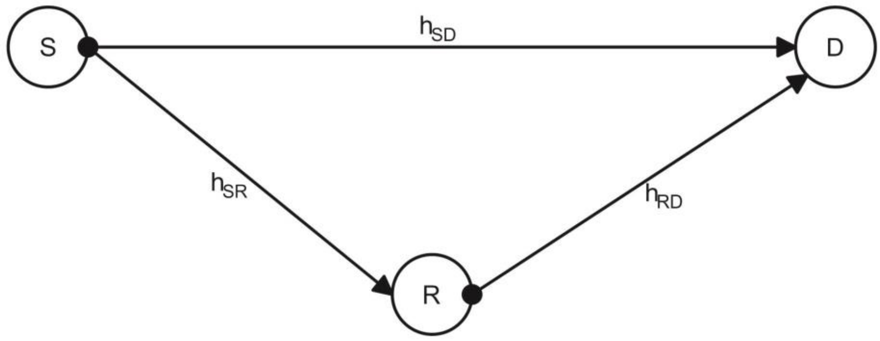

Figure 2.1 Common cooperative communication network model [27].

In Figure 2.1, the source node (S) transmits a message to both the relay node (R) and the destination node (D), [27]. The signals received at the destination node and the relay node denoted by y_{SD} and y_{SR} respectively can be expressed as

$$y_{SD} = \sqrt{P_s} h_{SD} x + \eta_{SD} \tag{2.1}$$

$$y_{SR} = \sqrt{P_s} h_{SR} x + \eta_{SR} \tag{2.2}$$

where P_S, is the transmit power at the source, h_{SD}, h_{RD} and h_{SR} are channel coefficients between the source and destination node and source and relay node, respectively, x is the transmitted information symbol and η_{SD} and η_{SR} are the additive white Gaussian noise (AWGN) at the relay and destination, respectively, modeled with mean zero and variance σ^2. The received signal is forwarded to the destination, and the destination will decode the messages received from the direct link and the relaying link based on the processing method applied.

2.2.1 Fixed Amplify and Forward Scenario

Research done in [28-29] elaborates on a cooperative communication network with AF. The relay nodes forward the received signal from the source multiplied by an amplification factor. Relating to the setup in figure 2.1, a message is sent from the source to the relay and the destination simultaneously. The received signal at the destination and relay can be expressed as equation (2.1) and (2.2), respectively. In the AF case, the signal received at the destination from the relay is given by

$$y_{RD} = \sqrt{P_R} h_{RD} \left(\sqrt{P_s} h_{SR} x + \eta_{SR} \right) + \eta_{RD} \tag{2.3}$$

where P_R is the relay transmit power, η_{RD} is the AWGN also modelled as complex Gaussian random variables with zero mean and variance σ^2. In [30-31], the authors studied the impact of the AF model in a multi-relay setup and derived the outage probability performance of the system.

2.2.2 Fixed Decode and Forward Scenario

The authors in, [32-33] evaluated the DF setup, the relay starts by decoding the signal received from the source, re-encodes the information before forwarding to the intended destination. The received signal at the destination from the relay is given by

$$y_{RD} = \sqrt{P_R} h_{RD} \hat{x} + \eta_{RD} \tag{2.4}$$

where $\hat{x}$ is the information re-encoded by the relay. The main challenge with this scenario is that the relay may decode incorrectly; thus the relay will end up forwarding an error to the destination node leading to error propagation which can be detrimental to the system performance. Most studies assume perfect decoding to avoid error propagation.

2.2.3 Adaptive Relaying Scenario

Fixed relay is a simplified approach to implementation of a cooperative communication network because the relay always forwards the information to the destination in a deterministic manner. The major challenge with this method is the fact that it has low efficiency, since the received signals at the relay may not be good enough to be forwarded to the destination, which is often due to adverse channel conditions and high noise levels. Adaptive relaying [34-36] plays the role of mitigating the drawbacks of fixed relaying by employing different scenarios in forwarding information.

Selective relaying [37] is a common form of adaptive relaying. Selective relaying takes advantage of the SNR information on the relay to decide whether to transmit to the destination or not to transmit in that particular time slot. If the SNR of the received signal at the relay is lower than a set threshold, the probability of accurately decoding at the relay will be very low such that it will be better not to forward the transmission due to high chances of causing errors in the destination.

The second form of adaptive relaying is the incremental relaying [38-40]. This acts like the automatic repeat re-quest (ARQ) protocol to stop the relay from transmitting an erroneous signal. This setup allows a source to broadcast message to the destination and relay, and the destination then checks the received signal. If the signal fulfils the required SNR for the receiver, then the destination sends an acknowledgement to the source. Now if the SNR fails to meet the receiver requirement, then the destination can request the relay to forward the information and then combine the transmission from the relay and the source.

2.3 Background on Relay Selection

The studies in [41-42] have shown that incorporating a relay node in wireless transmissions increases both the capacity and the system diversity. It is important to note that there are three common relay selection strategies implemented in cooperative communications. In what follows, we focus on these strategies to understand the impact they have on the system performance.

2.3.1 Opportunistic Relay Selection Strategy

Based on [43], the selection scheme depends mainly on the best end-to-end link between the source and the destination. The channels from source to relay and relay to destination vary with time and directly impact system performance. These channels are considered to follow a Doppler shift inversely proportional to channel coherence [44]. The choosing of the most appropriate relay before the channel condition changes defines opportunistic relay selection (ORS).

In this scheme, the relays should always be aware of the instantaneous channel conditions towards the destination from the source to decide the most reliable channel for transmission before channel conditions change. There are, however, two common types of ORS: the proactive relay selection and reactive relay selection [45-47].

2.3.2 Proactive Relay Selection

Proactive relay selection can be referred to as opportunistic relay selection that is performed before source transmission. It offers energy efficiency [48] since only the selected relay is activated for receiving when the source transmits. It also reduces the probability of channel access data packet collisions. However, based on [49], the best relay should be chosen at each instant of transmission. The drawback of proactive relay selection is that the relay is selected based on channel conditions before transmission.

2.3.3 Reactive Relay Selection

Reactive relay selection is also referred to as partial relaying, and it is opportunistic relaying performed after the first hop transmission. In reactive mode [50], only relays with average received SNR higher than the threshold will form the relaying set. The relay with the maximum SNR received at the destination node chosen from the relaying set is then selected for forwarding the signal to the destination.

2.3.4 Max-min Relay Selection

In this scheme, performance is optimised by maximizing the end-to-end SNR through minimizing error rate and maximizing transmission rate, [51]. The choice of selection criteria for relaying depends on the system QoS requirements. Generally, this selection criterion maximizes the minimum end-to-end SNR.

Considering a dual-hop relaying scheme with source-relay and relay-destination hops, then the selection is based on the scheme below

$$k^* = \arg\max \min_{k \in \{1 \ldots\ldots K\}} (\gamma_{SR_k}, \gamma_{R_k D}), \tag{2.5}$$

where k^* denotes the selected relay, k is an element of a set of 1 to K relays and γ_{SR_k} is the SNR for the source-relay link while $\gamma_{R_k D}$, denotes the SNR for relay-destination link.

2.3.5 Max-max Relay Selection

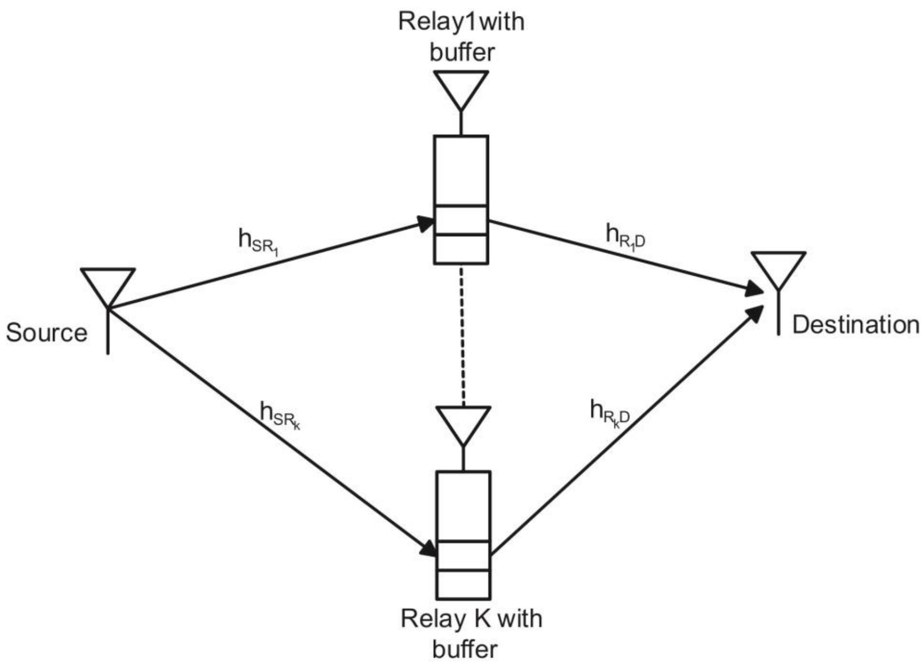

Figure 2.2 A model for max-max relay selection scheme with the source – relay link transmission in the 1st time slot and relay – destination transmission in the 2nd time slot.

In this type of selection, relays should have buffers as in figure 2.2, such that the relay with the best source-relay channel conditions is used for receiving [52]. The best relay-destination channel can also be selected for transmission to the destination while the relay with the best source-to-relay channels is used to receive packets from the source. It is practical only when the relay selected for source-relay reception can store the received packet in its buffer and retransmit in the second time slot. Based on the same concept the relay selected for relay-destination transmission can transmit the packet from the first time slot in the buffer queue, which is the source-relay received packet.

2.3.6 BER-based Relay Selection

In a BER-based relay selection strategy, the relay that can minimize the BER at the destination is selected for transmission. Based on [53] this is determined by first deriving the BER expression of the system, then the approximate BER expression based on the relation between the SNR of relay-to-destination link and the error propagation.

Considering a dual-hop relaying scheme with source-relay, relay-destination hops and also a direct source-destination link, then the selection is based on the scheme below

$$k^* = \arg\min_k \left\{ P_e(\varepsilon_{d(k)}) \right\} \approx \arg\min_k \min \left\{ (\gamma_{SR_{(k)}}, \gamma_{R_{(k)}D} + \ln(1 + \gamma_{SD}) \right\} \tag{2.6}$$

Where k^* denotes the selected relay, $P_e(\varepsilon_{d(k)})$ is the BER at the destination when the kth relay is selected as the best relay to forward the received signals from the source. $\min\left\{ (\gamma_{SR_{(k)}}, \gamma_{R_{(k)}D} + \ln(1 + \gamma_{SD}) \right\}$ is an effective method for measuring the BER at the destination proposed in this paper. γ_{SR_k} is the SNR for the source-relay link while γ_{R_kD}, denotes the SNR for relay-destination link and γ_{SD}, is the SNR of the source-destination link.

2.4 Non-Orthogonal Multiple Access (NOMA)

NOMA is a communication principle which ensures spectrum resource sharing/reuse at different power ratios. The spectrum resources shared are mainly time, space, frequency and code, [54-56]. NOMA allows the simultaneous serving of multiple users by using the entire system bandwidth to transmit data with the help of superposition coding at the base station and successive interference cancellation (SIC) decoding techniques at the users; this is in contrast with the traditional orthogonal multiple access in which spectrum resources are exclusively allocated per user.[57]

2.4.1 NOMA in Uplink Transmission Scenario

In the uplink NOMA [58-59], we have multiple antennas of different user equipment non –orthogonally transmitting to a single receiver antenna at the base station using the same spectrum resources. The transmission is non-orthogonal; each user transmits its signal at a power dependent on its channel gain. Superposed message signals received at the receiver (BS) cause interference to each other. There is a need to distinguish the different received messages when considering SIC accurately.

Based on NOMA the received signal from the highest channel gain user will be the strongest at the BS receiver and will be decoded first but will also experience interference from the other NOMA users while the lowest channel gain user experiences zero interference from other users.

2.4.2 NOMA in Downlink Transmission Scenario

According to [58] and [60], the power domain NOMA system can serve multiple users in the same time slot. The multiple access trait is achieved by allocating different power levels to different users. The base station transmits a linear superposition of N users' data by allocating a fraction α_i of the total power to each such that the power allocated to the i^{th} user U_i is $P_i = \alpha_i$P, where P is the total transmit power.

On the receiving end, each user decodes the signal of the stronger user i.e. U_i can decode the messages for each strong user and perform SIC with $N < i$. Signals from stronger users are then subtracted from the received signal to decode the actual signal of the user U_i itself treating the signals of the weaker user U_N with $N > i$, as interference termed intra-cell or intra-cluster interference.

The received signal at the user U_i can be represented as

$$y_i = h_i x + n_i \tag{2.7}$$

where $x = \sum_{i=1}^{N} \sqrt{\alpha_i \mathrm{P}} s_i$, refers to the superposed signal transmitted by the base station with s_i being the signal for U_i and n_i is the additive white Gaussian noise of the user U_i with zero mean and variance σ_i^2.

Considering a NOMA downlink scenario with a single antenna base station and N single antenna users with distinct channel gains. The base station non-orthogonally transmits N different signals by superposing them on the same spectrum resources, but all N user equipment receivers will get their desired signals along with interference caused by the messages of other users.

2.5 NOMA and Relay Selection

Among the many promising wireless communication techniques, relay-based networks have emerged as a critical concept, primarily when employed with NOMA, [61-62]. The key idea is that the mobile users relay signals to each other to emulate an antenna array. Since the deployment of multiple relays offers even more significant performance improvements in dual-hop cooperative networks, special attention has been given to the analysis of relay selection techniques mainly the opportunistic relay selection and the partial relay selection.

Due to the benefits of relay selection and NOMA as separate concepts. It is essential to develop NOMA systems under relay selection jointly. A cooperative NOMA system with simultaneous wireless information and power transfer which was studied in [63], where NOMA users located near the source act as energy harvesting relays to help far NOMA users. Different from cooperative NOMA [64], a cooperative relay system employing the NOMA scheme was proposed in [65-67] to improve spectral efficiency. The design of NOMA with one relay was also studied in [68]. Recently, [69] studied the implementation of NOMA in a multi-relay network system investigating a scheme assuming joint NOMA and PRS. The researches on NOMA and relay selection are broad some of the more recent works in literature are as explained in the section that follows.

2.5.1 NOMA schemes in partial relay selection

In this scheme the authors consider joint NOMA and PRS using an AF relay network. Based on this model, the authors in [19] investigated the outage performance and the sum rate of the NOMA scheme in AF relay system.

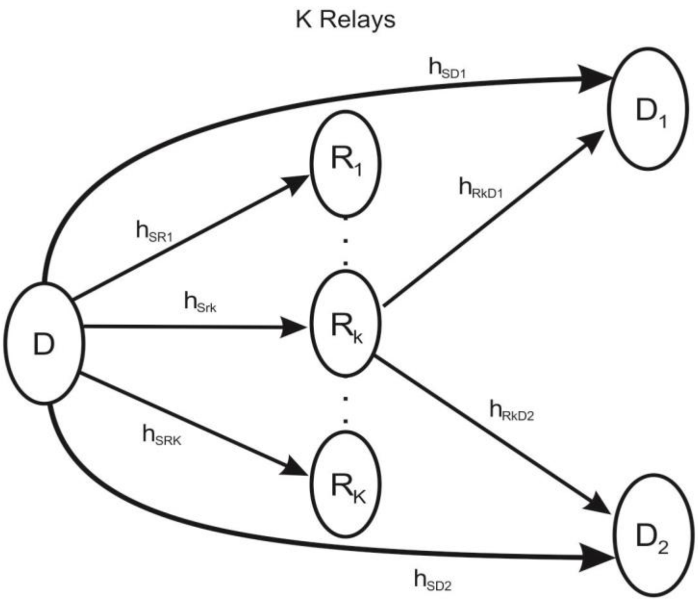

Figure 2.3 System model for NOMA model will PRS [19]

The system model of this scheme is shown in Figure 2.3 where the authors consider a downlink cooperative dual-hop relay system with a base station (BS) intending to transmit the signal to two users (i.e., D_1 and D_2) with the help of one out of K AF relays (i.e., $\{R_1, \ldots.., R_k\}$. The selected relay is determined using PRS criteria. The system is considered to exhibit frequency non-selective Rayleigh block fading and additive white Gaussian noise (AWGN).

The authors showed using numerical results that the ergodic capacity at the weak user relies on the power allocation ratio in the high SNR region. It was also demonstrated that NOMA with PRS improves performance gain as the number of relays increases and this only significant for a maximum of 2 relays, outage performance is almost constant for more than two relays.

2.5.2 Joint user and relay selection for cooperative NOMA networks

The work done in [70] considered AF cooperative NOMA to derive approximate and asymptotic expressions on average sum rate with relay selection. Inspired by this work, authors [69] focused on investigating a joint user and relay selection for AF cooperative NOMA network. Based on a candidate subset, they proposed an optimal selection criterion to improve the outage performance of the system and derive the exact expressions on the outage probability. They also noted the effects of several physical parameters, including transmission power, the number of relays and target data rate on outage probability were revealed. The authors' results showed that when the target data rate is low enough, the diversity order of the outage probability equals to the number of relays, whereas when the target data rate tends to infinity, the outage probability occurs one.

The research considered two-slot AF cooperative NOMA networks, as shown in Figure 2.4, in which multiple users transmit messages to two destinations with the help of multiple AF relays. In this system, they had M users, N relays and two destinations. The destinations share channel resource simultaneously through NOMA, and they are categorized by their quality of service (QoS) requirements. Hence D_1 required a low data rate with short packet size for urgent scenarios, while D_2 is served opportunistically for a long time. All nodes were assumed to be equipped with single antennas and operate in the half-duplex time-division mode. Due to severe fading, there were no direct links between the user and the destination, and all links were assumed to be quasi-static Rayleigh block fading and independent

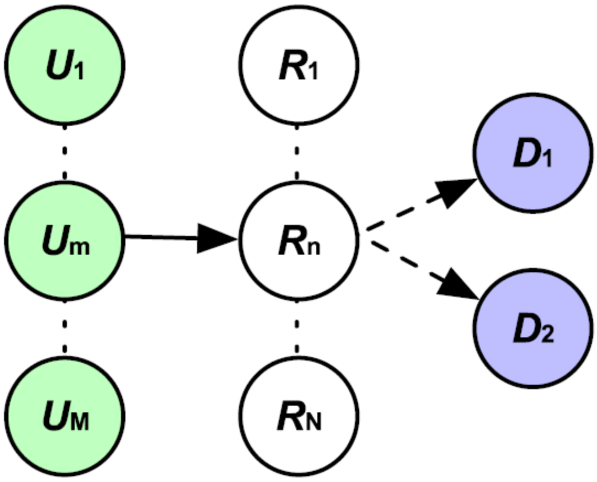

Figure 2.4 Two-slot AF cooperative NOMA system model [69].

In this model, a system analysis was done by deriving closed-form analytical expressions and asymptotic results. The asymptotic outage performance revealed that the number of relays and target data rate affect diversity order. The number of users has no positive impact on the diversity order of outage performance but help in improving transmission quality.

The authors in [71] also considered a dual-hop AF NOMA model but subjected to Nakagami-m fading. In this model, they evaluated the impact of the number of relays, the Nakagami-m fading severity parameter and NOMA power allocation on the outage performance of the system. In [72], a NOMA-based transmission between two sources and two users through a set of full-duplex/half-duplex relays. In this model, they also consider channel variance to be exponentially dependent on the transmitted power of the relay.

2.5.3 Underlay cognitive networks with cooperative NOMA

In another research that focused on NOMA and relay selection, the author [21] focused on an underlay cognitive radio network with cooperative NOMA. In this research, they focused on developing a cooperative NOMA scheme for a CR [73] network subject to an underlay approach. In their work, a cooperative scheme is used to enhance the outage performance at a cell edge user for user fairness, and NOMA aims to improve its decreased spectral efficiency, with this in mind they proposed this system to enhance both spectral efficiency and user fairness. In the analysis, a number of secondary users employed cooperative NOMA, in which a user with strong channel gains is selected (to act as a relay) by a multi-antenna BS to assist another user with weak channel gains in the presence of a primary network.

Closed-form expressions for the outage probabilities were derived, and some useful insights into the behaviour of outage performances in different cases were given. These results showed that the outage at both users decreases significantly by increasing the number of antennas at the BS. Also, an outage floor which relies on the maximum tolerable interference was observed in the outage probability. Furthermore, the impact of multiple antennas on the outage floor was discussed, and the impact of the number of multiple cooperative secondary users in multi-user scenarios.

In their model, they considered a cooperative NOMA scheme for an underlay CR network in which a secondary BS intends to transmit to two groups of secondary users in the presence of one primary transmitter and one primary receiver as shown in Figure 2.5. Assuming that the BS is equipped with M antennas and adopts a transmit beamforming technique, while all other nodes are equipped with a single antenna. They considered that user U_1 is located far away from the BS while the user U_{2k} is near to the BS. The preliminary analysis was performed considering only two secondary users U_1 and U_2, and afterwards, it was generalised for the multi-user case.

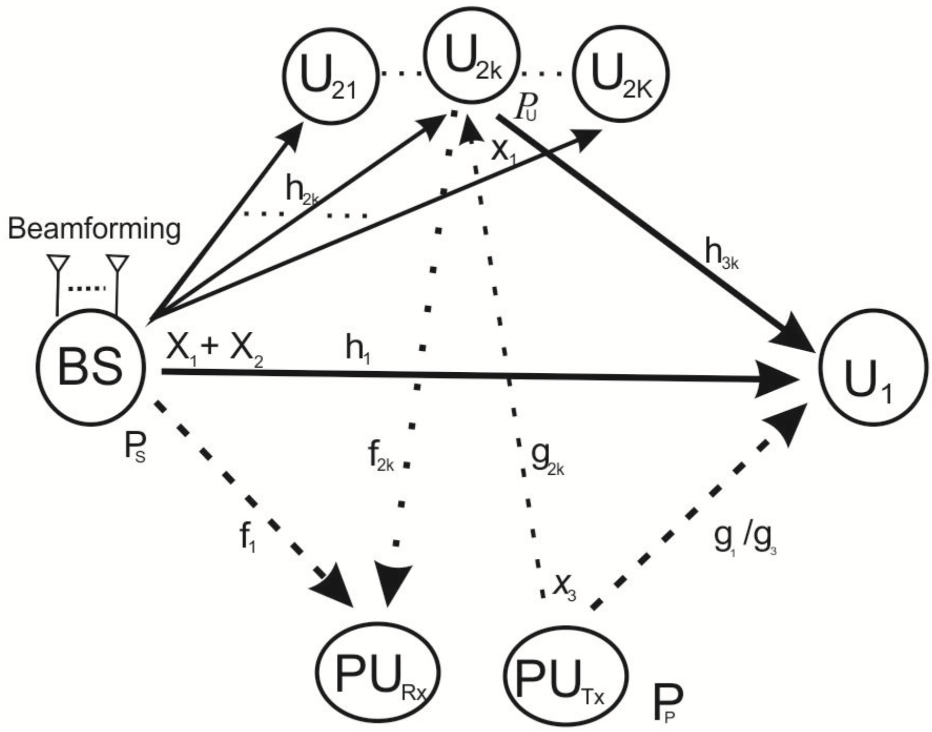

Figure 2.5 Cognitive radio network with cooperative NOMA [73].

The other derived closed-form expressions for the outage performance of a single cooperative NOMA user. They also showed that the outage performance at both users increased significantly as the number of antennas at the secondary BS increased. An outage floor existed which was dependent on the maximum tolerable interference power, and this outage floor reduced as the number of antennas increased. They concluded using these results that for an underlay cognitive cooperative NOMA system, selecting the optimal number of antennas and maximum tolerable interference power results in an improved outage performance of the system.

2.6 NOMA and Successive Interference Cancellation

Based on the downlink NOMA concept, all individual user information signals are superimposed into a single waveform at the BS. SIC distinguishes all multiplexed users that are using the same spectrum resources (time, code, frequency, space, etc.) through successive subtraction of the decoded signal from the overall received signal. According to [74], the decoding time increases as the number of users increases and also the power allocation gets complicated when trying to distinguish the users. The receiver needs to determine the phase and amplitude of each user accurately, according to [75]. This is crucial as it helps in the subtraction of other messages through SIC.

2.6.1 NOMA with imperfect SIC Implementation

The work of [76], focused on a NOMA network with SIC for the downlink channel and the associated security issues. NOMA signals for all users are superimposed and encoded then transmitted from the source, at the destination each user uses SIC for the decoding process. A user performs SIC by subtracting unwanted signals for the other NOMA users in a well-defined sequence until it decodes its intended signal. The sequence at each user should tally with the user index in SIC, however, in the event of a cancellation mismatch the user will not get its intended signal and will re-request the source which will increase processing time. The increase in processing times poses security threats to transmitted messages [77-78]. The authors present an analysis of the impact on the performance of having perfect SIC and ling decoding times associated with imperfect SIC.

It is revealed that the time for decoding varies according to the order of user connected to the network. The order/sequence depends on the distance of the user from the base station; this distance is also used to determine the power allocation coefficients. Time to decode signal for the first user gradually increases as the number of NOMA users increases. The authors simulated a scenario where the user mistakenly decodes the message of the neighbouring user with an error index of two users. A way to prevent interception and optimize security is through the addition of layers from complex algorithms and intelligent transmission.

2.6.2 Exploiting NOMA in cooperative relay sharing

The work of [22], was motivated by the need for strategies that can increase capacity gains and provide connectivity to more users in cooperative relaying schemes (CRS) [79] using NOMA systems. The authors carried out investigations in the impact of relay schemes (RS) on the performance of cooperative NOMA.

They proposed and analyzed a dual-hop CRS using NOMA where two sources are allowed to transmit in parallel, and the decoded signals at the relay are re-encoded and forwarded in parallel again to the destination NOMA users as illustrated in Figure 2.6

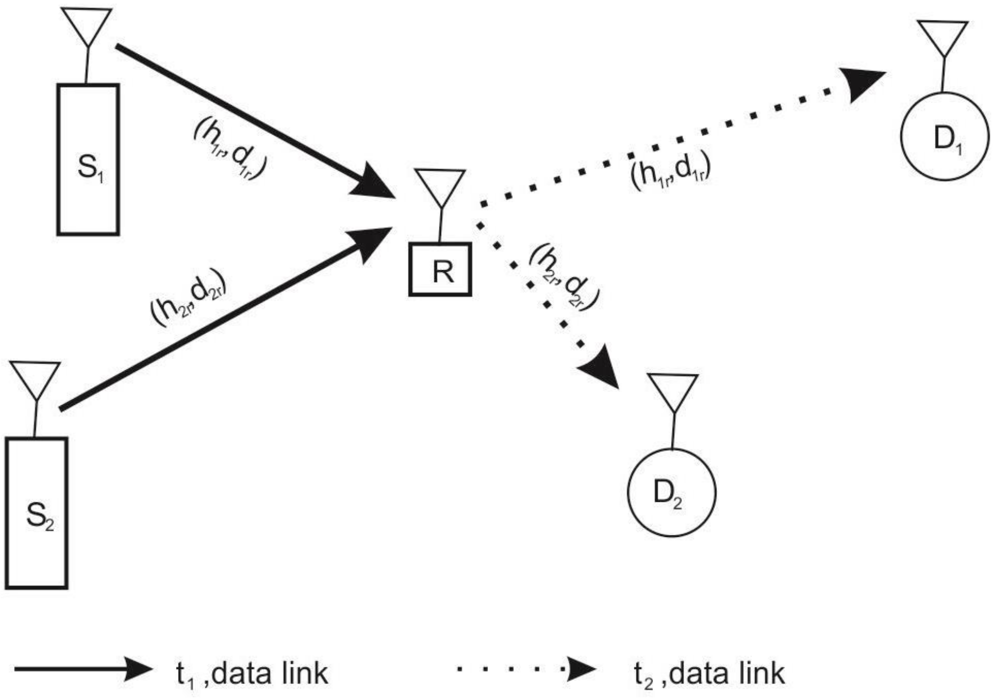

Figure 2.6 System model for NOMA-RS [22].

They derived the ergodic sum capacity of NOMA-RS under both perfect and imperfect SIC scenarios, and simulation results validated these results. The authors also used a cooperative network using orthogonal multiple access as a benchmark. Results showed that NOMA-RS outperformed OMA under perfect SIC, whereas performance gains under imperfect SIC were significantly dependent on the level of the residual interference. The results showed that power allocation coefficients have a substantial impact on ergodic sum capacity of NOMA-RS and also the fact that more users can be served at the same instance.

2.6.3 Cooperative NOMA systems with imperfect SIC in cognitive Radio Networks

The work done in [23], a NOMA system with imperfect SIC in an underlay cognitive radio network. The model in Figure 2.7 assumes that all channel coefficients follow Rayleigh distribution. They derive an exact closed-form of the outage probability for each secondary destination.

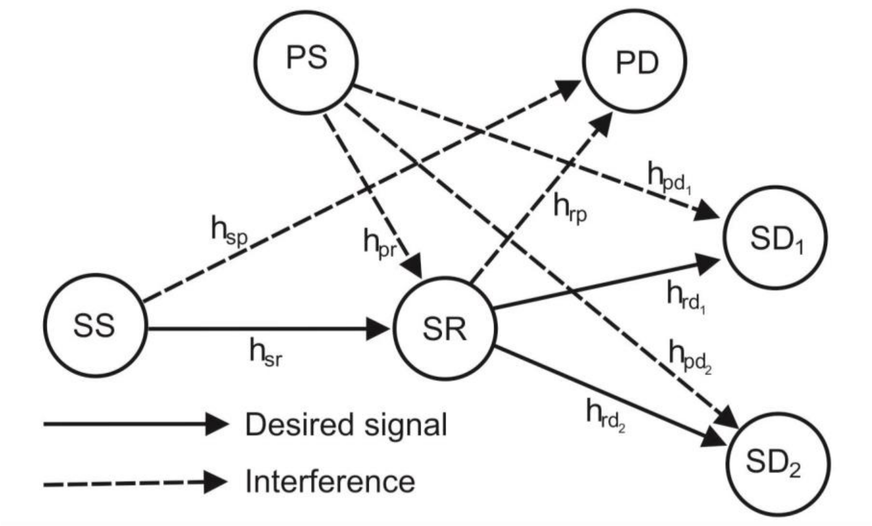

Figure 2.7 System model of an underlay cognitive NOMA network where, $h_{i,j}$ $(i \neq j, i \in \{p, s, r\}, j \in \{p, r, d_1, d_2\})$ is the channel coefficient [23].

Imperfect SIC scenario, as defined in [23], is investigated in an underlay cognitive radio network. Derivations for the asymptotic outage probability are analyzed, and it is noted that the diversity order of zero is achieved, which results in error floor ah high transmit power regions. Simulations results are used to validate the mathematical derivations.

2.7 Spectrum Sharing in Cognitive Radio Networks

Cognitive radio refers to an intelligent wireless device that exploits the existing wireless spectrum opportunistically to improve spectrum utilization. The main issue addressed by cognitive radios is spectrum usage, which allows for spectrum sharing. According to [80-81], there are three main categories for spectrum sharing in CRs; overlay, underlay or interweave.

- Underlay: Code Side Information- this is when a secondary transmitter knows the channel strengths to the non-cognitive (primary) receiver. The secondary user can transmit simultaneously with the primary user as long as interference caused is below a set threshold. The secondary user's power is limited by the interference constraint (set threshold). The interference caused by the secondary user can be estimated via reciprocity if the secondary transmitter can overhear a transmission from the secondary receiver's location. The secondary transmitter can also be very conservative in its transmit power to ensure that its signal stays below the predefined interference threshold. Since the interference constraints in underlay are restrictive, secondary users in this paradigm are limited to short range communication.
- Overlay: Codebook Side Information (CSI)-[82] cognitive nodes know channel gains, codebooks and the messages of the non-cognitive users. Codebook information can be obtained if the primary user follow a uniform standard for communication based on a publicised codebook or through broadcasting of the codebook periodically. In the overlay paradigm it is assumed that the primary message is known at the secondary transmitter when the primary user starts transmission (more practical in a case of retransmission where the secondary user manages to decode the signal while the primary receiver fails due to fading.Cognitive users can transmit simultaneously with the non-cognitive user; the interference to a non-cognitive user can be offset by using part of the cognitive user's power to relay the non-cognitive user's message. The cognitive user can transmit at any power; the interference to the non-cognitive user can be offset by relaying the non-cognitive user's message.
- Interweave: Activity Side Information (ASI) - [83-84] Cognitive user knows the spectral holes in space, time or frequency when the non-cognitive user is not using these holes. The cognitive user transmits simultaneously with a non-cognitive user only in the event of a false

spectral hole-detection. The cognitive user's transmit power is limited by the range of its spectral hole-sensing. The utilization of spectrum is improved by opportunistic frequency reuse over the spectrum holes. The interweave technique requires knowledge of the activity information of the primary users in the spectrum. The interweave paradigm allows a secondary user to periodically monitor the radio spectrum, intelligently detect occupancy in the different parts of the spectrum holes with minimal interference to the active primary users.

2.8 Cognitive Radio Network with Relay Selection

CRs, according to [83], exploits side information about its environment to improve spectral utilization. This side information can be activity channels, codebooks and messages of the nodes. CRs utilizes advanced radio and signal processing technology along with novel spectrum-allocation policies to support new wireless users operating in the existing crowded spectrum without degrading the performance of the entrenched users.

2.8.1 Cognitive Coded Cooperation in Underlay Spectrum sharing network

Due to the high demand for a means to deal with the strain on the radio spectrum, cognitive radio networks have been exploited as a possible solution. Work done in [85], proposed integrating CRs with cooperative relaying techniques. It analysed the outage and bit error probabilities of a dual-hop cognitive turbo-coded relaying network with outdated channel state information (CSI) [86] Rayleigh block fading. The model assumed a transmit power that is constrained by the maximum allowable transmit power at the secondary source and an interference power constraint determined by the primary network. The model, as shown in Figure 2.8, incorporates the effect of interference from the primary transmitter on the secondary network relays and a destination user. The best relay is selected from a set of DF relays. Motivated by [87-89], they assume that the relays are corrupted by cochannel interference (CCI) while the destination is only affected by additive noise

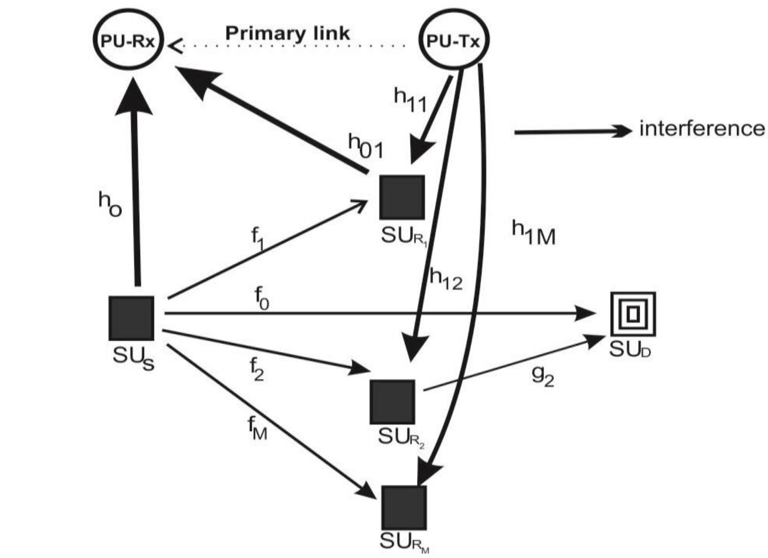

Figure 2.8 System model of coded cooperation with relay selection in an underlay spectrum sharing environment [85].

To efficiently analyze the main parameters of the system performance, the authors derived analytical expressions of the end-to-end bit error rate (BER) and outage probability of the proposed model. The authors derived upper bound of the probability in the high SNR regime assuming binary phase-shift keying. The author also provided corresponding simulation results to validate all these mathematical derivations. In conclusion, this study revealed that the diversity gain on the outage probability was found to solely depend on the desired CSI without being affected by the interference CSI.

2.8.2 Underlay Cognitive Multiple relay Networks

Motivated by another scenario, [90] investigated underlay cognitive network systems with multiple intermediate relays. In this model, the authors assumed that there was a direct link from the secondary source to the destination and a relaying link as well. The relaying link was implemented using two modes: (i) DF and (ii) incremental decode and forward (IDF).

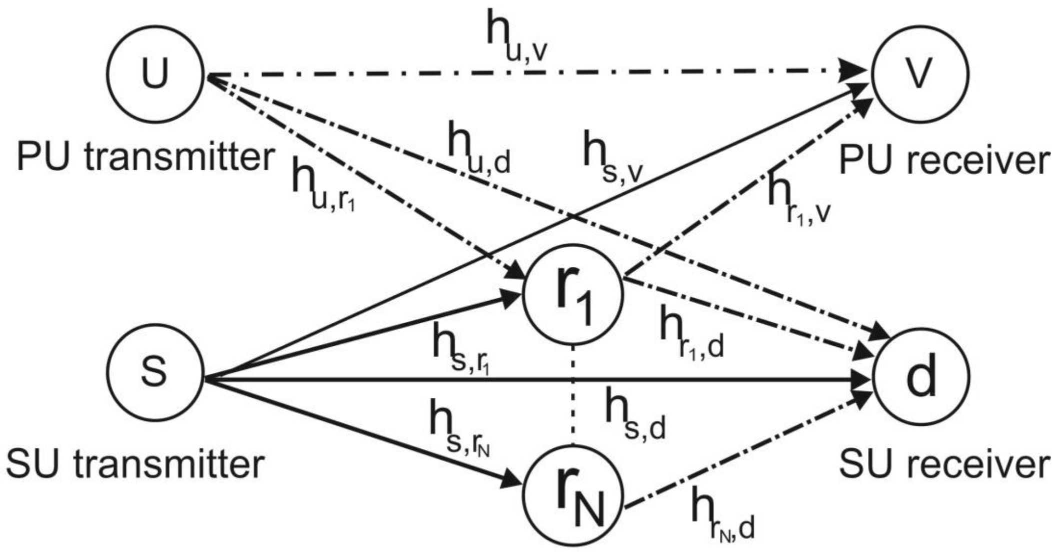

Figure 2.9 Model of an underlay cognitive radio network with multiple relays [90].

Illustrated in Figure 2.9, the author investigated an underlay cognitive relaying network with mutual interference between SU and PU. Insightful analysis of the outage performance gap between DF and IDF relaying was done. In particular, based on the characteristics of cognitive relay networks, the authors considered a direct link between SU source and destination, and a set of relays.

In this model, it was assumed that all nodes are equipped with a single omnidirectional antenna and are in half-duplex mode with time division multiple access (TDMA) [91]. This study revealed that the outage gap between DF and IDF relaying reduces with an increase in the number of available relays. The direct link and increasing number of relays also compensated the performance loss resulting from the PU transmitter's interference.

2.9 Conclusion

The main focus of this chapter is to explain the work that exists in the literature that motivated us into doing this research. We cover NOMA, Cognitive Radios and Cooperative relaying models that have been studied in the past. NOMA has been considered the future of multiple access radio network due to its capabilities of enhancing spectrum efficiency by transmitting using the same spectrum resources without spreading redundancy. Cognitive radios are intelligent wireless communication devices that utilize side information about the transmission environment to improve spectrum utilization. These radios use advanced radio and signal process technology and comprehensive spectrum utilization policies to support wireless users in the crowded spectrum without the performance of established/licensed users. Cooperative communication is vital in transmission since it increases capacity performance. System reliability increases with the existence of a relaying link as it reduces end-to-end channel fading by being an intermediate node. Due to all these different positive attributes research work is expanding to the integration of these models as a way of optimising the overall system. Now in the chapters that follow motivated by these concepts, we propose a model that integrates these three key concepts. The main aim of this study is to understand the impact of relay selection in a cognitive NOMA radio network model concerning outage performance.

Chapter 3 NOMA in Spectrum-Sharing Network under Interference Power Constraints

3.1 Introduction

This chapter focuses on non-orthogonal multiple access in a cognitive radio network with spectrum sharing and transmission power constrained. The model incorporates a dual-hop transmission through a set of decode and forward relays. A secondary source node communicates with two destination nodes through the help of a single relay node selected from the set of DF relays making sure that the multiple cognitive transmissions do not compromise the primary networks' quality of service (QoS).

The relay nodes are used to improve the reliability and coverage of the cognitive network since there exists a strict power constraint on the secondary cognitive source. Closed-form expressions for the outage probabilities at both destination nodes are obtained. Monte Carlo simulations are provided to assess the accuracy of the proposed analytical framework.

3.2 System Model

As shown in Figure. 3.1, motivated by [19] we consider a downlink cooperative underlay CR-NOMA wireless system, where concurrent primary transmissions and secondary transmissions with NOMA take place. On the one hand, the secondary network consists of a cognitive source SU_S, a set of K relays denoted by R_k where $k = 1, \dots, K$, and two destination nodes, $D_1$and D_2 while on the other hand, the primary network includes a primary transmitter PU_{Tx} and a primary receiver PU_{Rx}.

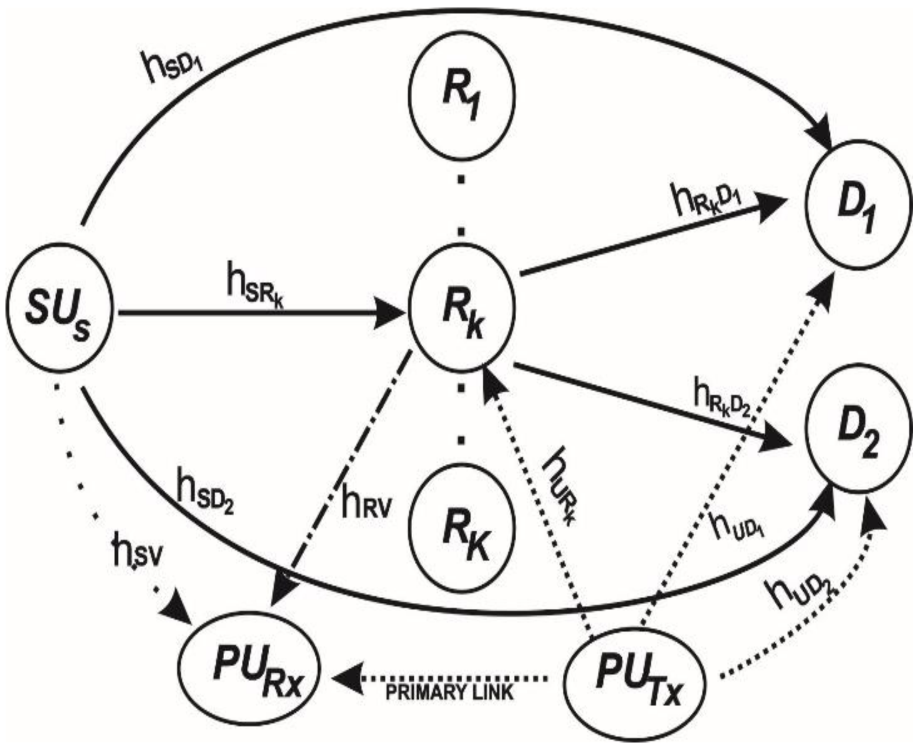

Figure 3.1 Illustration of a cooperative underlay CR-NOMA wireless system with DF partial relay selection.

The secondary transmissions take place in two-time slots. In the first phase, SU_S broadcasts information x_S to all the relay nodes R_k, and both the destination nodes D_1 and D_2. The received signals at R_k, D_1 and D_2 are given respectively by

$$y_{R_k} = h_{SR_k} x_s + \sqrt{P_P} h_{UR_k} x' + n_{SR_k}, \tag{3.1}$$

$$y_{D_1} = h_{SD_1} x_s + \sqrt{P_P} h_{UD_1} x' + n_{SD_1}, \tag{3.2}$$

$$y_{D_2} = h_{SD_2} x_s + \sqrt{P_P} h_{UD_2} x' + n_{SD_2}, \tag{3.3}$$

where x' is the transmitted signal from the primary transmitter in the first phase, P_P is the transmit power of the primary transmitter, and the transmitted signal x_S is given by

$$x_s = \sqrt{a_1 P_S} x_1 + \sqrt{a_2 P_S} x_2, \tag{3.4}$$

with x_1 and x_2 being the messages for D_1 and D_2, respectively, and a_1 and a_2 are the power allocation coefficients. We assume that $|a_1| > |a_2|$, with $|a_1| + |a_2| = 1$ according to NOMA. Also, $h_{EF} \sim \mathcal{CN}(0, \Omega_{EF})$ denotes the complex channel fading coefficient, with the subscripts $E = \{S, R_k, U\}$ and $F = \{R_k, D_1, D_2, V\}$. Moreover, the noises at the receivers R_k and D_i with $i = \{1,2\}$ denoted by n_{SR_k} and n_{SD_i} respectively, are additive white Gaussian noise (AWGN) with zero mean and variance $\mathcal{N}_0$, i.e., $\sim \mathcal{CN}(0, \mathcal{N}_0)$. Both the users D_1 and D_2 form a NOMA downlink system with channel $h_{SD_1} \leq h_{SD_2}$ [10]. In (4), the transmit power at the secondary source is given by

$$P_S = \min\left(P_t, \frac{I_p}{|h_{SV}|^2}\right), \tag{3.5}$$

where P_t represents the maximum allowable transmit power, I_p is the interference temperature limit which guarantees that the secondary transmissions do not violate the primary transmissions at the primary receiver.

In the second phase, a relay selected from a set of relay nodes that have successfully received the source information in the first time slot is used to assist the source by forwarding its message to both D_1 and D_2. The relay selection criterion will be defined subsequently. For now, we assume that R_k is selected to transmit in the second time slot. Similar to the source, the transmit power of R_k is also limited and given by

$$P_{R_k} = \min\left(P_t, \frac{I_p}{\left|h_{R_kV}\right|^2}\right). \tag{3.6}$$

The received signals at both D_1 and D_2, emanating from R_k in the second phase are given respectively by

$$y_{R_kD_1} = h_{R_KD_1} x_{R_k} + \sqrt{P_P} h_{UD_1} x'' + n_{R_KD_1}, \tag{3.7}$$

$$y_{R_kD_2} = h_{R_KD_2} x_{R_k} + \sqrt{P_P} h_{UD_2} x'' + n_{R_KD_2}, \tag{3.8}$$

where $x_{R_k}$the transmitted signal from the selected relay node is expressed as $x_{R_k} = \sqrt{d_1 P_{R_k}} x_1 + \sqrt{d_2 P_{R_k}} x_2$, with the assumption that $|d_1| > |d_2|$ given $|d_1| + |d_2| = 1$, x'' is the transmitted signal from the primary transmitter in the second phase, and $n_{R_{kD_i}} \sim \mathcal{CN}(0, \mathcal{N}_0)$ is AWGN. Next, we derive the received signal-to-interference-plus-noise ratio (SINR) at D_1, and, D_2 as shown in appendix A1.1-A1.2. After substituting (3.4) into (3.2) and after some manipulations, the received instantaneous SINR at D_1 to detect x_1 is given by

$$\gamma_{SD_1} = \frac{a_1 X_1}{a_2 X_1 + B_{D_1} + 1}, \tag{3.9}$$

where $X_1 = \gamma_0 |h_{SD_1}|^2$ and $B_{D_1} = \gamma_2 |h_{UD_1}|^2$. Using the approach in Appendix A1.3, the received SNR at D_2 used to detect x_1 is given by

$$\gamma_{SD_{12}} = \frac{a_1 X_2}{a_2 X_2 + B_{D_2} + 1}, \tag{3.10}$$

where $X_2 = \gamma_0 |h_{SD_2}|^2$ and $B_{D_2} = \gamma_2 |h_{UD_2}|^2$. Note that, $B_{D_i} = \gamma_2 |h_{UD_i}|^2$ represents the instantaneous signal-to-noise ratio (SNR) for the links $P \to D_i$, with $i = \{1, 2\}$. D_2 decode the symbol x_2 by cancelling x_1 using SIC. To this end, the received SNR at D_2 for receiving x_2 according to Appendix A1.4-A1.5 is expressed as

$$\gamma_{SD_2} = \frac{a_2 X_2}{B_{D_2} + 1}. \tag{3.11}$$

Note that B_{D_2} refers to the interference caused by the primary transmitter on the destination D_2. In the second phase, the selected relay transmits the source information to both the destination nodes. Using the above definition of x_{R_k} and equation (3.7) and after derivations shown in A2.1-A2.2, the instantaneous SINR at D_1 is given

$$\gamma_{R_k D_1} = \frac{d_1 Z_{1_k}}{d_2 Z_{1_k} + B_{D_1} + 1}, \tag{3.12}$$

where $Z_{1_k} = \gamma_1 \left|h_{R_k D_1}\right|^2$ with $\gamma_1 = \min\left(\gamma_P \ , \frac{\gamma_I}{\left|h_{R_k V}\right|^2}\right)$. With the help of x_{R_k} in (3.8), the received instantaneous SINR used for D_2 to detect x_1 based on Appendix A2.3-A2.4 is given by

$$\gamma_{R_k D_{12}} = \frac{d_1 Z_{2_k}}{d_2 Z_{2_k} + B_{D_2} + 1}, \tag{3.13}$$

While the instantaneous SINR used for D_2 to detect x_2 according to Appendix A2.5-A2.6 is given by

$$\gamma_{R_k D_2} = \frac{d_2 Z_{2_k}}{B_{D_2} + 1}. \tag{3.14}$$

It is assumed that both D_1 and D_2 employ a selection combining (SC) scheme. Hence, as mentioned above, the received instantaneous SINR at D_1 and D_2 are given respectively by

$$\gamma_{D_1} = \max\left(\gamma_{SD_1}, \gamma_{R_k D_1}\right), \tag{3.15}$$

$$\gamma_{D_2} = \max\left(\gamma_{SD_2}, \gamma_{R_k D_2}\right). \tag{3.16}$$

It is previously assumed that R_k is selected as the best relay node. Here, a partial relay selection scheme is used according to the following criterion

$$k = \arg \max_{j=1,\dots,K} \left\{\gamma_{R_j D_i}\right\}. \tag{3.17}$$

For mathematical tractability, the relay with the highest SNR link between any of the relay node and the two destinations is selected.

3.3 Outage Performance Analysis

In this section, we derive the outage performance of each destination node using the statistics of the received SINR obtained previously. It is defined as the probability that the received SINR at a particular user falls below a pre-defined threshold. In this case, it is assumed that both destinations D_1 and D_2 have the same outage threshold $\gamma_{\text{th}} = 2^{2R_{\text{th}}} - 1$, where R_{th} denotes the target transmission rate.

3.3.1 Outage Probability at $\mathbf{D_1}$

Here, an outage event occurs if neither the direct transmission nor the relaying transmission succeeds at D_1. Using the above definition, the corresponding outage probability can be expressed mathematically as

$$OP_1 = \Pr\left(\max\left[\gamma_{SD_1}, \gamma_{R_k D_1}\right] \le \gamma_{\text{th}}\right). \tag{3.18}$$

Since the random variables (RV) γ_{SD_1} and $\gamma_{R_k D_1}$ are independent, (3.18) can further be written in terms of the cumulative distribution function (CDF) as

$$OP_1 = F_{\gamma_{SD_1}}(\gamma_{\text{th}}) F_{\gamma_{R_k D_1}}(\gamma_{\text{th}}). \tag{3.19}$$

In what follows, we derive the expressions of the CDFs in (3.19). Starting with the CDF of the RV γ_{SD_1} and using (3.9), we get

$$F_{\gamma_{SD_1}}(\gamma_{\text{th}}) = Pr\left(\frac{a_1 X_1}{a_2 X_1 + B_{D_1} + 1} \le \gamma_{\text{th}}\right). \tag{3.20}$$

Using the definitions of X_1 and B_{D_1} given above, and with the condition on the transmit power at the source node, (3.20) can further be expressed as

$$F_{\gamma_{SD_1}}(\gamma_{\text{th}}) = Pr\left(\frac{\frac{\mu_1}{|h_{SV}|^2}\left|h_{SD_1}\right|^2}{\frac{\mu_2}{|h_{SV}|^2}\left|h_{SD_1}\right|^2 + \left|h_{UD_1}\right|^2\gamma_2 + 1} \le \gamma_{\text{th}}, \frac{\gamma_I}{|h_{SV}|^2} \le \gamma_P\right)$$

$$+ Pr\left(\frac{\left|h_{SD_1}\right|^2 a_1\gamma_P}{\left|h_{SD_1}\right|^2 a_2\gamma_P + \left|h_{UD_1}\right|^2\gamma_2 + 1} \le \gamma_{\text{th}}, \frac{\gamma_I}{|h_{SV}|^2} \ge \gamma_P\right), \tag{3.21}$$

where $\mu_1 = a_1\gamma_I$ and $\mu_2 = a_2\gamma_I$. To derive (3.21) in closed-form, we deal with the two expressions in (3.21) separately. In what follows, we denote I_1 as the first part of the summation and I_2 as the second part. We start with the first part of the summation which can be rewritten after some algebraic manipulations as

$$I_1 = \Pr\left(\left|h_{SD_1}\right|^2 \le \left(\frac{\gamma_{\text{th}}}{(\mu_1 - \mu_2\gamma_{\text{th}})}\right)\left(\gamma_2\left|h_{UD_1}\right|^2 + 1\right)|h_{SV}|^2\right)$$

$$\times \Pr\left(|h_{SV}|^2 \ge \frac{\gamma_I}{\gamma_P}\right). \quad (3.22)$$

By taking $\emptyset = \mu_1 - \mu_2\gamma_{\text{th}}$ and after performing some manipulations and using the moment generating function (MGF) of the chi-square distribution as shown in Appendix B.1, we obtain

$$I_1 = \Pr\left(\left|h_{SD_1}\right|^2 \le \mathscr{g}_1\right)\Pr\left(|h_{SV}|^2 \ge \frac{\gamma_I}{\gamma_P}\right)$$

$$I_1 = \left[1 - \exp\left(-\frac{\mathscr{g}_1}{\Omega_{SD_1}}\right)\right]\left(e^{-\frac{\gamma_I}{\gamma_P\Omega_{SV}}}\right)$$

$$I_1 = \left[1 - \mathbb{E}_{|h_{SV}|^2,\left|h_{UD_1}\right|^2}\left[e^{-\frac{\mathscr{g}_1}{\Omega_{SD_1}}}\right]\right]\left(e^{-\frac{\gamma_I}{\gamma_P\Omega_{SV}}}\right), \quad (3.23)$$

where $\mathscr{g}_1 = \left(\frac{\gamma_{\text{th}}}{\emptyset}\right)\left(\gamma_2\left|h_{UD_1}\right|^2 + 1\right)|h_{SV}|^2$. It turns out that the exact expression of (3.23) is difficult to obtain. Therefore, we derive an approximate expression with the help of Jensen's inequality, which yields

$$I_1 \cong \left[1 - \left[\left(1 + \frac{\gamma_{\text{th}}\gamma_2\Omega_{h_{SV}}\Omega_{UD_1}}{\emptyset\Omega_{SD_1}}\right)^{-1}\left(1 + \frac{\gamma_{th}\Omega_{h_{SV}}}{\emptyset\Omega_{SD_1}}\right)^{-1}\right]\right]\left(e^{-\frac{\gamma_I}{\gamma_P\Omega_{h_{SV}}}}\right) \quad (3.24)$$

A detailed derivation of (3.24) is given in appendix A. Using the same approach, I_2 can be approximated as shown in (3.25), where $\psi = \beta_1 - \beta_2\,\gamma_{\text{th}}$ with $\beta_1 = a_1\gamma_P$, and $\beta_2 = a_2\gamma_P$ for notational convenience.

$$I_2 \cong \left[1 - \left[\left(1 + \frac{\gamma_{th}\gamma_2\Omega_{UD_1}}{\psi\Omega_{SD_1}}\right)^{-1} e^{-\frac{\gamma_{th}}{\psi\Omega_{SD_1}}}\right]\right]\left(1 - e^{-\frac{\gamma_I}{\gamma_P\Omega_{h_{SV}}}}\right). \quad (3.25)$$

After substituting (3.24) and (3.25) in (3.21), we obtain a closed-form analytical expression for the approximate of $F_{\gamma_{SD_1}}(\gamma_{\text{th}})$. Next, we focus on deriving an analytical expression of $F_{\gamma_{R_kD_1}}(\gamma_{\text{th}})$. Based on (3.14), the CDF of $\gamma_{R_kD_1}$ can further be expressed as

$$F_{\gamma_{R_kD_1}}(\gamma_{\text{th}}) = \Pr\left(\frac{d_1 Z_{1_k}}{d_2 Z_{1_k} + B_{D_1} + 1} \leq \gamma_{\text{th}}\right). \tag{3.26}$$

Using the definitions of Z_{1_k} and B_{D_1}given above, and with the condition on the transmit power at the relay node, (3.26) is provided by

$$F_{\gamma_{R_kD_1}}(\gamma_{\text{th}}) = \Pr\left(\frac{\frac{\alpha_1}{\left|h_{R_kV}\right|^2}\left|h_{R_kD_1}\right|^2}{\frac{\alpha_2\left|h_{R_kD_1}\right|^2}{\left|h_{R_kV}\right|^2} + \left|h_{UD_1}\right|^2\gamma_2 + 1} \leq \gamma_{\text{th}}, \left|h_{R_kV}\right|^2 \geq \frac{\gamma_I}{\gamma_P}\right)$$

$$+\Pr\left(\frac{\left|h_{R_kD_1}\right|^2\omega_1}{\left|h_{R_kD_1}\right|^2\omega_2 + \left|h_{UD_1}\right|^2\gamma_2 + 1} \leq \gamma_{\text{th}}, \frac{\gamma_I}{\left|h_{h_{R_kV}}\right|^2} \geq \gamma_P\right), \tag{3.27}$$

where $\alpha_1 = d_1\gamma_I$ $,\alpha_2 = d_2\gamma_I$ $\omega_1 = d_1\gamma_P$, and $\omega_2 = d_2\gamma_P$ for notational convenience. After rearranging (3.27), and using $\eta = \alpha_1 - \alpha_2\gamma_{\text{th}}$ and $\vartheta = \omega_1 - \omega_2\gamma_{\text{th}}$, we can express (3.27) as

$$F_{\gamma_{R_kD_1}}(\gamma_{\text{th}}) = \left(\Pr\left(\left|h_{R_kD_1}\right|^2 \leq \varphi_1\right) Pr\left(\left|h_{R_kV}\right|^2 \geq \frac{\gamma_I}{\gamma_P}\right)\right)$$

$$+\Pr\left(\left|h_{R_kD_1}\right|^2 \leq \sigma_1\right)\Pr\left(\left|h_{R_kV}\right|^2 \leq \frac{\gamma_I}{\gamma_P}\right), \tag{3.28}$$

where we define $\varphi_1 = \left(\frac{\gamma_{\text{th}}}{\eta}\right)\left(\gamma_2\left|h_{UD_1}\right|^2 + 1\right)\left|h_{R_kV}\right|^2$and from the second part of (3.28), $\sigma_1 = \left(\frac{\gamma_{\text{th}}}{\vartheta}\right)\left(\gamma_2\left|h_{UD_1}\right|^2 + 1\right)$, and we denote the first and second parts of the summation in (3.28) by J_1 and J_2, respectively. It is easy to obtain the closed-form expression of J_1 as

$$J_1 = \left[1 - e^{-\frac{\varphi_1}{\Omega_{R_kD_1}}}\right]^K\left(e^{-\frac{\gamma_I}{\gamma_P\Omega_{R_kV}}}\right).$$

$$J_1 \cong \left[1 - \sum_{m=1}^{K}\binom{K}{m}(-1)^{m-1}\left[\left(1 + \frac{m\gamma_{\text{th}}\gamma_2\Omega_{R_kV}\Omega_{UD_1}}{\eta\Omega_{R_kD_1}}\right)^{-1}\left(1 + \frac{m\gamma_{\text{th}}\Omega_{R_kV}}{\eta\Omega_{R_kD_1}}\right)^{-1}\right]\right]\left(e^{-\frac{\gamma_I}{\gamma_P\Omega_{R_kV}}}\right) \tag{3.29}$$

Next, to evaluate J_2, we use the same approach as the one used to obtain J_1. Hence, J_2 can be approximated by

$$J_2 \cong \left[1-\sum_{n=1}^{K}\binom{K}{n}(-1)^{n-1}\left[\left(1+\frac{n\gamma_{\text{th}}\gamma_2\Omega_{UD_1}}{\vartheta\Omega_{R_kD_1}}\right)^{-1}\left(e^{-\frac{\gamma_{\text{th}}}{\vartheta\Omega_{R_kD_1}}}\right)\right]\right]\left(1-\left(e^{-\frac{\gamma_I}{\gamma_P\Omega_{R_kV}}}\right)\right).$$

(3.30)

Plugging (3.29) and (3.30) into (3.28) and substituting the resulting expression together with the analytical expression of $F_{\gamma_{SD_1}}(\gamma_{\text{th}})$ previously derived in (3.20), yields the analytical expression for the approximate of the outage probability at D_1 as shown in (3.31).

$$OP_1 = \Bigg[\bigg[1-\sum_{m=1}^{K}\binom{K}{m}(-1)^{m-1}\bigg[\left(1+\frac{m\gamma_{\text{th}}\gamma_2\Omega_{R_kV}\Omega_{UD_1}}{\eta\Omega_{R_kD_1}}\right)^{-1}\left(1+\frac{m\gamma_{\text{th}}\Omega_{R_kV}}{\eta\Omega_{R_kD_1}}\right)^{-1}\bigg]\bigg]\left(e^{-\frac{\gamma_I}{\gamma_P\Omega_{R_kV}}}\right)$$

$$+\bigg[1-\textstyle\sum_{n=1}^{K}\binom{K}{n}(-1)^{n-1}\bigg[\left(1+\frac{n\gamma_{\text{th}}\gamma_2\Omega_{UD_1}}{\vartheta\Omega_{R_kD_1}}\right)^{-1}\left(e^{-\frac{\gamma_{\text{th}}}{\vartheta\Omega_{R_kD_1}}}\right)\bigg]\bigg]\left(1-\left(e^{-\frac{\gamma_I}{\gamma_P\Omega_{R_kV}}}\right)\right)\bigg]$$

$$\Bigg[\bigg[1-\bigg[\left(1+\frac{\gamma_{\text{th}}\gamma_2\Omega_{h_{SV}}\Omega_{UD_1}}{\emptyset\Omega_{SD_1}}\right)^{-1}\left(1+\frac{\gamma_{th}\Omega_{h_{SV}}}{\emptyset\Omega_{SD_1}}\right)^{-1}\bigg]\bigg]\left(e^{-\frac{\gamma_I}{\gamma_P\Omega_{h_{SV}}}}\right)$$

$$+\bigg[1-\bigg[\left(1+\frac{\gamma_{th}\gamma_2\Omega_{UD_1}}{\psi\Omega_{SD_1}}\right)^{-1}e^{-\frac{\gamma_{th}}{\psi\Omega_{SD_1}}}\bigg]\bigg]\left(1-e^{-\frac{\gamma_I}{\gamma_P\Omega_{h_{SV}}}}\right)\bigg]$$

(3.31)

3.3.2 Outage Probability at D_2

An outage event at D_2 occurs when both the first phase and the second-phase transmissions are not successful. Based on NOMA and SIC, the outage will occur when D_2 can detect x_1 successfully but fails to detect its signal x_2, or when D_2 fails to detect x_1 due to the significant impact of the interference from the primary network, i.e., B_{D_2}. The outage probability at D_2 is given by

$$OP_2 = F_{\gamma_{SD_2}}(\gamma_{\text{th}}) F_{\gamma_{SR_kD_2}}(\gamma_{\text{th}}). \tag{3.32}$$

First, our attention is on deriving an analytical expression of $F_{\gamma_{SD_2}}(\gamma_{\text{th}})$ which can be expressed as

$$F_{\gamma_{SD_2}}(\gamma_{\text{th}}) = \Pr\left(\frac{a_2 X_2}{B_{D_2}+1} \leq \gamma_{\text{th}}, \frac{a_1 X_2}{a_2 X_2 + B_{D_2} + 1} > \gamma_{\text{th}}\right)$$

$$+\Pr\left(\frac{a_1 X_2}{a_2 X_2 + B_{D_2} + 1} \leq \gamma_{\text{th}}\right). \tag{3.33}$$

With the constraints on the transmit power, the first part of (3.33) denoted by G_1 can be rewritten as

$$G_1 = \Pr\left(\frac{a_2 X_2}{B_{D_2} + 1} \leq \gamma_{\text{th}}, \frac{\gamma_I}{|h_{SV}|^2} \leq \gamma_P\right) + \Pr\left(\frac{a_2 X_2}{B_{D_2} + 1} \leq \gamma_{\text{th}}, \frac{\gamma_I}{|h_{SV}|^2} \geq \gamma_P\right), \tag{3.34}$$

And can further be expressed as

$$G_1 \cong \left[1 - \left[\left(1 + \frac{\gamma_{\text{th}}\gamma_2 \Omega_{h_{SV}} \Omega_{UD_2}}{\mu_2 \Omega_{SD_2}}\right)^{-1} \left(1 + \frac{\gamma_{\text{th}} \Omega_{h_{SV}}}{\mu_2 \Omega_{SD_2}}\right)^{-1}\right]\right] \left(e^{-\frac{\gamma_I}{\gamma_P \Omega_{h_{SV}}}}\right)$$

$$+\left[1 - \left[\left(1 + \frac{\gamma_{\text{th}}\gamma_2 \Omega_{UD_2}}{\beta_2 \Omega_{SD_2}}\right)^{-1} \times e^{-\frac{\gamma_{\text{th}}}{\beta_2 \Omega_{SD_2}}}\right]\right] \left(1 - e^{-\frac{\gamma_I}{\gamma_P \Omega_{h_{SV}}}}\right), \tag{3.35}$$

Similarly, the second part of (3.33) denoted by G_2 can be analytically obtained using the above approach. First, we rewrite G_2 in (3.33), as

$$G_2 = \Pr\left(\frac{a_1 X_2}{a_2 X_2 + B_{D_2} + 1} \leq \gamma_{\text{th}}, \frac{\gamma_I}{|h_{SV}|^2} \leq \gamma_P\right) + \Pr\left(\frac{a_1 X_2}{a_2 X_2 + B_{D_2} + 1} \leq \gamma_{\text{th}}, \frac{\gamma_I}{|h_{SV}|^2} \geq \gamma_P\right), \tag{3.36}$$

Equation (3.36) can be given in closed form as

$$G_2 = \left[1 - \left[\left(1 + \frac{\gamma_{\text{th}}\gamma_2 \Omega_{h_{SV}} \Omega_{UD_2}}{\emptyset \Omega_{SD_2}}\right)^{-1} \left(1 + \frac{\gamma_{\text{th}} \Omega_{h_{SV}}}{\emptyset \Omega_{SD_2}}\right)^{-1}\right]\right] \left(e^{-\frac{\gamma_I}{\gamma_P \Omega_{h_{SV}}}}\right)$$

$$+ \left[1 - \left[\left(1 + \frac{\gamma_{\text{th}}\gamma_2 \Omega_{UD_2}}{\psi \Omega_{SD_2}}\right)^{-1} e^{-\frac{\gamma_{\text{th}}}{\psi \Omega_{SD_2}}}\right]\right] \left(1 - e^{-\frac{\gamma_I}{\gamma_P \Omega_{h_{SV}}}}\right). \tag{3.37}$$

Also, note that

$$\Pr\left(\frac{a_1 X_2}{a_2 X_2 + B_{D_2} + 1} > \gamma_{\text{th}}\right) = 1 - \Pr\left(\left(\frac{a_1 X_2}{a_2 X_2 + B_{D_2} + 1} \leq \gamma_{\text{th}}\right)\right),$$

$$\Pr\left(\frac{a_1 X_2}{a_2 X_2 + B_{D_2} + 1} > \gamma_{\text{th}}\right) = 1 - G_2$$

(3.38)

The analytical expression of $F_{\gamma_{SD_2}}(\gamma_{\text{th}})$ based on (3.33) can be expressed as

$$F_{\gamma_{SD_2}}(\gamma_{\text{th}}) = G_1(1 - G_2) + G_2$$

(3.39)

Equation (3.39) reduces to

$$F_{\gamma_{SD_2}}(\gamma_{\text{th}}) = \left[\left[1-\left[\left(1+\frac{\gamma_{\text{th}}\gamma_2\Omega_{h_{SV}}\Omega_{UD_2}}{\mu_2\Omega_{SD_2}}\right)^{-1}\left(1+\frac{\gamma_{\text{th}}\Omega_{h_{SV}}}{\mu_2\Omega_{SD_2}}\right)^{-1}\right]\right]\left(e^{\frac{\gamma_I}{\gamma_P\Omega_{h_{SV}}}}\right)\right.$$

$$+\left[1-\left[\left(1+\frac{\gamma_{\text{th}}\gamma_2\Omega_{UD_2}}{\beta_2\Omega_{SD_2}}\right)^{-1}\times e^{-\frac{\gamma_{\text{th}}}{\beta_2\Omega_{SD_2}}}\right]\right]\left(1-e^{-\frac{\gamma_I}{\gamma_P\Omega_{h_{SV}}}}\right)\Bigg]$$

$$\times\left[1-\left[\left[1-\left[\left(1+\frac{\gamma_{\text{th}}\gamma_2\Omega_{h_{SV}}\Omega_{UD_2}}{\emptyset\Omega_{SD_2}}\right)^{-1}\left(1+\frac{\gamma_{\text{th}}\Omega_{h_{SV}}}{\emptyset\Omega_{SD_2}}\right)^{-1}\right]\right]\left(e^{-\frac{\gamma_I}{\gamma_P\Omega_{h_{SV}}}}\right)\right.\right.$$

$$+\left[1-\left[\left(1+\frac{\gamma_{\text{th}}\gamma_2\Omega_{UD_2}}{\psi\Omega_{SD_2}}\right)^{-1}e^{\frac{\gamma_{\text{th}}}{\psi\Omega_{SD_2}}}\right]\right]\left(1-e^{-\frac{\gamma_I}{\gamma_P\Omega_{h_{SV}}}}\right)\Bigg]\Bigg]$$

$$+\left[\left[1-\left[\left(1+\frac{\gamma_{\text{th}}\gamma_2\Omega_{h_{SV}}\Omega_{UD_2}}{\emptyset\Omega_{SD_2}}\right)^{-1}\left(1+\frac{\gamma_{\text{th}}\Omega_{h_{SV}}}{\emptyset\Omega_{SD_2}}\right)^{-1}\right]\right]\left(e^{-\frac{\gamma_I}{\gamma_P\Omega_{h_{SV}}}}\right)\right.$$

$$+\left[1-\left[\left(1+\frac{\gamma_{\text{th}}\gamma_2\Omega_{UD_2}}{\psi\Omega_{SD_2}}\right)^{-1}e^{-\frac{\gamma_{\text{th}}}{\psi\Omega_{SD_2}}}\right]\right]\left(1-e^{-\frac{\gamma_I}{\gamma_P\Omega_{h_{SV}}}}\right)\Bigg]$$

(3.40)

Next, we turn our attention to deriving an analytical expression of $F_{\gamma_{SR_kD_2}}(\gamma_{\text{th}})$ Using (3.13) and (3.14), the term $F_{\gamma_{SR_kD_2}}(\gamma_{\text{th}})$ can further be expressed as

$$F_{\gamma_{SR_kD_2}}(\gamma_{\text{th}}) = \Pr\left(\frac{d_2 Z_{2_k}}{B_{D_2}+1} \leq \gamma_{\text{th}}, \frac{d_1 Z_{2_{k*}}}{d_2 Z_{2_k}+B_{D_2}\ 1} > \gamma_{\text{th}}\right) + \Pr\left(\frac{d_1 Z_{2_k}}{d_2 Z_{2_k}+B_{D_2}+1} \leq \gamma_{\text{th}}\right).$$

(3.41)

We denote the first part of (3.41) by H_1. After some expansion, H_1 is given by

$$H_1 = \Pr\left(\frac{d_2 Z_{2_k}}{B_{D_2} + 1} \leq \gamma_{\text{th}}, \frac{\gamma_I}{\left|h_{R_k V}\right|^2} \leq \gamma_P\right)$$

$$+\Pr\left(\frac{d_2 Z_{2_k}}{B_{D_2} + 1} \leq \gamma_{\text{th}}, \frac{\gamma_I}{\left|h_{R_k V}\right|^2} \geq \gamma_P\right), \quad (3.42)$$

And can be obtained analytically through tome approximations and given by

$$H_1 \cong \left[1 - \sum_{m=1}^{K}\binom{K}{m}(-1)^{m-1}\left[\left(1 + \frac{m\gamma_{\text{th}}\Omega_{R_k V}}{\alpha_2 \Omega_{R_k D_2}}\right)^{-1}\left(1 + \frac{m\gamma_{\text{th}}\gamma_2\Omega_{R_k V}\Omega_{UD_2}}{\alpha_2\Omega_{R_k D_2}}\right)^{-1}\right]\right]\left(e^{-\frac{\gamma_I}{\gamma_P \Omega_{R_k V}}}\right)$$

$$+\left[1 - \sum_{n=1}^{K}\binom{K}{n}(-1)^{n-1}\left[\left(1 + \frac{n\gamma_{\text{th}}\gamma_2\Omega_{UD_2}}{\omega_2\Omega_{R_k D_2}}\right)^{-1} e^{-\frac{\gamma_{\text{th}}}{\omega_2\Omega_{R_k D_1}}}\right]\right]\left(1 - e^{-\frac{\gamma_I}{\gamma_P\Omega_{R_k V}}}\right). \quad (3.43)$$

Subsequently, the second part of (3.41) is denoted by H_2. Expanding H_2 in (3.41) yields

$$H_2 = \Pr\left(\frac{d_1 Z_{2_k}}{d_2 Z_{2_k} + B_{D_2} + 1} \leq \gamma_{\text{th}}, \frac{\gamma_I}{\left|h_{R_k V}\right|^2} \leq \gamma_P\right) + \Pr\left(\frac{d_1 Z_{2_k}}{d_2 Z_{2_k} + B_{D_2} + 1} \leq \gamma_{\text{th}}, \frac{\gamma_I}{\left|h_{R_k V}\right|^2} \geq \gamma_P\right),$$

(3.44)

And further given by

$$H_2 \cong \left[1 - \sum_{m=1}^{K}\binom{K}{m}(-1)^{m-1}\left(1 + \frac{k\gamma_{\text{th}}\Omega_{R_k V}}{\eta\Omega_{R_k D_2}}\right)^{-1}\left(1 + \frac{m\gamma_{\text{th}}\gamma_2\Omega_{R_k V}\Omega_{UD_2}}{\eta\Omega_{R_k D_2}}\right)^{-1}\right]\left(e^{-\frac{\gamma_I}{\gamma_P\Omega_{R_k V}}}\right)$$

$$+\left[1 - \sum_{n=1}^{K}\binom{K}{n}(-1)^{n-1}\left[\left(1 + \frac{n\gamma_{\text{th}}\gamma_2\Omega_{UD_2}}{\vartheta\Omega_{R_k D_2}}\right)^{-1} e^{-\frac{\gamma_{\text{th}}}{\vartheta\Omega_{R_k D_1}}}\right]\right]\left(1 - e^{-\frac{\gamma_I}{\gamma_P\Omega_{R_k V}}}\right).$$

(3.45)

Based on (3.43) we have the below

$$\Pr\left(\frac{d_1 Z_{2_k}}{d_2 Z_{2_k} + B_{D_2}\ 1} > \gamma_{\text{th}}\right) = 1 - \Pr\left(\left(\frac{d_1 Z_{2_k}}{d_2 Z_{2_k}\ +\ B_{D_2}\ +\ 1} \leq \gamma_{\text{th}}\right)\right)$$

$$\Pr\left(\frac{d_1 Z_{2_k}}{d_2 Z_{2_k} + B_{D_2}\ 1} > \gamma_{\text{th}}\right) = 1 - H_{2.} \tag{3.46}$$

After plugging (3.43) and (3.45) into (3.41), we come up with the closed-form expression of $F_{\gamma_{SR_k D_2}}(\gamma_{\text{th}})$ shown below

$$\begin{aligned} F_{\gamma_{SR_k D_2}}(\gamma_{\text{th}}) = &\left[\left[1 - \left[\left(1 + \frac{\gamma_{\text{th}}\gamma_2 \Omega_{h_{SV}} \Omega_{UD_2}}{\mu_2 \Omega_{SD_2}}\right)^{-1} \left(1 + \frac{\gamma_{\text{th}} \Omega_{h_{SV}}}{\mu_2 \Omega_{SD_2}}\right)^{-1}\right]\right] \left(e^{-\frac{\gamma_I}{\gamma_P \Omega_{h_{SV}}}}\right)\right. \\ &+ \left[1 - \left[\left(1 + \frac{\gamma_{\text{th}}\gamma_2 \Omega_{UD_2}}{\beta_2 \Omega_{SD_2}}\right)^{-1} \times e^{-\frac{\gamma_{\text{th}}}{\beta_2 \Omega_{SD_2}}}\right]\right] \left(1 - e^{-\frac{\gamma_I}{\gamma_P \Omega_{h_{SV}}}}\right)\Bigg] \\ &\times \left[1 - \left[\left[1 - \left[\left(1 + \frac{\gamma_{\text{th}}\gamma_2 \Omega_{h_{SV}} \Omega_{UD_2}}{\emptyset \Omega_{SD_2}}\right)^{-1} \left(1 + \frac{\gamma_{\text{th}} \Omega_{h_{SV}}}{\emptyset \Omega_{SD_2}}\right)^{-1}\right]\right] \left(e^{-\frac{\gamma_I}{\gamma_P \Omega_{h_{SV}}}}\right)\right.\right. \\ &+ \left.\left[1 - \left[\left(1 + \frac{\gamma_{\text{th}}\gamma_2 \Omega_{UD_2}}{\psi \Omega_{SD_2}}\right)^{-1} e^{-\frac{\gamma_{\text{th}}}{\psi \Omega_{SD_2}}}\right]\right] \left(1 - e^{-\frac{\gamma_I}{\gamma_P \Omega_{h_{SV}}}}\right)\right]\Bigg] \\ &+ \left[\left[1 - \left[\left(1 + \frac{\gamma_{\text{th}}\gamma_2 \Omega_{h_{SV}} \Omega_{UD_2}}{\emptyset \Omega_{SD_2}}\right)^{-1} \left(1 + \frac{\gamma_{\text{th}} \Omega_{h_{SV}}}{\emptyset \Omega_{SD_2}}\right)^{-1}\right]\right] \left(e^{-\frac{\gamma_I}{\gamma_P \Omega_{h_{SV}}}}\right)\right. \\ &+ \left[1 - \left[\left(1 + \frac{\gamma_{\text{th}}\gamma_2 \Omega_{UD_2}}{\psi \Omega_{SD_2}}\right)^{-1} e^{-\frac{\gamma_{\text{th}}}{\psi \Omega_{SD_2}}}\right]\right] \left(1 - e^{-\frac{\gamma_I}{\gamma_P \Omega_{h_{SV}}}}\right)\Bigg] \end{aligned} \tag{3.47}$$

Substituting the resulting expression together with the analytical expression of $F_{\gamma_{SD_2}}(\gamma_{\text{th}})$ as above obtained in (3.41), yields the outage probability at D_2

3.4 Numerical Results

In this section, we present numerical results to evaluate the performance of the proposed system. Monte Carlo simulations are also provided to assess the correctness of the mathematical derivations. Without loss of generality, we use the following parameters: $a_1 = 0.8$, $a_2 = 0.2$, $d_1 = 0.8$ and $d_2 = 0.2$. Also, the threshold SINR at D_1 and D_2 is the same and is given by $\gamma_{\text{th}} = 2^{2R_{\text{th}}} - 1$, where $R_{\text{th}} = 1$ bit/s/Hz. It is observed in the subsequent figures that Monte Carlo simulations corroborate our proposed analytical framework.

In Figure 3.2, we investigate the impact of the interference constraint on the outage performance of the system. We consider a case wherein, and all channels are subjected to the same conditions and the maximum allowable transmit power of the secondary network. As can be observed, the outage probability decreases as SNR increases until it reaches a specific fixed value. This result shows that outage performance improves until a particular floor of outage value determined by interference constraints of the system.

In Figure 3.3, we consider a case wherein, the maximum allowable transmit power of the secondary network takes fixed values, and the interference power varies. This result implies that the outage probability decreases as the interference power increases until it reaches a given outage floor which depends on the maximum allowable transmit power of the secondary nodes. There is a small discrepancy between the analytical and simulated results for Figure. 3.2 and Figure. 3.3, these are mainly because the closed-form analytical expressions for outage probability are approximated using moment generating function.

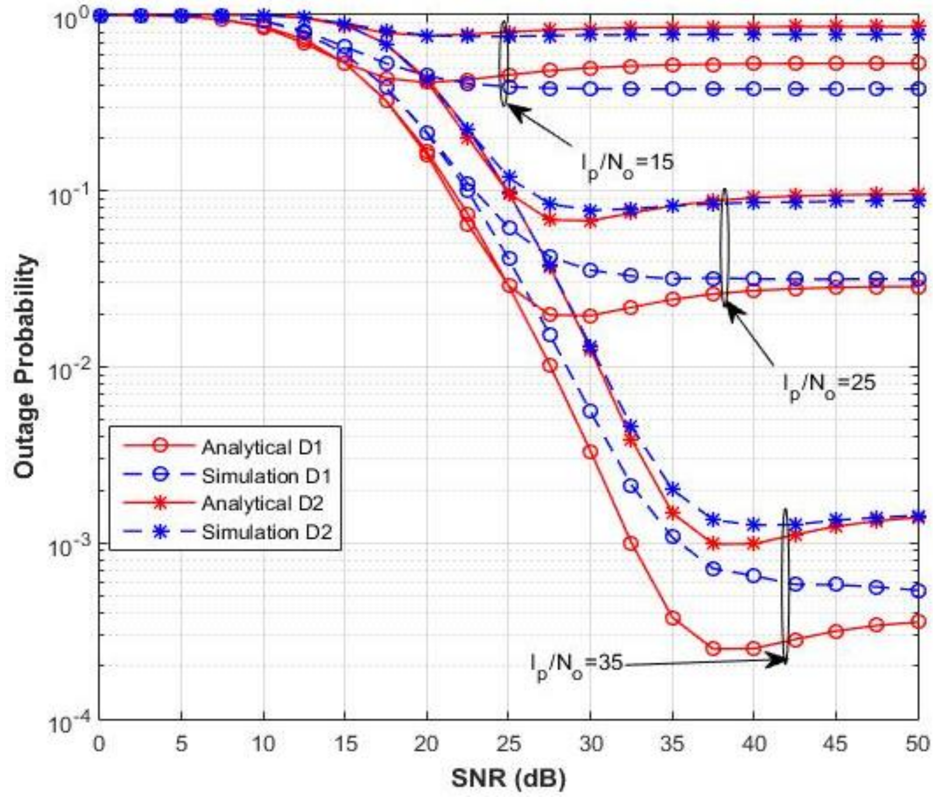

Figure 3.2 Outage probability of D_1 and D_2 versus γ_P for $\gamma_I = 15, 25$ and 35 dB.

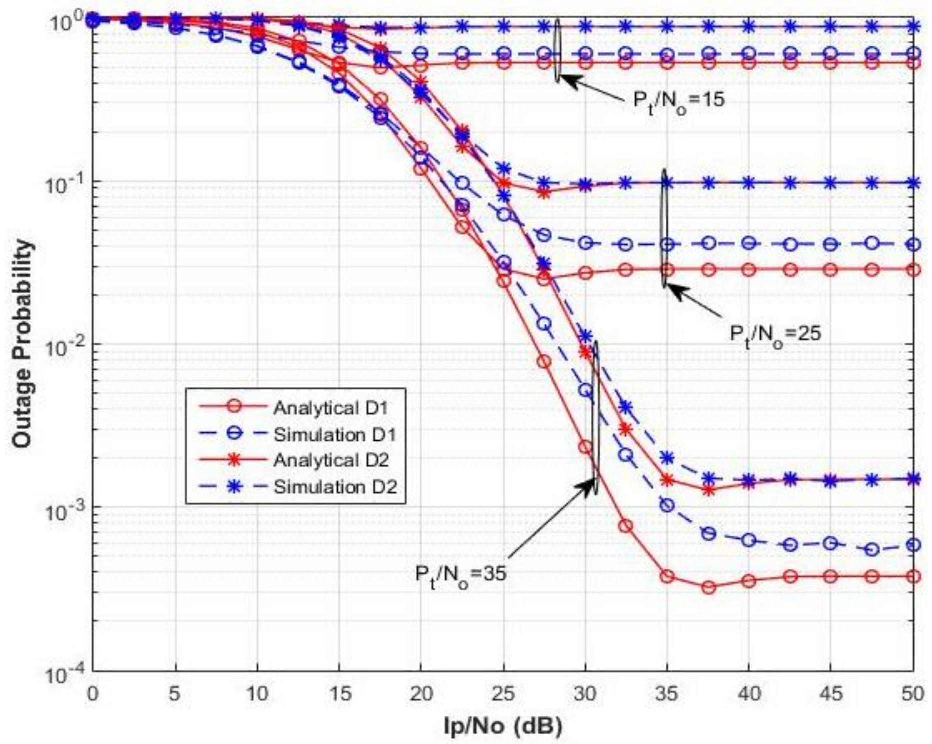

Figure 3.3 Outage probability of D_1 and D_2 versus γ_I for $\gamma_P = 15, 25$ and 35 dB.

To show the impact of the number of relays, Figure 3.4 considers a scenario where we vary the amount of DF relays with fixed interference power while maximum allowable transmit power for secondary nodes increases. The results show that the outage performance improves significantly when we change the number of relays from one to two. It is essential also to note that there is a continual improvement when we increase to three relays even though the difference is not very significant. This result implies that for a NOMA system in a cognitive radio network, increasing the number of relays results in outage performance improvement but employing a high number of relays is relatively insignificant in the improvement of outage performance.

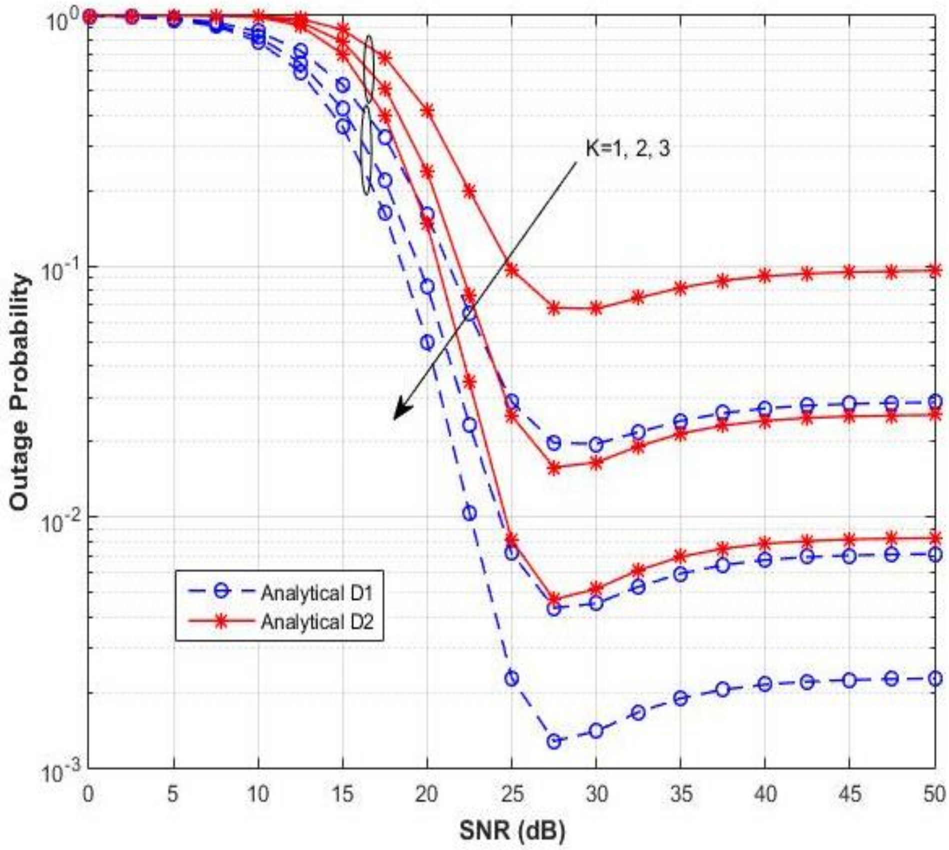

Figure 3.4 Outage probability of $D_1$and D_2 versus γ_P (SNR) with different number of DF relays (K=1, 2 and 3) when $\gamma_I = 25$ dB.

Figure 3.5 refers to a case where we include or exclude the secondary relay-to-destination link for D_2 with a fixed interference power and varying the maximum allowable transmit power of secondary nodes. Results indicate that excluding the $R_k \rightarrow D_2$ link results in higher outage probability implying poor system performance. It justifies why our model incorporates both a direct link and a relaying link to transmit to the two destinations. Given these results, it is essential to note that using D_2 as a relaying NOMA user results in poor performance on D_2 as it will be receiving it is signal direct from the secondary source only.

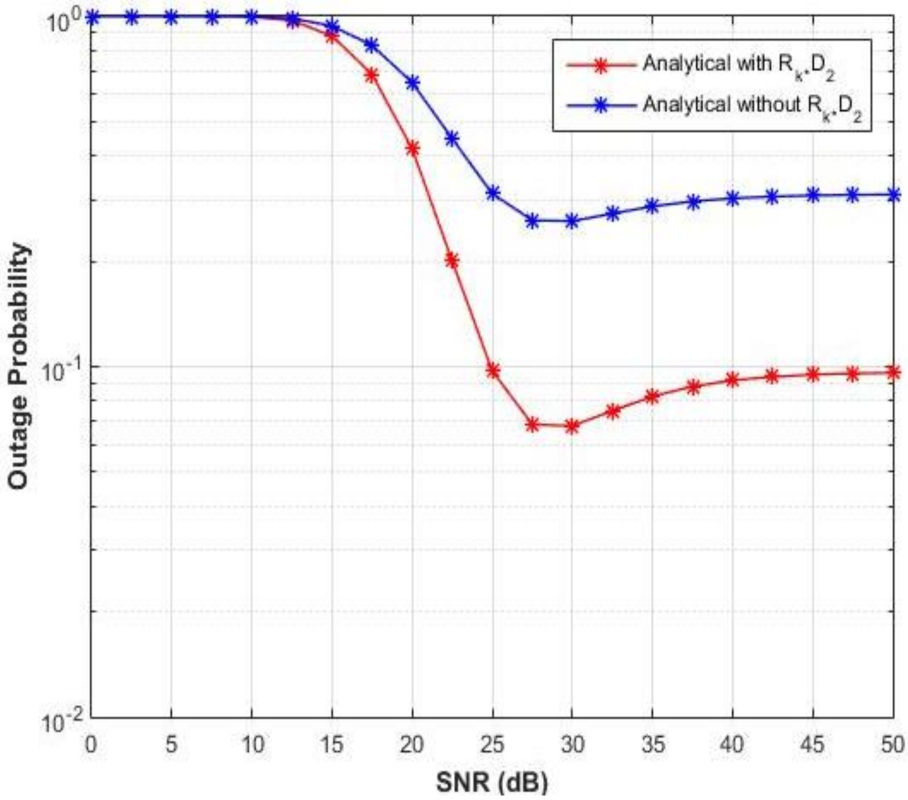

Figure 3.5 Outage probability of D_2 versus γ_P (SNR) with and without $R_k \rightarrow D_2$ link, when $\gamma_I = 25$ dB.

In Figure 3.6, we consider a case where the relay is a cooperative NOMA user such that it does SIC before forwarding the signal to D_1. In this case, it means the received signal no longer includes interference from the user D_2, as shown in [23], the outage probability decreases because there is no interference from the stronger destination. This result indicates that using D_2 as a relaying NOMA user will lower its outage performance but in turn improve the performance of D_1.

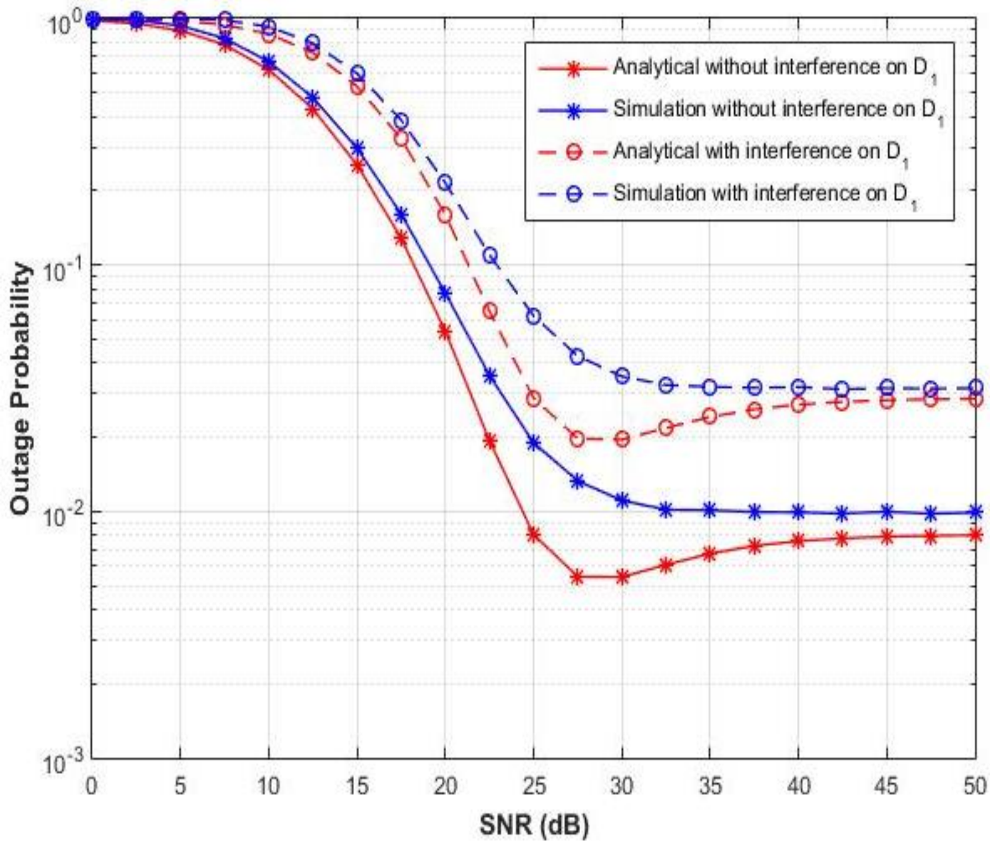

Figure 3.6 Outage probability of D_1 versus γ_P (after SIC assuming D_2 is a cooperative NOMA user and when D_2 signal is treated as interference) with $\gamma_I =$ 25 dB.

3.5 Conclusion

In this chapter, we presented a NOMA network in a cooperative spectrum-sharing network with partial DF relay selection under interference power constraints. Closed-form expressions of the outage probabilities of both destination nodes were derived. Monte Carlo simulations were provided to corroborate the proposed mathematical derivations. There is a small difference between the simulated and analytical results which is due to the use of the Jensen's inequality. It was concluded that the outage probabilities of the two secondary destinations improved significantly with an increasing number of relay nodes. Furthermore, results showed that for a fixed interference power, the outage probability decreases as the average SNR or maximum allowable transmit power of the secondary source increases. However, this decrease had an error floor which is dependent on the interference power constraint.

Chapter 4 Underlay Spectrum Sharing NOMA network with Imperfect SIC

4.1 Introduction

This chapter investigates the performance of a cooperative non-orthogonal multiple access (NOMA) cognitive network with imperfect successive interference cancellation (SIC) under Rayleigh fading conditions. We consider an underlay cognitive network that consists of a primary transmitter-receiver pair and a secondary system where a source node communicates with two destinations nodes directly and directly through a relay node selected from a set of decode-and-forward (DF) relays. SIC receivers face several challenges, for instance, the decoding time increases as the number of users grow, and a sophisticated power control mechanism is needed to differentiate the users successfully [74]. The receiver needs to accurately estimate the amplitude and phase of each user, this is vital in imitating the information waveforms of each user at the receiver for further subtraction [75]. Based on these factors, perfect SIC is not always possible in realistic scenarios which is why we investigate NOMA under imperfect SIC.

A partial relay selection scheme is implemented to determine the best relay used for the source transmissions. For this analytical framework, we derive closed-form analytical expressions for the outage probabilities at the two destinations. Moreover, to simplify the analysis and to provide further insights into the impact of key system parameters, asymptotic studies of the outage probabilities are carried out. To this end, we focus on two cases: a) the maximum allowable transmit power of the secondary network grows sufficiently large; b) the interference power approaches infinity. Finally, Monte Carlo simulations are provided to assess the accuracy of the proposed mathematical framework.

4.2 System Model

Motivated by [73], we consider an underlay cognitive radio network which consists of a primary source-primary destination pair denoted by *PS* and *PU*, respectively, and a downlink cooperative NOMA wireless scheme with a secondary source *S*, a set of secondary *J* relays denoted by R_j, where $j = 1, \ldots, J$, and two secondary destination nodes, U_1 and U_2 as illustrated in Fig. 4.1. We assume that all links undergo frequency non-selective Rayleigh block fading and all the nodes are equipped with a single antenna.

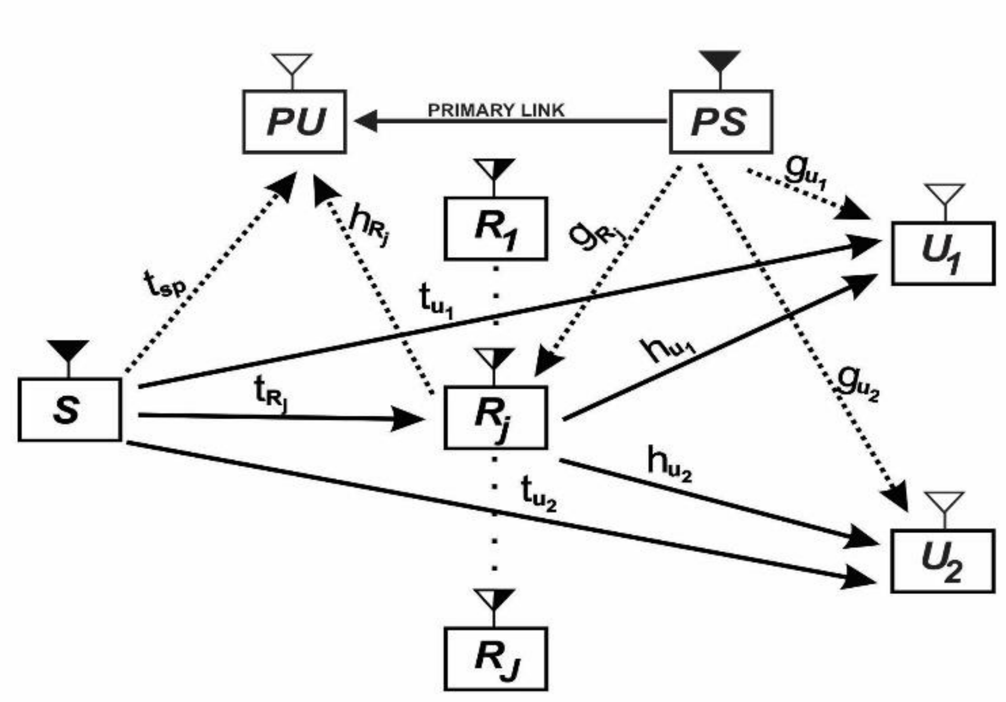

Figure 4.1 Illustration of an underlay spectrum-sharing network with downlink cooperative NOMA.

The secondary transmissions are divided into two-time slots. In the first time slot, *S* transmits the signal $v = \sqrt{\delta_1 P_S} v_1 + \sqrt{\delta_2 P_S} v_2$, to the two secondary destinations U_1 and U_2, and all the relay nodes R_j, where δ_1 andδ_2 are the power allocation coefficients for U_1 and U_2, respectively, with $\delta_1 + \delta_2 = 1$ and $\delta_1 < \delta_2$, the transmit power P_S of the secondary source is given by

$$P_S = \min\left(P, \frac{I_p}{\left|t_{s_p}\right|^2}\right), \tag{4.1}$$

where I_p is the interference temperature limit, P represents the maximum allowable transmit power at the source node, and t_{s_p} is the complex channel fading coefficient between S and PU. The received signal at the relay node is given by

$$y_{R_j} = t_{R_j}\left(\sqrt{\delta_1 P_S} v_1 + \sqrt{\delta_2 P_S} v_2\right) + \sqrt{P_P} g_{R_j} v' + n_{R_j}, \tag{4.2}$$

Where v_1 and v_2 are the messages for U_1 and U_2, respectively. In Figure 4.1, complex channel fading exponentially distributed coefficients are denoted by $A_X \sim \mathcal{CN}\left(0, \Omega_{A_X}\right)$, with $\{A_X\} \in \left\{t_{s_p}, t_{U_1}, t_{U_2}, t_{R_j}, g_{U_1}, g_{U_2}, g_{R_j}, , h_{U_1}, h_{U_2}, h_{R_j}\right\}$The noise at the secondary users U_1 and U_2, and at the relay nodes R_j are denoted by additive white Gaussian noise (AWGN) with mean zero and variance $\mathcal{N}_0$. v' is the transmitted signal from the primary network and P_P is transmit power of the primary source. The received signals at U_1 and U_2 are given respectively by

$$y_{U_1} = t_{U_1} v + \sqrt{P_P} g_{U_1} v' + n_{U_1}, \tag{4.3}$$

$$y_{U_2} = t_{U_2} v + \sqrt{P_P} g_{U_2} v' + n_{U_2}. \tag{4.4}$$

Using (4.2), the received instantaneous signal-to-interference-plus-noise ratio (SINR) used to decode v_1 is given by

$$\gamma_{R_{j1}} = \frac{\delta_1 \gamma_1}{\delta_2 \gamma_1 + \gamma_2 + 1}, \tag{4.5}$$

where $\gamma_1 = \min\left(\frac{P}{\mathcal{N}_0}, \left(\frac{I_p}{\mathcal{N}_0}\right) / \left|t_{s_p}\right|^2\right) \left|t_{R_j}\right|^2$ and$\gamma_2 = \left(\frac{P}{\mathcal{N}_0}\right) \left|g_{R_j}\right|^2$. Similarly, with the aid of (4.3), the received instantaneous SINR at U_1 to decode v_1 is given by

$$\gamma_{U_1}^{v_1} = \frac{\delta_1 \gamma_3}{\delta_2 \gamma_3 + \gamma_4 + 1}, \quad (4.6)$$

where $\gamma_3 = \min\left(\frac{P}{\mathcal{N}_0}\ ,\left(\frac{I_p}{\mathcal{N}_0}\right)/\left|t_{s_p}\right|^2\right)\left|t_{U_1}\right|^2$and $\gamma_4 = \left(\frac{P}{\mathcal{N}_0}\right)\left|g_{U_1}\right|^2$ with the aid of (4.4), the received SNR at U_2 used to detect v_1 is given by

$$\gamma_{U_2}^{v_1} = \frac{\delta_1 \gamma_5}{\delta_2 \gamma_5 + \gamma_6 + 1}, \quad (4.7)$$

Where $\gamma_5 = \min\left(\frac{P}{\mathcal{N}_0}\ ,\left(\frac{I_p}{\mathcal{N}_0}\right)/\left|t_{s_p}\right|^2\right)\left|t_{U_2}\right|^2and\gamma_6 = \left(\frac{P}{\mathcal{N}_0}\right)\left|g_{U_2}\right|^2$. Both R_j and U_2 decode the symbol v_2 by cancelling v_1 using SIC. It is assumed that the SIC performed at R_j and at U_2 for receiving v_2 is imperfect, and the resulting SINRs are expressed respectively as

$$\gamma_{R_{j2}} = \frac{\delta_2 \gamma_1}{\delta_2 \gamma_{1\_1} + \gamma_2 + 1}, \quad (4.8)$$

$$\gamma_{U_2}^{v_2} = \frac{\delta_2 \gamma_5}{\delta_1 \gamma_{5\_1} + \gamma_6 + 1}. \quad (4.9)$$

In (4.9), we define $\gamma_{5\_1} = \min\left(\frac{P}{\mathcal{N}_0}\ ,\left(\frac{I_p}{\mathcal{N}_0}\right)/\left|t_{s_p}\right|^2\right)\left|t_{U_{2\_1}}\right|^2$, $t_{U_{2\_1}} \sim \mathcal{CN}\left(0, \zeta_{2\_1}\Omega_{t_{U_2}}\right)$ and the variable ζ_{2_1} denotes the level of residual interference from imperfect SIC with $0 \leq \zeta_{2\_1} \leq 1$, $\gamma_{1\_1} = \min\left(\frac{P}{\mathcal{N}_0}\ ,\left(\frac{I_p}{\mathcal{N}_0}\right)/\left|t_{s_p}\right|^2\right)\left|t_{R_{j\_1}}\right|^2$, where $t_{R_{j\_1}} \sim \mathcal{CN}\left(0, \zeta_{j\_1}\Omega_{t_{R_j}}\right)$ and variable $0 \leq \zeta_{j\_1} \leq 1$. We also assume for simplicity that $\zeta_{j_1}$is some residual interference from imperfect SIC.[1*]

[1*]The SIC error used in this model follows a Gaussian distribution as in [22]. The assumption made in (4.9) is such that when $\zeta_{2\_1} = 1$ then we have 100% SIC error and when $\zeta_{2\_1} = 0$, perfect SIC occurred.

In the second time slot, a single relay selected from a set of J relay nodes decodes and transmits the source message with $P_{R_j} = \min\left(P, I_p/\left|h_{R_j}\right|^2\right)$. As aforementioned, a PRS scheme is used to select the best relay according to the following criterion

$$j^* = \arg \max_{j=1\ldots\ldots J} \left\{\gamma_{SR_j}\right\}, \tag{4.10}$$

where γ_{SR_j} is the average SNR of the jth relay. The received signals to interference at both U_1 and U_2, forwarded by R_j in the second phase are given respectively by

$$y_{U_1}^{R_j} = h_{U_1} v_{R_j} + \sqrt{P_P} g_{U_1} v'' + n_{U_1}^{R_j}, \tag{4.11}$$

$$y_{U_2}^{R_j} = h_{U_2} v_{R_j} + \sqrt{P_P} g_{U_2} v'' + n_{U_2}^{R_j}, \tag{4.12}$$

where v'', is the transmitted signal from PS in the second time slot and $v_{R_j} = \sqrt{b_1 P_{R_j}} \breve{v_1} + \sqrt{b_2 P_{R_j}} \breve{v_2}$ is the transmitted signal from the selected relay node assuming $b_1 = \delta_1$ and $b_2 = \delta_2$.

In the second time slot, the best relay transmits the re-encoded information to the two secondary destination nodes. Using (4.11), the instantaneous SINR at U_1 to decode $\breve{v_1}$ is given by

$$\gamma_{R_j U_1}^{\breve{v_1}} = \frac{b_1 \gamma_7}{b_2 \gamma_7 + \gamma_4 + 1}, \tag{4.13}$$

where $\gamma_7 = \min\left(\frac{P}{\mathcal{N}_0}, \left(\frac{I_p}{\mathcal{N}_0}\right) / \left|h_{R_j}\right|^2\right) \left|h_{U_1}\right|^2$. Using the same approach to obtain (4.9), the received instantaneous SINRs at U_2 to detect $\breve{v_1}$ and $\breve{v_2}$ are given respectively by

$$\gamma_{R_j U_2}^{\breve{v_1}} = \frac{b_1 \gamma_8}{b_2 \gamma_8 + \gamma_6 + 1}, \tag{4.14}$$

$$\gamma_{R_j U_2}^{\breve{v_2}} = \frac{b_2 \gamma_8}{b_1 \gamma_{8\_1} + \gamma_6 + 1}, \tag{4.15}$$

where $\gamma_{8\_1} = \min\left(\mathrm{P}/\mathcal{N}_0, \left(\frac{I_p}{\mathcal{N}_0}\right)/\left|h_{R_j}\right|^2\right)\left|h_{U_{2\_1}}\right|^2$ for $h_{U_{2\_1}} \sim \mathcal{CN}(0, \zeta_{j\_2}\Omega_{h_{U_{2\_1}}})$ with the range of SIC error being $0 \leq \zeta_{j\_1} \leq 1$ and $\gamma_8 = \min\left(P/\mathcal{N}_0, \left(\frac{I_p}{\mathcal{N}_0}\right)/\left|h_{R_j}\right|^2\right)\left|h_{U_2}\right|^2$

Based on selection combining (SC), the received instantaneous SINR at U_1 and U_2 are given respectively by

$$\gamma_{U_1} = \max\left(\gamma_{U_1}^{v_1}, \gamma_{R_jU_1}^{\breve{v}_1}\right), \tag{4.16}$$

$$\gamma_{U_2} = \max\left(\gamma_{U_2}^{v_2}, \gamma_{R_jU_2}^{\breve{v}_2}\right). \tag{4.17}$$

4.3 Outage Probability Analysis

In this section, due to mathematical tractability, we investigate the approximate outage performance of the underlying scheme taking into account the imperfectness of the SIC. To this end, we derive the outage probabilities at both destination nodes. Before delving into that, we first define the outage probability as the probability that the received SINR falls below a preset threshold, γ_{th}. Here, it is assumed that both destination nodes U_1 and U_2 have equal outage threshold $\gamma_{\mathrm{th}} = 2^{2R_{\mathrm{th}}} - 1$, where R_{th} denotes the target transmission rate. It is worthwhile noting that the proposed approach applies to the case where both U_1 and U_2 have unequal outage thresholds.

4.3.1 Outage Probability at U_1

In this proposed system, an outage occurs when U_1 fails to detect v_1 or $\breve{v}_1$ from the received signals through the direct link and the indirect link (via the relay node), respectively. Based on the above definition, the outage probability can be expressed mathematically as

$$OP_{U_1} = \Pr\left(\gamma_{U_1} \leq \gamma_{\mathrm{th}}\right), \tag{4.18}$$

where Pr(x) denotes the probability of x. With the help of (4.15), (4.18) is given in terms of the cumulative distribution functions (CDFs) of the random variables (RVs) $\gamma_{U_1}^{v_1}$ and $\gamma_{R_jU_1}^{\widetilde{v_1}}$ as

$$OP_{U_1} = F_{\gamma_{U_1}^{v_1}}(\gamma_{\text{th}})F_{\gamma_{R_jU_1}^{\widetilde{v_1}}}(\gamma_{\text{th}}). \tag{4.19}$$

The expressions of the CDFs in (4.19) can be expanded using the law of total probability, and the resulting expression of the outage probability is given by OP_{U_1}

$$\begin{aligned} OP_{U_1} = &\left[\Pr\left(\frac{\left(\mu_1/\left|t_{s_p}\right|^2\right)\left|t_{U_1}\right|^2}{\left(\mu_2/\left|t_{s_p}\right|^2\right)\left|t_{U_1}\right|^2+\left|g_{U_1}\right|^2\gamma_P+1}\leq\gamma_{\text{th}},\frac{\gamma_I}{\left|t_{s_p}\right|^2}\leq\gamma_0\right)\right.\\ &\left.+\Pr\left(\frac{\left|h_{U_1}\right|^2\delta_1\gamma_0}{\left|h_{U_1}\right|^2\delta_2\gamma_0+\left|g_{U_1}\right|^2\gamma_P+1}\leq\gamma_{\text{th}},\frac{\gamma_I}{\left|t_{s_p}\right|^2}\geq\gamma_0\right)\right]\\ &\times\left[\Pr\left(\frac{\left(\alpha_1/\left|h_{R_j}\right|^2\right)\left|h_{U_1}\right|^2}{\left(\alpha_2/\left|h_{R_j}\right|^2\right)\left|h_{U_1}\right|^2+\left|g_{U_1}\right|^2\gamma_P+1}\leq\gamma_{\text{th}},\left|h_{R_j}\right|^2\geq\frac{\gamma_I}{\gamma_P}\right)\right.\\ &\left.+\Pr\left(\frac{\left|h_{U_1}\right|^2b_1}{\left|h_{U_1}\right|^2b_2+\left|g_{U_1}\right|^2\gamma_2+1}\leq\gamma_{\text{th}},\frac{\gamma_I}{\left|h_{h_{R_j}}\right|^2}\geq\gamma_P\right)\right] \end{aligned} \tag{4.20}$$

where $\gamma_P = \frac{P_P}{\mathcal{N}_0}\,\gamma_I=\frac{I_p}{\mathcal{N}_0},\gamma_0 = \frac{P}{\mathcal{N}_0},\ \alpha_i = b_i\gamma_I$ and $\mu_i = \delta_i\gamma_I$ for $i \in \{1,2\}$.

In what follows, we evaluate the CDF $F_{\gamma_{U_1}^{v_1}}(\gamma_{\text{th}})$. Before that, we rewrite the expression of $F_{\gamma_{U_1}^{v_1}}(\gamma_{\text{th}})$ as

$$F_{\gamma_{U_1}^{v_1}}(\gamma_{\text{th}}) = \left[\Pr\left(\frac{\left(\mu_1/\left|t_{s_p}\right|^2\right)\left|t_{U_1}\right|^2}{\left(\mu_2/\left|t_{s_p}\right|^2\right)\left|t_{U_1}\right|^2 + \left|g_{U_1}\right|^2\gamma_P + 1} \leq \gamma_{\text{th}}, \frac{\gamma_I}{\left|t_{s_p}\right|^2} \leq \gamma_0\right)\right.$$

$$\left. +\Pr\left(\frac{\left|t_{U_1}\right|^2\delta_1\gamma_0}{\left|t_{U_1}\right|^2\delta_2\gamma_0 + \left|g_{U_1}\right|^2\gamma_P + 1} \leq \gamma_{\text{th}}, \frac{\gamma_I}{\left|t_{s_p}\right|^2} \geq \gamma_0\right)\right]$$

. (4.21)

To derive the analytical expression of (4.21), we separate (for the sake of clarity) it into two expressions, D_1 and D_2, such that

$$D_1 = \Pr\left(\frac{\left(\mu_1/\left|t_{s_p}\right|^2\right)\left|t_{U_1}\right|^2}{\left(\mu_2/\left|t_{s_p}\right|^2\right)\left|t_{U_1}\right|^2+\left|g_{U_1}\right|^2\gamma_P+1} \leq \gamma_{\text{th}}, \frac{\gamma_I}{\left|t_{s_p}\right|^2} \leq \gamma_0\right) \tag{4.22}$$

$$D_2 = \Pr\left(\frac{\left|t_{U_1}\right|^2\delta_1\gamma_0}{\left|t_{U_1}\right|^2\delta_2\gamma_0 + \left|g_{U_1}\right|^2\gamma_P + 1} \leq \gamma_{\text{th}}, \frac{\gamma_I}{\left|t_{s_p}\right|^2} \geq \gamma_0\right). \tag{4.23}$$

Using the approach as in Appendix 1, the analytical expression for the approximation of D_1 yields

$$D_1 \cong \beth_1\left[1 - \left[\left(1 + \frac{\gamma_{\text{th}}\gamma_P\Omega_{t_{SP}}\Omega_{g_{U_1}}}{\Delta_1\Omega_{t_{U_1}}}\right)^{-1}\left(1 + \frac{\gamma_{th}\Omega_{t_{SP}}}{\Delta_1\Omega_{t_{U_1}}}\right)^{-1}\right]\right], \tag{4.24}$$

where $\beth_1 = e^{-\frac{\gamma_I}{\gamma_0\Omega_{t_{SP}}}}$ and $\Delta_1 = \mu_1 - \mu_2\gamma_{\text{th}}$. Based on the same approach, D_2 can be approximated by

$$D_2 \cong (1 - \beth_1)\left[1 - \left[\left(1 + \frac{\gamma_{th}\gamma_P\Omega_{g_{U_1}}}{\Delta_2\Omega_{t_{U_1}}}\right)^{-1} e^{-\frac{\gamma_{th}}{\Delta_2\Omega_{t_{U_1}}}}\right]\right]. \tag{4.25}$$

To derive the analytical expression of $F_{\gamma_{R_jU_1}^{\widetilde{v_1}}}(\gamma_{\text{th}})$, we also separate it into two expressions, E_1 and E_2, such that $F_{\gamma_{R_jU_1}^{\widetilde{v_1}}}(\gamma_{\text{th}}) = E_1 + E_2$ where

$$E_1 = \Pr\left(\frac{\left(\alpha_1/\left|h_{R_j}\right|^2\right)\left|h_{U_1}\right|^2}{\left(\alpha_2/\left|h_{R_j}\right|^2\right)\left|h_{U_1}\right|^2+\left|g_{U_1}\right|^2\gamma_P+1} \le \gamma_{\text{th}}, \left|h_{R_j}\right|^2 \ge \frac{\gamma_I}{\gamma_P}\right), \tag{4.26}$$

$$E_2 = \Pr\left(\frac{\left|h_{U_1}\right|^2 b_1}{\left|h_{U_1}\right|^2 b_2 + \left|g_{U_1}\right|^2\gamma_2+1} \le \gamma_{\text{th}}, \frac{\gamma_I}{\left|h_{h_{R_j}}\right|^2} \ge \gamma_P\right). \tag{4.27}$$

Similarly, using the same method as shown in Appendix 1, we derive an analytical expression of E_1 which is given by

$$E_1 \cong \left[1 - \sum_{m=1}^{J}\binom{J}{m}(-1)^{m-1}\left[\left(1+\frac{m\gamma_{\text{th}}\gamma_P\Omega_{h_{R_j}}\Omega_{g_{U_1}}}{\phi_1\Omega_{h_{U_1}}}\right)^{-1}\left(1+\frac{m\gamma_{\text{th}}\Omega_{h_{R_j}}}{\phi_1\Omega_{h_{U_1}}}\right)^{-1}\right]\right]\beth_2, \tag{4.28}$$

where $\beth_2 = e^{-\frac{\gamma_I}{\gamma_0\Omega_{h_{R_j}}}}$ and $\phi_1 = \alpha_1 - \alpha_2\gamma_{\text{th}}$. Similarly, the analytical expression of the approximation of E_2 can be obtained and expressed as

$$E_2 \cong (1-\beth_2)\left[1 - \sum_{n=1}^{J}\binom{J}{n}(-1)^{n-1}\left[\left(1+\frac{n\gamma_{\text{th}}\gamma_P\Omega_{g_{U_1}}}{\phi_2\Omega_{h_{U_1}}}\right)^{-1} e^{-\frac{\gamma_{\text{th}}}{\phi_2\Omega_{h_{U_1}}}}\right]\right], \tag{4.29}$$

where $\phi_2 = b_1\gamma_0 - b_2\gamma_0\gamma_{\text{th}}$. Substituting the derived expressions into (4.19) gives the analytical expression for the approximate outage probability of U_1 as shown (4.30).

$$OP_{U_1} = \left[\left[1 - \sum_{m=1}^{J} \binom{J}{m} (-1)^{m-1} \left[\left(1 + \frac{m\gamma_{\text{th}}\gamma_P \Omega_{h_{R_j}} \Omega_{g_{U_1}}}{\phi_1 \Omega_{h_{U_1}}}\right)^{-1} \left(1 + \frac{m\gamma_{\text{th}} \Omega_{h_{R_j}}}{\phi_1 \Omega_{h_{U_1}}}\right)^{-1}\right]\right] \beth_2\right.$$

$$\left. +(1-\beth_2)\left[1 - \sum_{n=1}^{J} \binom{J}{n} (-1)^{n-1} \left[\left(1 + \frac{n\gamma_{\text{th}}\gamma_P \Omega_{g_{U_1}}}{\phi_2 \Omega_{h_{U_1}}}\right)^{-1} e^{-\frac{\gamma_{\text{th}}}{\phi_2 \Omega_{h_{U_1}}}}\right]\right]\right]$$

$$\left[\beth_1 \left[1 - \left[\left(1 + \frac{\gamma_{\text{th}}\gamma_P \Omega_{t_{SP}} \Omega_{g_{U_1}}}{\Delta_1 \Omega_{t_{U_1}}}\right)^{-1} \left(1 + \frac{\gamma_{th} \Omega_{t_{SP}}}{\Delta_1 \Omega_{t_{U_1}}}\right)^{-1}\right]\right]\right.$$

$$\left. +(1-\beth_1)\left[1 - \left[\left(1 + \frac{\gamma_{th}\gamma_P \Omega_{g_{U_1}}}{\Delta_2 \Omega_{t_{U_1}}}\right)^{-1} e^{-\frac{\gamma_{th}}{\Delta_2 \Omega_{t_{U_1}}}}\right]\right]\right] \quad (4.30)$$

4.3.2 Outage Probability at U_2

An outage event occurs at U_2 under two scenarios: 1) when U_2 can detect v_1 successfully but fails to detect its signal v_2; 2) when D_2 fails to detect v_1 due to high interference from the primary network. Based on NOMA and SIC, U_2 should decode v_1, subtract it and then decode its intended signal v_2. Hence, the outage probability at U_2 is given by

$$OP_{U_2} = \Pr\left(\gamma_{U_2} \le \gamma_{\text{th}}\right). \quad (4.31)$$

Using (4.16), the expression in (4.30) can further be expressed as

$$OP_{U_2} = F_{\gamma_{U_2}^{v_2}}(\gamma_{\text{th}}) F_{\gamma_{R_j U_2}^{\widetilde{v_2}}}(\gamma_{\text{th}}), \quad (4.32)$$

Where $F_{\gamma_{U_2}^{v_2}}(\gamma_{\text{th}})$ and $F_{\gamma_{R_j U_2}^{\widetilde{v_2}}}(\gamma_{\text{th}})$ are given by (4.33) and (4.34) respectively

$$F_{\gamma_{U_2}^{v_2}}(\gamma_{\text{th}}) = \left[\Pr\left(\frac{\delta_2\gamma_5}{\delta_1\gamma_{5\_1} + \gamma_6 + 1} \le \gamma_{\text{th}}, \frac{\delta_1\gamma_5}{\delta_2\gamma_5 + \gamma_6 + 1} >\right) + \Pr\left(\frac{\delta_1\gamma_5}{\delta_2\gamma_5 + \gamma_6 + 1} \le \gamma_{\text{th}}\right)\right], \quad (4.33)$$

$$F_{\gamma_{R_jU_2}^{\widetilde{v2}}}(\gamma_{\text{th}}) = \left[\Pr\left(\frac{b_2\gamma_8}{b_1\gamma_{8\_1}+\gamma_6+1} \le \gamma_{\text{th}}, \frac{b_1\gamma_8}{b_2\gamma_8+\gamma_6+1} > \gamma_{\text{th}}\right)\right.$$

$$\left. +\Pr\left(\frac{b_1\gamma_8}{b_2\gamma_8+\gamma_6+1} \le \gamma_{\text{th}}\right)\right] \quad (4.34)$$

After some mathematical manipulations and using the constraints on the transmit power of the source, (4.33) can further be expressed, as shown in (4.35).

$$F_{\gamma_{U_2}^{v2}}(\gamma_{th}) \cong \left[\left[\left(1+\frac{\gamma_{th}\gamma_P\Omega_{t_{SP}}\Omega_{g_{U_2}}}{\mu_2\Omega_{t_{U_2}}}\right)^{-1} \times \left(1+\frac{\gamma_{th}\Omega_{t_{SP}}}{\mu_2\Omega_{t_{U_2}}}\right)^{-1} \left(1+\frac{\mu_1\gamma_{th}\zeta_{2_1}\Omega_{t_{U_2}}}{\mu_2\Omega_{t_{U_2}}}\right)^{-1}\right](\beth_1)\right.$$

$$+\left[1-\left[\left(1+\frac{\gamma_{th}\gamma_P\Omega_{g_{U_2}}}{\delta_2\gamma_0\Omega_{t_{U_2}}}\right)^{-1} e^{\frac{\gamma_{th}}{\delta_2\gamma_0\Omega_{t_{U_2}}}}\left(1+\frac{\delta_1\gamma_0\gamma_{th}\zeta_{2\_1}\Omega_{t_{U_2}}}{\delta_2\gamma_0\Omega_{t_{U_2}}}\right)^{-1}\right]\right](1-\beth_1)\Bigg]$$

$$\times\left[1-\left[\left[1-\left[\left(\begin{matrix}1\\+\dfrac{\gamma_{th}\gamma_P\Omega_{t_{SP}}\Omega_{g_{U_2}}}{\Delta_1\Omega_{t_{U_2}}}\end{matrix}\right)^{-1} \times \left(1+\frac{\gamma_{th}\Omega_{t_{SP}}}{\Delta_1\Omega_{t_{U_2}}}\right)^{-1}\right]\right](\beth_1)\right.\right.$$

$$\left.\left.+\left[1-\left[\left(\begin{matrix}1+\\\dfrac{\gamma_{th}\gamma_P\Omega_{g_{U_2}}}{\Delta_2\Omega_{t_{U_2}}}\end{matrix}\right)^{-1} \times e^{-\frac{\gamma_{th}}{\Delta_2\Omega_{t_{U_2}}}}\right]\right](1-\beth_1)\right]\right]$$

$$+\left[\left[1-\left[\left(1+\frac{\gamma_{th}\gamma_P\Omega_{t_{SP}}\Omega_{g_{U_2}}}{\Delta_1\Omega_{t_{U_2}}}\right)^{-1} \times \left(1+\frac{\gamma_{th}\Omega_{t_{SP}}}{\Delta_1\Omega_{t_{U_2}}}\right)^{-1}\right]\right](\beth_1)\right.$$

$$\left.+\left[1-\left[\left(1+\frac{\gamma_{th}\gamma_P\Omega_{g_{U_2}}}{\Delta_2\Omega_{t_{U_2}}}\right)^{-1} \times e^{-\frac{\gamma_{th}}{\Delta_2\Omega_{t_{U_2}}}}\right]\right](1-\beth_1)\right]$$

(4.35)

The analytical expression of the approximation of $F_{\gamma_{R_jU_2}^{\tilde{v}_2}}(\gamma_{\text{th}})$ is given by (4.36)

$$
\begin{aligned}
F_{\gamma_{R_jU_2}^{\tilde{v}_2}}(\gamma_{th}) = \Bigg[1 - \Bigg[\Bigg[1 - \sum_{m=1}^{J}\binom{J}{m}(-1)^{m-1}\left(1+\frac{m\gamma_{th}\Omega_{h_{R_j}}}{\phi_1\Omega_{h_{U_2}}}\right)^{-1}\left(1+\frac{m\gamma_{th}\gamma_P\Omega_{h_{R_j}}\Omega_{g_{U_2}}}{\phi_1\Omega_{h_{U_2}}}\right)^{-1}\Bigg](\beth_2) \\
+\Bigg[1-\sum_{n=1}^{J}\binom{J}{n}(-1)^{n-1}\Bigg[\left(1+\frac{n\gamma_{th}\gamma_P\Omega_{g_{U_2}}}{\phi_2\Omega_{h_{U_2}}}\right)^{-1}\times e^{\frac{\gamma_{th}}{\phi_2\Omega_{h_{U_2}}}}\Bigg]\Bigg](1-\beth_2\Bigg]\Bigg] \\
\Bigg[\Bigg[1-\sum_{m=1}^{J}\binom{J}{m}(-1)^{m-1}\Bigg[\left(1+\frac{m\gamma_{th}\Omega_{h_{R_j}}}{\alpha_2\Omega_{h_{U_2}}}\right)^{-1}\times\left(1+\frac{m\gamma_{th}\gamma_P\Omega_{h_{R_j}}\Omega_{g_{U_2}}}{\alpha_2\Omega_{h_{U_2}}}\right)^{-1} \\
\times\left(1+\frac{\alpha_1 m\gamma_{th}\zeta_{j1}\Omega_{h_{U_2}}}{\alpha_2\Omega_{h_{U_2}}}\right)^{-1}\Bigg]\Bigg](\beth_2) \\
+\Bigg[1-\sum_{n=1}^{J}\binom{J}{n}(-1)^{n-1}\Bigg[\left(1+\frac{n\gamma_{th}\gamma_P\Omega_{g_{U_2}}}{b_2\gamma_0\Omega_{h_{U_2}}}\right)^{-1}\times e^{-\frac{n\gamma_{th}}{b_2\gamma_0\Omega_{h_{U_2}}}} \\
\times\left(1+\frac{b_1\gamma_0 n\gamma_{th}\zeta_{j1}\Omega_{h_{U_2}}}{b_2\gamma_0\Omega_{h_{U_2}}}\right)^{-1}\Bigg]\Bigg]\times(1-\beth_2)\Bigg] \\
+\Bigg[\Bigg[1-\sum_{m=1}^{J}\binom{J}{m}(-1)^{m-1}\left(1+\frac{m\gamma_{th}\Omega_{h_{R_j}}}{\phi_1\Omega_{h_{U_2}}}\right)^{-1}\left(\frac{m\gamma_{th}\gamma_P\Omega_{h_{R_j}}\Omega_{g_{U_2}}}{\phi_1\Omega_{h_{U_2}}}\right)^{-1}\Bigg](\beth_2) \\
+\Bigg[1-\sum_{n=1}^{J}\binom{J}{n}(-1)^{n-1}\Bigg[\left(1+\frac{n\gamma_{th}\gamma_P\Omega_{g_{U_2}}}{\phi_2\Omega_{h_{U_2}}}\right)^{-1}\times e^{-\frac{\gamma_{th}}{\phi_2\Omega_{h_{U_2}}}}\Bigg]\Bigg](1-\beth_2)\Bigg]
\end{aligned}
$$

(4.36)

4.4 Asymptotic Performance Analysis

In this section, we investigate the asymptotic expressions for the outage probability of the two NOMA users. We mainly focus on two scenarios; 1) when the maximum tolerable interference power grows sufficiently large; 2) when the maximum allowable transmit power at the secondary source, and relay becomes very large.

4.4.1 Asymptotic Analysis for the scenario with $\gamma_I \to \infty$

Assuming that maximum tolerable interference power grows sufficiently large, i.e., $\gamma_I \to \infty$ the following approximations can be used:

$$\lim_{\gamma_I \to \infty} e^{-\frac{\gamma_I}{\gamma_0 \Omega_{t_{SP}}}} \simeq 0, \tag{4.37}$$

$$\lim_{\gamma_I \to \infty} e^{-\frac{\gamma_I}{\gamma_0 \Omega_{h_{R_j}}}} \simeq 0. \tag{4.38}$$

The asymptotic outage probability for U_1 when $\gamma_I \to \infty$ can be derived as

$$OP_{U_1}^{\gamma_I \to \infty} = F_{\gamma_{U_1}}^{\gamma_I \to \infty}(\gamma_{\text{th}}) F_{\gamma_{R_j U_1}}^{\gamma_I \to \infty}(\gamma_{\text{th}}), \tag{4.39}$$

where $F_{\gamma_{U_1}}^{\gamma_I \to \infty}(\gamma_{\text{th}})$ and $F_{\gamma_{R_j U_1}}^{\gamma_I \to \infty}(\gamma_{\text{th}})$ represent the CDFs for sufficiently large values of γ_I and are given respectively by

$$F_{\gamma_{U_1}}^{\gamma_I \to \infty}(\gamma_{\text{th}}) = \left[1 - \left[\left(1 + \frac{\gamma_{th}\gamma_P \Omega_{g_{U_1}}}{\Delta_2 \Omega_{t_{U_1}}}\right)^{-1} e^{-\frac{\gamma_{th}}{\Delta_2 \Omega_{t_{U_1}}}}\right]\right], \tag{4.40}$$

$$F_{\gamma_{R_j U_1}}^{\gamma_I \to \infty}(\gamma_{\text{th}}) = \left[1 - \sum_{n=1}^{J} \binom{J}{n} (-1)^{n-1} \times \left[\left(1 + \frac{n\gamma_{\text{th}}\gamma_P \Omega_{g_{U_1}}}{\phi_2 \Omega_{h_{U_1}}}\right)^{-1} e^{-\frac{\gamma_{\text{th}}}{\phi_2 \Omega_{h_{U_1}}}}\right]\right]. \tag{4.41}$$

Note that (4.40) and (4.41) are independent of γ_I since the maximum allowable transmit power will always be the minimum for high values of interference power.

For D_2, based on the approximations given in (4.37) and (4.38), the asymptotic outage probability expression when $\gamma_I \to \infty$ can be expressed as (4.42).

$$OP_{U_2}^{\gamma_I \to \infty} = F_{\gamma_{U_2}}^{\gamma_I \to \infty}(\gamma_{\text{th}}) F_{\gamma_{R_j U_2}}^{\gamma_I \to \infty}(\gamma_{\text{th}}). \tag{4.42}$$

In what follows, we derive the analytical expressions $F_{\gamma_{U_2}}^{\gamma_I \to \infty}$ and $F_{\gamma_{R_j U_2}}^{\gamma_I \to \infty}(\gamma_{\text{th}})$. The former expression is given by

$$F_{\gamma_{U_2}}^{\gamma_I \to \infty}(\gamma_{\text{th}}) = S_1^{\gamma_I \to \infty}\left(1 - S_2^{\gamma_I \to \infty}\right) + S_2^{\gamma_I \to \infty} \ . \tag{4.43}$$

It should be noted that (4.43) represents the asymptotic outage expression for (4.32) as $\gamma_I \to \infty$, where $S_1^{\gamma_I \to \infty}$ and $S_2^{\gamma_I \to \infty}$ are given below, for the sake of clarity by

$$S_1^{\gamma_I \to \infty} = \left[1 - \left[\left(1 + \frac{\gamma_{\text{th}}\gamma_P \Omega_{g_{U_2}}}{\delta_2 \gamma_0 \Omega_{t_{U_2}}}\right)^{-1} \times e^{-\frac{\gamma_{\text{th}}}{\delta_2 \gamma_0 \Omega_{t_{U_2}}}} \times \left(1 + \frac{\delta_1 \gamma_0 \gamma_{th} \zeta_{2\_1} \Omega_{t_{U_2}}}{\delta_2 \gamma_0 \Omega_{t_{U_2}}}\right)^{-1}\right]\right] \tag{4.44}$$

$$S_2^{\gamma_I \to \infty} = \left[1 - \left[\left(1 + \frac{\gamma_{\text{th}}\gamma_P \Omega_{g_{U_2}}}{\Delta_2 \Omega_{t_{U_2}}}\right)^{-1} e^{-\frac{\gamma_{\text{th}}}{\Delta_2 \Omega_{t_{U_2}}}}\right]\right]. \tag{4.45}$$

The same approach as above is used to derive an analytical expression of $F_{\gamma_{R_j U_2}}^{\gamma_I \to \infty}(\gamma_{\text{th}})$ which is given by

$$F_{\gamma_{R_j U_2}}^{\gamma_I \to \infty}(\gamma_{\text{th}}) = T_1^{\gamma_I \to \infty}\left(1 - T_2^{\gamma_I \to \infty}\right) + T_2^{\gamma_I \to \infty}, \tag{4.46}$$

where $T_1^{\gamma_I \to \infty}$ and $T_2^{\gamma_I \to \infty}$ are given respectively by (4.47) and (4.48)

$$T_1^{\gamma_I \to \infty} = \left[1 - \sum_{n=1}^{J} \binom{J}{n} (-1)^{n-1} \times \left[\left(1 + \frac{n\gamma_{\text{th}}\gamma_P \Omega_{g_{U_2}}}{b_2 \gamma_0 \Omega_{h_{U_2}}}\right)^{-1} e^{-\frac{n\gamma_{\text{th}}}{b_2 \gamma_0 \Omega_{h_{U_2}}}} \times \left(1 + \frac{b_1 \gamma_0 n \gamma_{th} \zeta_{j1} \Omega_{h_{U_2}}}{b_2 \gamma_0 \Omega_{h_{U_2}}}\right)^{-1}\right]\right] \tag{4.47}$$

$$T_2^{\gamma_I \to \infty} = \left[1 - \sum_{n=1}^{J} \binom{J}{n} (-1)^{n-1} \times \left[\left(1 + \frac{n\gamma_{\text{th}}\gamma_P \Omega_{g_{U_2}}}{\phi_2 \Omega_{h_{U_2}}}\right)^{-1} e^{-\frac{\gamma_{\text{th}}}{\phi_2 \Omega_{h_{U_2}}}}\right]\right]. \tag{4.48}$$

From (4.39) and (4.42), it can be noticed that both the derived asymptotic outage probabilities are independent of γ_I, but depend on γ_P with a probability of one. This means that after the maximum allowable transmit power is attained, the system performance cannot longer improve. Using the definition of the diversity order [24], U_1 and U_2 have diversity orders given respectively by

$$OP_{\mathrm{U}_1}^{\gamma_I\to\infty} = -\lim_{\gamma_I\to\infty} \frac{\log OP_1^{\gamma_I\to\infty}(\gamma_I)}{\log(\gamma_I)} = 0, \tag{4.49}$$

$$OP_{\mathrm{U}_2}^{\gamma_I\to\infty} = -\lim_{\gamma_I\to\infty} \frac{\log OP_2^{\gamma_I\to\infty}(\gamma_I)}{\log(\gamma_I)} = 0, \tag{4.50}$$

4.4.2 Asymptotic Analysis with $\gamma_o \to \infty$

Assuming that maximum tolerable interference power grows sufficiently large, i.e.,$\gamma_o \to \infty$, the following approximations can be used:

$$\lim_{\gamma_o\to\infty} e^{-\frac{\gamma_I}{\gamma_0 \Omega_{t_{SP}}}} \simeq 1, \tag{4.51}$$

$$\lim_{\gamma_o\to\infty} e^{-\frac{\gamma_I}{\gamma_0 \Omega_{h_{R_j}}}} \simeq 1. \tag{4.52}$$

The asymptotic outage probability for U_1 when $\gamma_o \to \infty$ can be derived as

$$OP_{\mathrm{U}_1}^{\gamma_I\to\infty} = F_{\gamma_{U_1}}^{\gamma_o\to\infty}(\gamma_{\mathrm{th}}) F_{\gamma_{R_j U_1}}^{\gamma_o\to\infty}(\gamma_{\mathrm{th}}). \tag{4.53}$$

The expressions of $F_{\gamma_{U_1}}^{\gamma_o\to\infty}(\gamma_{\mathrm{th}})$ and $F_{\gamma_{R_j U_1}}^{\gamma_o\to\infty}(\gamma_{\mathrm{th}})$ for large values of γ_o are given respectively by (4.54) and (4.55)

$$F_{\gamma_{U_1}}^{\gamma_o\to\infty}(\gamma_{\mathrm{th}}) = \left[1 - \left[\left(1 + \frac{\gamma_{\mathrm{th}}\gamma_P \Omega_{t_{SP}} \Omega_{g_{U_1}}}{\Delta_1 \Omega_{t_{U_1}}}\right)^{-1} \left(1 + \frac{\gamma_{th} \Omega_{t_{SP}}}{\Delta_1 \Omega_{t_{U_1}}}\right)^{-1}\right]\right], \tag{4.54}$$

$$F_{\gamma_{R_j U_1}}^{\gamma_o\to\infty}(\gamma_{\text{th}}) = \left[1 - \sum_{m=1}^{J}\binom{J}{m}(-1)^{m-1}\left[\left(1+ \ \frac{m\gamma_{\text{th}}\gamma_P\Omega_{h_{R_j}}\Omega_{g_{U_1}}}{\phi_1\Omega_{h_{U_1}}}\right)^{-1}\right]\right.$$

$$\left.\times\left(1+\frac{m\gamma_{\text{th}}\Omega_{h_{R_j}}}{\phi_1\Omega_{h_{U_1}}}\right)^{-1}\right], \tag{4.55}$$

Both (4.54) and (4.55) are obtained from the asymptotic outage probability of (4.20) when $\gamma_0 \to \infty$ and are independent of γ_o. The asymptotic outage probability expression for D_2 can be obtained as

$$OP_2^{\gamma_o\to\infty} = F_{\gamma_{U_2}}^{\gamma_o\to\infty}(\gamma_{\text{th}})F_{\gamma_{R_j U_2}}^{\gamma_o\to\infty}(\gamma_{\text{th}}). \tag{4.56}$$

In the sequel, we find the analytical outage expressions of $F_{\gamma_{U_2}}^{\gamma_o\to\infty}(\gamma_{\text{th}})$ and $F_{\gamma_{R_j U_2}}^{\gamma_o\to\infty}(\gamma_{\text{th}})$ when $\gamma_o \to \infty$. We start with the former, which can be expressed as

$$F_{\gamma_{U_2}}^{\gamma_o\to\infty}(\gamma_{\text{th}}) = S_1^{\gamma_o\to\infty}\left(1 - S_2^{\gamma_o\to\infty}\right) + S_2^{\gamma_o\to\infty}, \tag{4.57}$$

where $S_1^{\gamma_o\to\infty}$ and $S_2^{\gamma_o\to\infty}$ are given respectively by

$$S_1^{\gamma_o\to\infty} \cong \left[\left(1+\frac{\gamma_{th}\gamma_P\Omega_{t_{SP}}\Omega_{g_{U_2}}}{\mu_2\Omega_{t_{U_2}}}\right)^{-1}\left(1+\frac{\gamma_{th}\Omega_{t_{SP}}}{\mu_2\Omega_{t_{U_2}}}\right)^{-1}\left(1+ \ \frac{\mu_1\gamma_{th}\zeta_{2_1}\Omega_{t_{U_2}}}{\mu_2\Omega_{t_{U_2}}}\right)^{-1}\right], \tag{4.58}$$

$$S_2^{\gamma_o\to\infty} \cong \left[1 - \left[\left(1+\frac{\gamma_{\text{th}}\gamma_P\Omega_{t_{SP}}\Omega_{g_{U_2}}}{\Delta_1\Omega_{t_{U_2}}}\right)^{-1}\left(1+\frac{\gamma_{\text{th}}\Omega_{t_{SP}}}{\Delta_1\Omega_{t_{U_2}}}\right)^{-1}\right]\right]. \tag{4.59}$$

The same approach used in (4.57) is applied to derive the analytical outage expression as

$$F_{\gamma_{R_j U_2}}^{\gamma_o\to\infty}(\gamma_{\text{th}}) = T_1^{\gamma_o\to\infty}\left(1 - T_2^{\gamma_o\to\infty}\right) + T_2^{\gamma_o\to\infty}, \tag{4.60}$$

where $T_1^{\gamma_o\to\infty}$ and $T_2^{\gamma_o\to\infty}$ are given in (4.61) and (4.62).

$$T_1^{\gamma_o\to\infty} = \left[1 - \sum_{m=1}^{J}\binom{J}{m}(-1)^{m-1}\left[\left(1 + \frac{m\gamma_{\text{th}}\Omega_{h_{R_j}}}{\alpha_2\Omega_{h_{U_2}}}\right)^{-1}\right.\right.$$

$$\left.\left.\times\left(1 + \frac{m\gamma_{th}\gamma_P\Omega_{h_{R_j}}\Omega_{g_{U_2}}}{\alpha_2\Omega_{h_{U_2}}}\right)^{-1}\left(1 + \frac{\alpha_1 m\gamma_{th}\zeta_{j1}\Omega_{h_{U_2}}}{\alpha_2\Omega_{h_{U_2}}}\right)^{-1}\right]\right] \quad (4.61)$$

and

$$T_2^{\gamma_o\to\infty} = \left[1 - \sum_{m=1}^{J}\binom{J}{m}(-1)^{m-1}\left(1 + \frac{m\gamma_{\text{th}}\Omega_{h_{R_j}}}{\phi_1\Omega_{h_{U_2}}}\right)^{-1}\left(1 + \frac{m\gamma_{\text{th}}\gamma_P\Omega_{h_{R_j}}\Omega_{g_{U_2}}}{\phi_1\Omega_{h_{U_2}}}\right)^{-1}\right]. \quad (4.62)$$

The diversity order at U_1 and U_2 when $\gamma_o \to \infty$ is given respectively by

$$div_{U_1}^{\gamma_o} = -\lim_{\gamma_o\to\infty}\frac{\log OP_1^{\gamma_o\to\infty}(\gamma_o)}{\log(\gamma_o)} = 0, \quad (4.63)$$

$$div_{U_2}^{\gamma_o} = -\lim_{\gamma_o\to\infty}\frac{\log OP_2^{\gamma_o\to\infty}(\gamma_o)}{\log(\gamma_o)} = 0. \quad (4.64)$$

As γ_o grows sufficiently large, the transmit power of the secondary source and the selected relay depends on the interference power with probability one. This means we will experience error floors after a given interference power constraint.

4.5 Numerical Results and Discussions

Here, we provide Monte Carlo simulations for some scenarios to assess the accuracy of the proposed mathematical analysis. We highlight the outage and asymptotic performances of the underlying network. For simplicity and without loss of generality, it is assumed that $\delta_1 = 0.8$, $\delta_2 = 0.2$, $b_1 = 0.8$ and $b_2 = 0.2$.

Figure 4.2 shows the outage probability versus $\frac{\mathrm{I_p}}{\mathcal{N}_0}$ wherein $\xi = 0.01$, $\frac{P}{\mathcal{N}_0} = \{15, 25, 35\}$ dB. It is shown that the outage probability decreases as the interference SNR increases until error floors occur for high interference SNR values. This result shows that when we experience some error in the SIC manifested by $\xi = 0.01$, the outage probability of U_2 increases

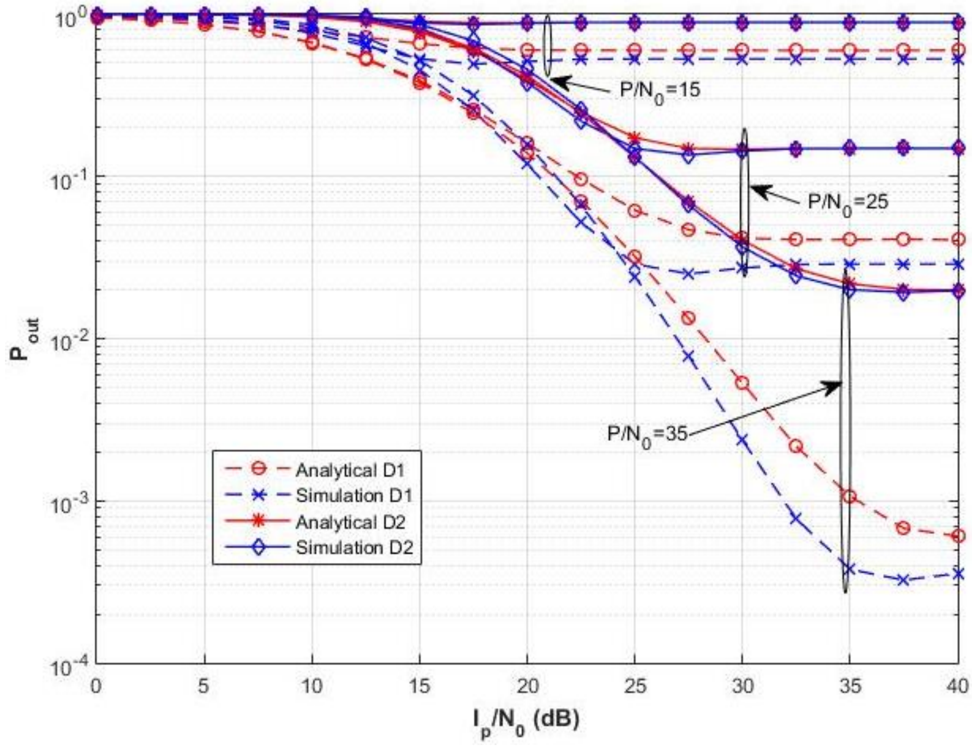

Figure 4.2 Outage probability versus interference power constraint with $\xi = 0.01$ and $\frac{I_p}{N_o} = \{15, 25, 35\}$ dB.

Figure 4.3 shows the outage probability versus the maximum allowable transmit power of the secondary network in a case where $\xi = 0.01$, $\frac{I_p}{N_o} = \{15, 25, 35\}$ dB. It is shown that the outage probability decreases as the maximum available transmit power increases, as expected error floors occur at high $\frac{P}{N_o}$ values. When we experience an error in the SIC manifested by $\xi = 0.01$, the outage probability of U_2 increases as opposed to the case of perfect SIC (as shown in [21]).

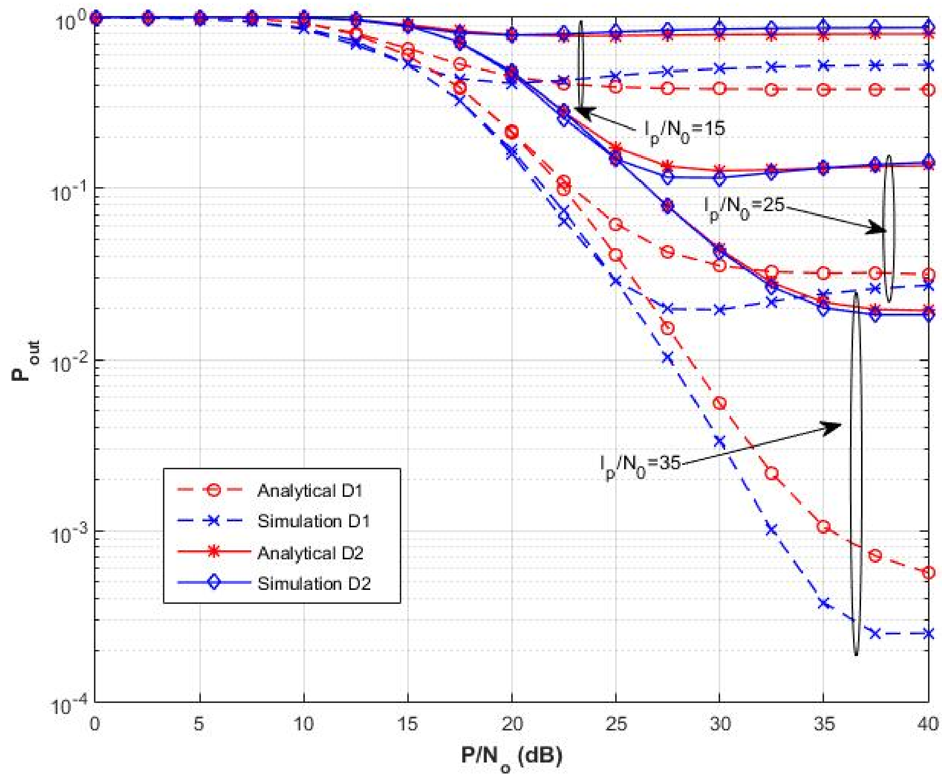

Figure 4.3 Outage probability versus maximum available transmit power with $\xi = 0.01$ and $\frac{I_p}{N_o} = \{15, 25, 35\}$ dB.

Figure 4.4 plots the outage performance versus average SNR for a various number of relays. We consider two cases: 1) perfect SIC, 2) imperfect SIC manifested in this particular setup by $\xi = 0.05$. Here, the number of relays varies from J= {1, 2, 3….}, with a fixed interference power while the maximum allowable transmit power for the secondary nodes increases. The results show that implementing a NOMA system with multiple relays improves outage performance. The set of results with SIC error also improve although the performance is not as good as in the case of perfect SIC. This result also shows that for a NOMA system, outage performance improvement is most significant for up to two relays.

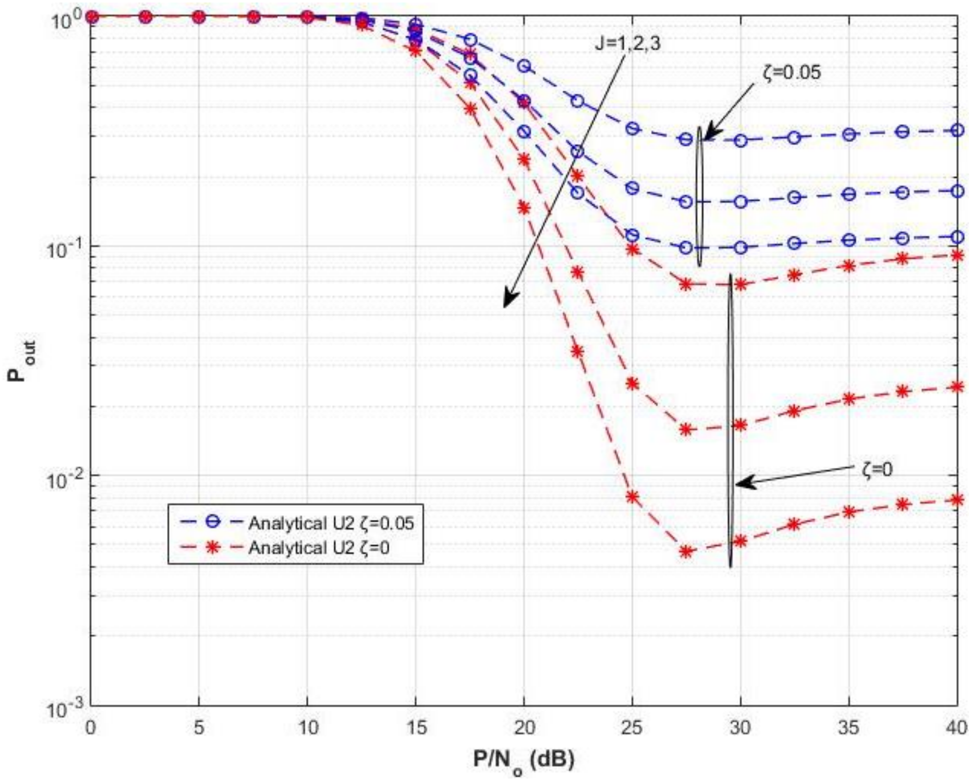

Figure 4.4 Outage probability of U_2 versus $\frac{P}{\mathcal{N}_0}$ with different number of relays, $J = \{1, 2, 3\}$ when $\gamma_I = 25$ dB and $\xi = \{0, 0.05\}$.

To investigate the impact of the relaying link on the outage performance, Figure 4.5 considers a scenario where we include or exclude the secondary relay-to-destination link for U_2 with $\gamma_I = 25$ dB and varying γ_o. Our results show that eliminating the $R_j \rightarrow U_2$ link results in reduced system outage performance. Our model performs better by incorporating both a direct link and a relaying link to transmit to the two destinations. These results show that using U_2 as a relaying NOMA user results in poor performance on U_2 due to the absence of a relaying link.

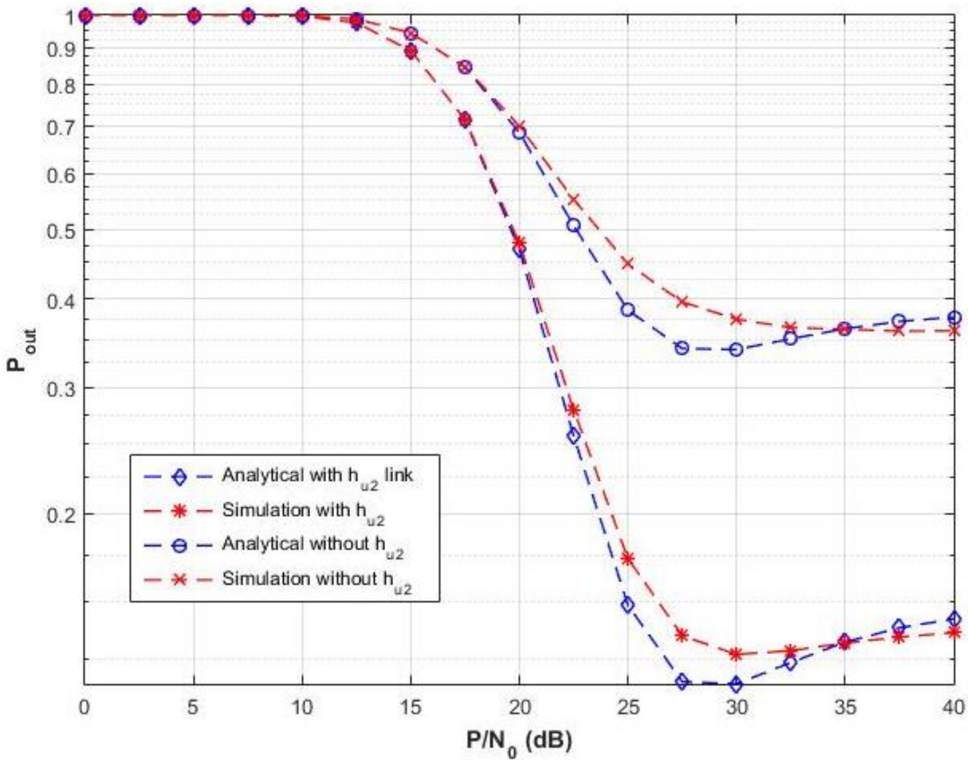

Figure 4.5 Outage probability of U_2 versus maximum allowable transmit power (SNR) in cases where the h_{U_2}link is includes and excludes, with $\gamma_I = 25$ dB.

In Figure 4.6, we consider the outage performance versus interference power for $\frac{P}{\mathcal{N}_0} = 25$dB and $\xi = 0.05$. In this case, it is shown that outage probability increases as ξ increases. Also, as expected, error floors exist for high interference power values. It is important to note that the outage performance becomes independent of interference power for high values, which justifies our asymptotic outage analysis.

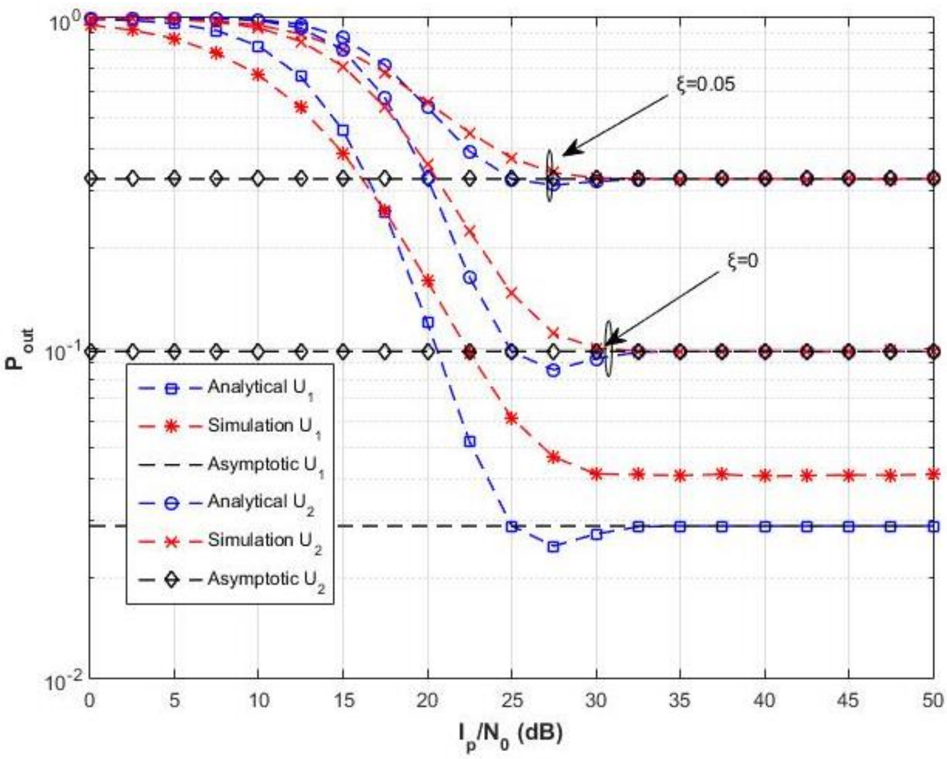

Figure 4.6 Outage probability versus interference power constraint with, $\xi = 0.05$, and $\frac{P}{\mathcal{N}_0} = 25$ dB.

Figure 4.7 shows the outage probability against maximum allowable transmit power taking $\gamma_I = 25$dB and $\xi = \{0, 0.05, 0.1\}$. Similar to Figure 4.6, the outage performance decreases as ξ increases. Error floors exist for high maximum allowable transmit power values because outage performance is now independent on the maximum allowable transmit power. The improvement in outage performance is limited, and for high values, it becomes independent of the maximum allowable transmit power which validates our asymptotic outage analysis.

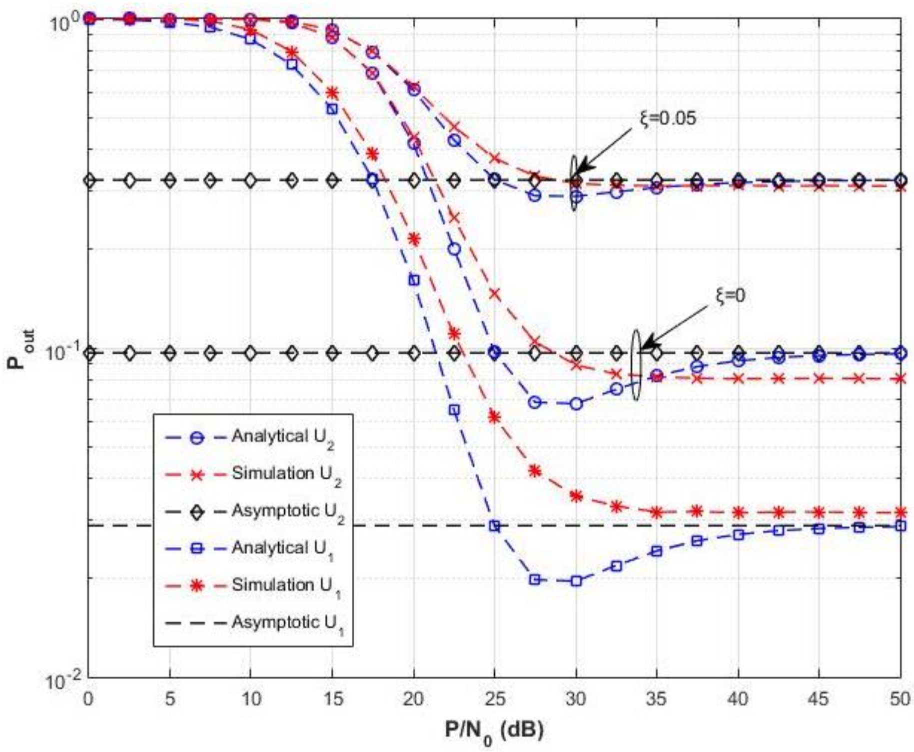

Figure 4.7 Outage probability versus maximum allowable transmit power with, $\xi = 0.05$ and $\gamma_I = 25$ dB.

4.6 Conclusions

In this work, we analyzed the performance of a NOMA system in a cooperative spectrum-sharing network with partial DF relay selection under interference power constraints assuming the presence of SIC error. We derived closed-form expressions of the outage probabilities of the secondary network destination users. Monte Carlo simulations were provided to validate our mathematical derivations. There is a small difference between the simulated and analytical results which is due to the use of the Jensen's inequality. It was shown that SIC error has a significant impact on the performance of the system. Moreover, the asymptotic analysis is provided to approximate the derive outage probabilities in for large values of interference power and the maximum tolerable transmit power.

Chapter 5 NOMA in Spectrum Sharing with Amplify and Forward Relaying

5.1 Introduction

This chapter considers NOMA in an underlay cognitive radio network with cooperative amplify and forward relaying in the secondary network. In this model, a secondary source node transmits to two destination nodes through a direct link (source-to-destination) and indirectly through an AF relay node. The transmission of the secondary network is constrained by a threshold (interference power constraint) which ensures that there is no compromise on the quality of service of the primary network.

The AF relays improve network reliability and increase the network coverage considering that the primary network constrains the transmission. The remainder of this chapter is organized as follows. In Section 5.2, the system model is described, followed by the performance analysis in Section 5.3. Numerical results are discussed in Section 5.4. Finally, Section 5.5 summarizes the main findings and provides concluding remarks.

5.2 System Model

We consider a downlink cooperative NOMA wireless scheme for an underlay cognitive radio network which comprises of a primary source PS, primary destination PU, a secondary source S, a set of J relays denoted by R_j where $j = 1, \dots, J$ in the secondary network and two secondary destination nodes, U_1 and U_2 as illustrated in Fig. 5.1. We consider a condition where all links are frequency non-selective Rayleigh block fading and additive white Gaussian noise (AWGN).

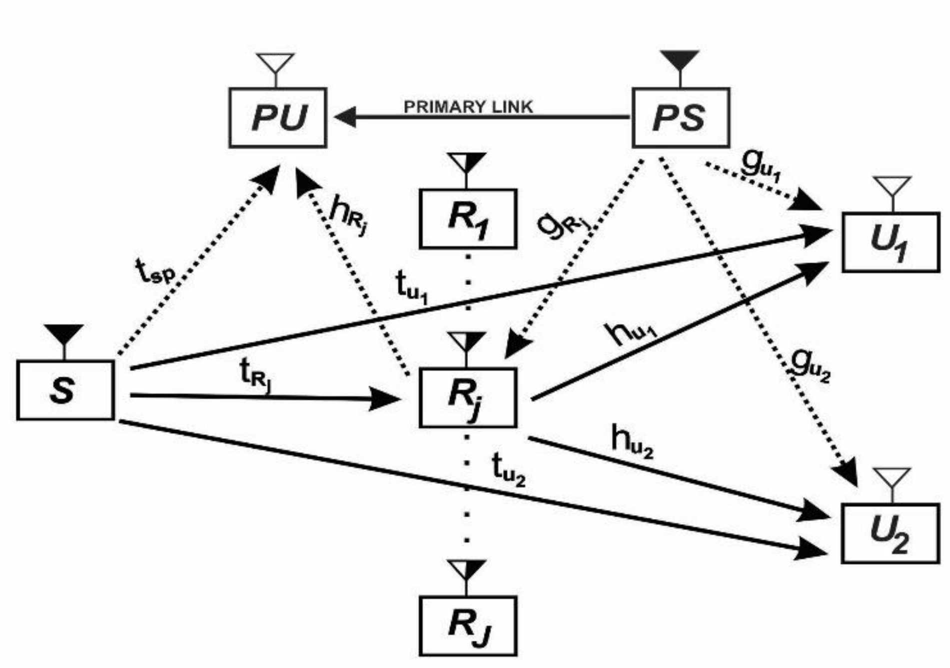

Figure 5.1 System model of a downlink cooperative NOMA system in an underlay cognitive radio network with AF relaying.

5.2.1 Phase 1

The secondary transmissions are divided into two-time slots. In the first time slot, S transmits the signal $v = \sqrt{\delta_1 P_S} v_1 + \sqrt{\delta_2 P_S} v_2$, to the two secondary destinations U_1 and U_2, and all the relay nodes R_j, where δ_1 andδ_2 are the power allocation coefficients for U_1 and U_2, respectively, with $\delta_1 + \delta_2 = 1$ and $\delta_1 < \delta_2$, the transmit power P_S of the secondary source is given by

$$P_S = \min\left(P, \frac{I_p}{\left|t_{s_p}\right|^2}\right), \tag{5.1}$$

where I_p is the interference temperature limit, P represents the maximum allowable transmit power at the source node, and t_{s_p} is the complex channel fading coefficient between S and PU. The received signal at the relay node is given by

$$y_{R_j} = t_{R_j}\left(\sqrt{\delta_1 P_S} v_1 + \sqrt{\delta_2 P_S} v_2\right) + \sqrt{P_P} g_{R_j} v' + n_{R_j}, \tag{5.2}$$

where v_1 and v_2 are the messages for U_1 and U_2, respectively. In Figure 5.1, complex channel fading exponentially distributed coefficients are denoted by $A_X \sim \mathcal{CN}\left(0, \Omega_{A_X}\right)$, with $\{A_X\} \in \left\{t_{s_p}, t_{U_1}, t_{U_2}, t_{R_j}, g_{U_1}, g_{U_2}, g_{R_j}, , h_{U_1}, h_{U_2}, h_{R_j}\right\}$The noise at the secondary users U_1 and U_2, and at the relay nodes R_j are additive white Gaussian noise (AWGN) with mean zero and variance $\mathcal{N}_0$. v' is the transmitted signal from the primary network and P_P is transmit power of the primary source. The received signals at U_1 and U_2 are given respectively by

$$y_{U_1} = t_{U_1} v + \sqrt{P_P} g_{U_1} v' + n_{U_1}, \tag{5.3}$$

$$y_{U_2} = t_{U_2} v + \sqrt{P_P} g_{U_2} v' + n_{U_2}. \tag{5.4}$$

Using (5.3), the received instantaneous SINR at U_1 to decode v_1 is given by

$$\gamma_{U_1}^{v_1} = \frac{\delta_1 \gamma_3}{\delta_2 \gamma_3 + \gamma_4 + 1}, \tag{5.5}$$

where $\gamma_3 = \min\left(P / \mathcal{N}_0, \left(\frac{I_p}{\mathcal{N}_0}\right) / \left|t_{s_p}\right|^2\right) \left|t_{U_1}\right|^2$ and $\gamma_4 = (P_P / \mathcal{N}_0) \left|g_{U_1}\right|^2$ with the aid of (5.4), the received SNR at U_2 used to detect v_1 is given by

$$\gamma_{U_2}^{v_1} = \frac{\delta_1 \gamma_5}{\delta_2 \gamma_5 + \gamma_6 + 1}, \tag{5.6}$$

where $\gamma_5 = \min\left(P / \mathcal{N}_0, \left(\frac{I_p}{\mathcal{N}_0}\right) / \left|t_{s_p}\right|^2\right) \left|t_{U_2}\right|^2$ and $\gamma_6 = (P_P / \mathcal{N}_0) \left|g_{U_2}\right|^2$. U_2 , decodes the symbol v_2 by cancelling v_1 using SIC. It is assumed that the SIC performed at U_2 for receiving v_2 is perfect, and the resulting SINRs are expressed respectively as

$$\gamma_{U_2}^{v_2} = \frac{\delta_2 \gamma_5}{\gamma_6 + 1}. \tag{5.7}$$

5.2.2 Phase 2

In the second time slot R_j, transmits $\widetilde{v_{R_j}} = G_j y_{R_j}$ to both U_1 and U_2 with G_j denoting the amplifying gain of the j^{th} relay, and y_{R_j} denotes the received signal on the relay R_j in equation (5.2)

$$G_j{}^2 = \frac{P_{R_j}}{P_S\left|t_{R_j}\right|^2 + P_P\left|g_{R_j}\right|^2 + \mathcal{N}_0}, \quad (5.8)$$

where P_{R_j} is the maximum allowable transmit power of the selected relay and we also assume that $P_{R_j} = P$.

$$y_{R_jU_1} = h_{U_1}\widetilde{v_{R_j}} + \sqrt{P_P}g_{U_1}v'' + n_{U_1}^{R_j}, \quad (5.9)$$

$$y_{R_jU_2} = h_{U_2}\widetilde{v_{R_j}} + \sqrt{P_P}g_{U_2}v'' + n_{U_2}^{R_j}, \quad (5.10)$$

But since $\widetilde{v_{R_j}} = G_j y_{R_j}$

$$y_{R_jU_1} = h_{U_1}t_{R_j}G_j\sqrt{\delta_1 P_S}v_1 + h_{U_1}t_{R_j}G_j\sqrt{\delta_2 P_S}v_2 + t_{R_j}G_j\sqrt{P_P}g_{R_j}v' + n_{R_j}t_{R_j}G_j + \sqrt{P_P}g_{U_1}v' + n_{U_1}^{R_j}. \quad (5.11)$$

Now the SINR at U_1 to detect v_1 as shown in Appendix C.1 is given by

$$\gamma_{R_jU_1}^{v_1} = \frac{\delta_1\gamma_7\gamma_1}{\delta_2\gamma_7\gamma_1 + \gamma_7\gamma_2 + \gamma_7 + \gamma_4\gamma_1 + \gamma_4\gamma_2 + \gamma_4 + \gamma_1 + \gamma_2 + 1} \quad (5.12)$$

where $\gamma_7 = \min\left(\frac{P}{\mathcal{N}_0}, \left(\frac{I_p}{\mathcal{N}_0}\right) / \left|h_{R_j}\right|^2\right)\left|h_{U_1}\right|^2$. Using the same approach in (5.11) the SINR at U_2 to detect v_1 and v_2 is given by (5.13) and (5.14) respectively

$$\gamma_{R_jU_2}^{v_1} = \frac{\delta_1\gamma_8\gamma_1}{\delta_2\gamma_8\gamma_1 + \gamma_8\gamma_2 + \gamma_8 + \gamma_6\gamma_1 + \gamma_6\gamma_2 + \gamma_6 + \gamma_1 + \gamma_2 + 1} \quad (5.13)$$

$$\gamma_{R_jU_2}^{v_2} = \frac{\delta_2\gamma_8\gamma_1}{\gamma_8\gamma_2 + \gamma_8 + \gamma_6\gamma_1 + \gamma_6\gamma_2 + \gamma_6 + \gamma_1 + \gamma_2 + 1} \quad (5.14)$$

where $\gamma_8 = \min\left(\frac{P}{\mathcal{N}_0}, \left(\frac{I_p}{\mathcal{N}_0}\right) / \left|h_{R_j}\right|^2\right)\left|h_{U_2}\right|^2$. So the instantaneous SINR at U_1 and U_2 based on selection combining which has lower complexity than maximal ratio can be written as

$$\gamma_{U_1} = max\left(\gamma_{SU_1}, \gamma_{R_jU_1}\right) \quad (5.15)$$

$$\gamma_{U_2} = max\left(\gamma_{SU_2}, \gamma_{R_jU_2}\right) \quad (5.16)$$

The selected relay is given

$$j* = \arg \max_{j=1,\dots,J} \gamma_{SR_j}\ , \tag{5.17}$$

where γ_{SR_k} denotes the instantaneous SNR at the kth relay.

Based on selection combining (SC), the received instantaneous SINR at U_1 and U_2 are given respectively by

$$\gamma_{U_1} = \max\left(\gamma_{U_1}^{v_1}, \gamma_{R_jU_1}^{v_1}\right), \tag{5.18}$$

$$\gamma_{U_2} = \max\left(\gamma_{U_2}^{v_2}, \gamma_{R_jU_2}^{v_2}\right). \tag{5.19}$$

5.3 Numerical Results

In this proposed system, an outage occurs when U_1 fails to detect v_1 from the received signals through the direct link and the indirect link (via the relay node), respectively. An outage event occurs at U_2 under two scenarios: 1) when U_2 can detect v_1 successfully but fails to detect its signal v_2; 2) when U_2 fails to detect v_1 due to high interference from the primary network. Based on NOMA and SIC, U_2 should decode v_1, subtract it and then decode its intended signal v_2. Here, we provide Monte Carlo simulations for some scenarios to assess the performance of the model. We highlight the outage performances of the underlying network. For simplicity and without loss of generality, it is assumed that $\delta_1 = 0.8$, $\delta_2 = 0.2$, $b_1 = 0.8$ and $b_2 = 0.2$.

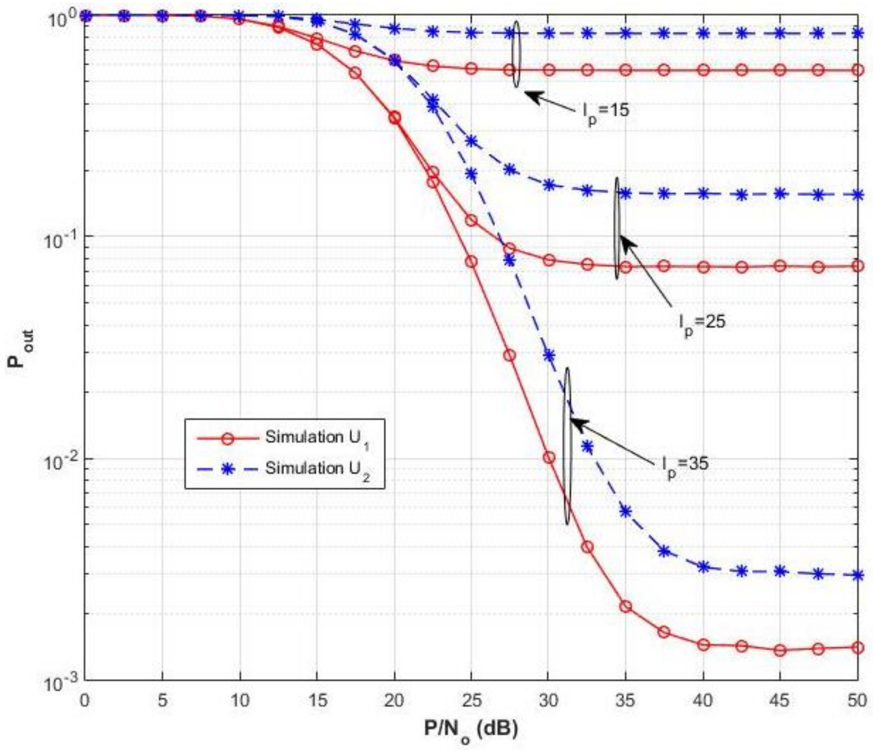

Figure 5.2 Outage probability against $\frac{P}{\mathcal{N}_0}$ for different interference power values, $\frac{I_p}{\mathcal{N}_0} = \{15, 25, 35\}$ dB.

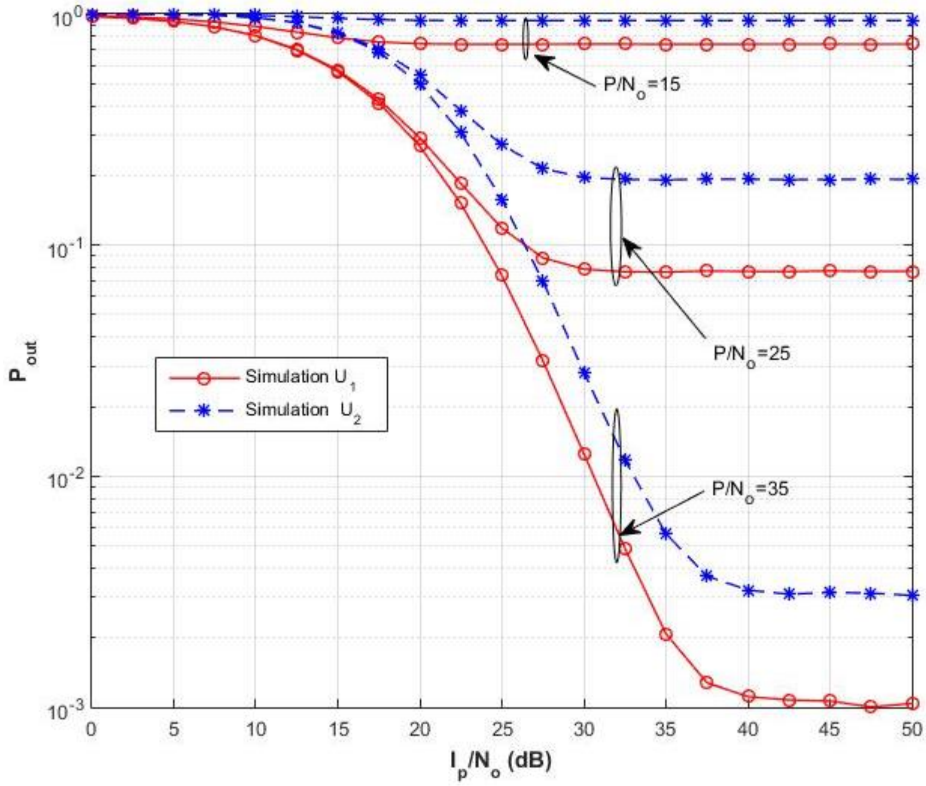

Figure 5.3 Outage probability against $\frac{I_p}{\mathcal{N}_0}$ with the maximum allowable transmit power taking values,$\{15, 25, 35\}$ dB.

In Figure 5.3, plots the outage probability of the system against interference power, $\frac{I_p}{\mathcal{N}_0}$ dB. The maximum allowable transmit power of the secondary network, $\frac{P}{\mathcal{N}_0}$ take values {15, 25, 35} dB and we assume that all channel conditions remain unchanged. The results indicate that the outage probability decreases as interference power increases but becomes constant at high $\frac{I_p}{\mathcal{N}_0}$ values. The results motivate us to conclude that outage performance improves in this case until a particular outage floor value determined by maximum allowable transmit power of the secondary source and selected relay of the system.

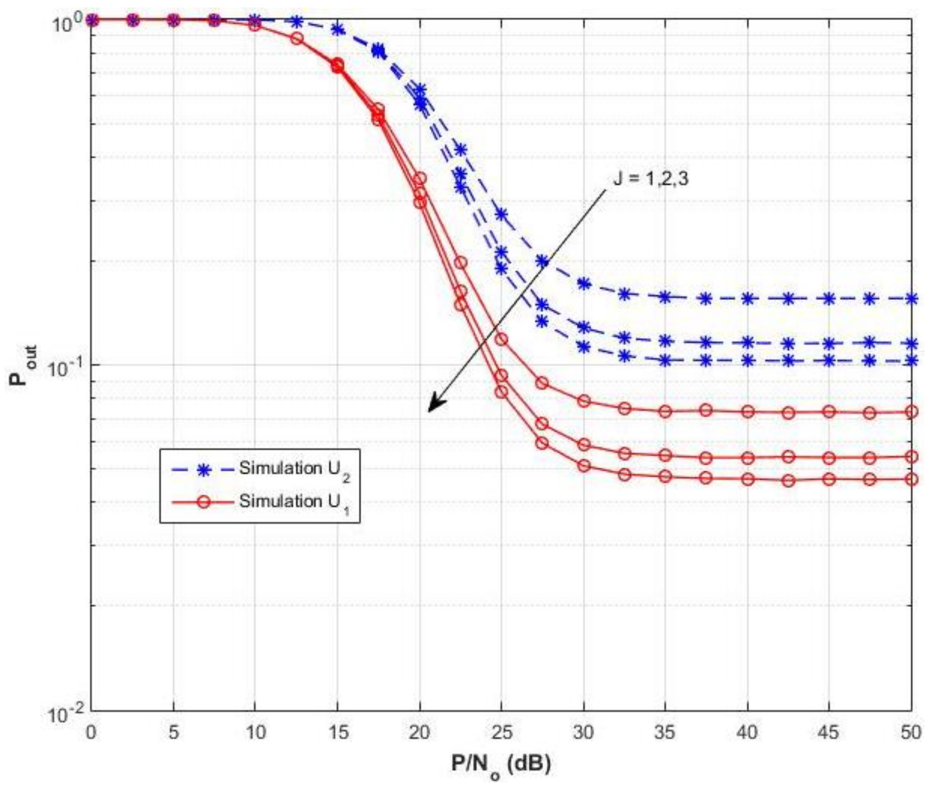

Figure 5.4 Outage probability against $\frac{P}{\mathcal{N}_0}$(dB) with different number of relays, $J = \{1, 2\ ,3\}$ when $\frac{I_p}{\mathcal{N}_0} = 25$ dB.

Figure 5.4 considers the effect of having multiple AF relays in the model with interference power fixed at 25 dB while $\frac{P}{\mathcal{N}_0}$ increases. There is a notable significant improvement in performance when the number of relays is increased to two. The small improvement that results when we have three relays shows that for a NOMA system in a cognitive radio network, an increase in the number of AF relays results in outage performance improvement, but it's unnecessary to go beyond two relays as improvement is insignificant.

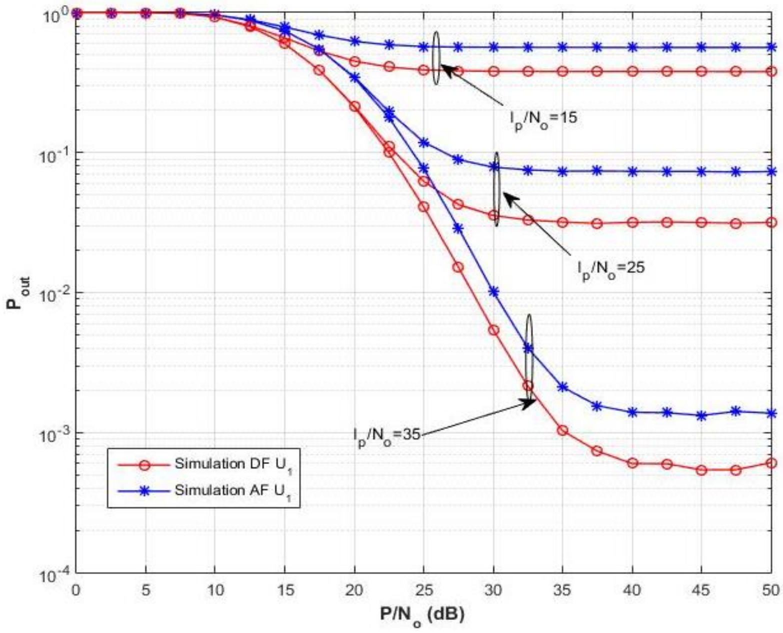

Figure 5.5 A comparison of the outage probability against $\frac{P}{\mathcal{N}_0}$ for different interference power values, $\frac{I_p}{\mathcal{N}_0} = \{15, 25, 35\}$ dB, using AF relaying vs DF relaying for U_1.

Figure 5.5 and Figure 5.6 show results for outage performance against average SNR at different fixed interference values. The results illustrate that the DF relaying scenario has better outage performance for all the different interference power values. It is important to note that in this model, the DF relaying outperforms AF relaying since we assumed that the selected DF relay perfectly decodes and re-encodes the signal for transmission without any errors. The AF relaying model has higher outage probability since the end-to-end SINR includes the amplified interference from the primary network to the relay and also the interference on the destination node.

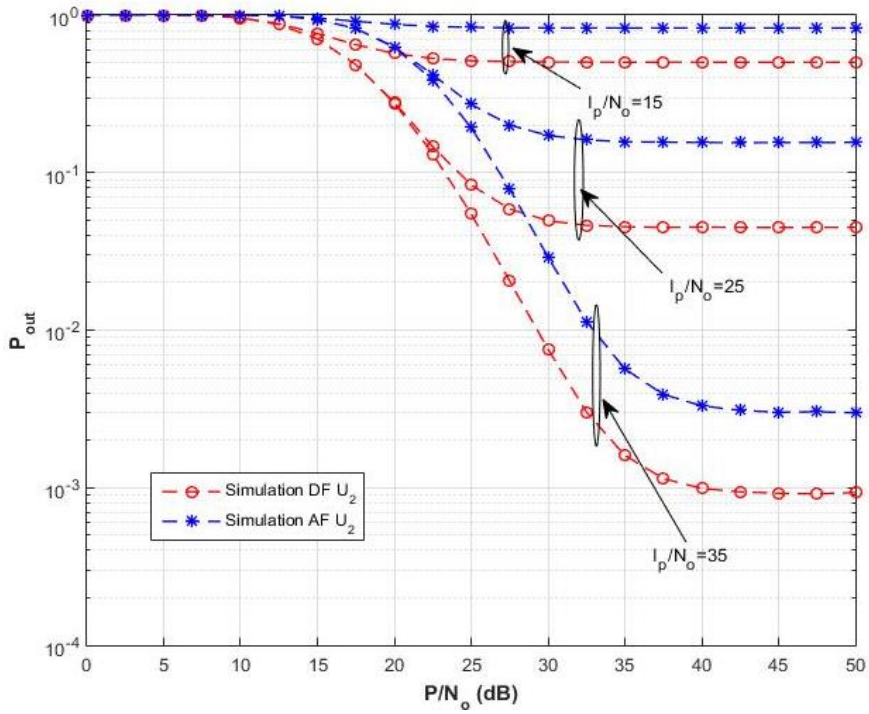

Figure 5.6 A comparison of the outage probability against $\frac{P}{\mathcal{N}_0}$ for different interference power values, $\frac{I_p}{\mathcal{N}_0} = \{15, 25, 35\}$ dB, using AF relaying vs DF relaying for U_2.

5.4 Conclusion

This chapter presented the model used in chapter 3 but employing AF relaying. The simulated outage performance of a NOMA system in a cooperative spectrum-sharing network with AF relay selection under interference power constraints is provided. Moreover, the performance of the underlying system from this model was also compared to the DF model, and it was shown that the AF model underperformed in this case this is also due to the fact that AF the noise and interference in the received signal leading to performance degradation. In most practical scenarios, DF relaying results in huge re-encoding errors since for a bad source-relay channel, a lot of wrong decisions will be made at the relay. However, from attained results, it can be concluded that the outage performance of the two secondary destinations improved significantly with an increase in the number of AF relays from one to two. Attained results also revealed that for a fixed interference power, the outage probability decreases as the average SNR or maximum allowable transmit power of the secondary selected relay (both AF and DF) or source increases, with error floors existing which are dependent on the interference power constraint.

Chapter 6 Conclusion

In this final chapter, we provide a concluding summary of the work done, focusing on the contributions, and we suggest potential improvements that have been identified as future works.

6.1 Summary

The work in this write-up mainly focused on the implementation of NOMA as a prospective solution to the challenges of spectrum extinction. The work was expanded to the incorporation of cognitive radios and cooperative relaying to the proposed model.

The introductory chapter (chapter 1) outlined the problem statement and motivation, and it models the research questions and research contributions. A section that thoroughly dealt with literature survey (chapter 2) follows, building up towards the gaps that exist in literature. Chapter 2 mainly focused on enlightening us on the NOMA implementations that have been done in past works. In chapter 3 we proposed a NOMA model in a cognitive underlay network implemented with an intermediate DF partial relaying link in the secondary network. In chapter 4, we remodel chapter 3, taking into account SIC error. We analysed the outage performance of the NOMA users to validate the theoretical derivations. The work covered in chapter 5 evaluated the implementation of a different relaying protocol (AF relaying) in the model proposed in chapter 3.

The performance of each model in terms of outage probability was analysed, and simulations were performed in Matlab to comprehend the theoretical framework with the simulated results for validation. Chapter 3 results from Fig. 3.2 and 3.3 outlined that outage performance improves with a gradual increase in the maximum allowable transmit power and interference power. However, both results show that the improvement is limited to a specific outage floor value determined by the interference constraint for fig. 3.2 and maximum allowable transmit power for Fig. 3.3. Results in Fig. 3.4 shows that for a NOMA system in a cognitive radio network, increasing the number of relays has a positive impact on the outage performance (optimal at two relays) but employing more than two relays in the model causes insignificant improvement of the outage performance. In Fig. 3.5, the results show that including two transmission links (relaying link and source –to- destination link) yields better results than having the direct link only, which justifies why our model implements both links for transmission in the secondary network. In the last figure (Fig. 3.6), we consider a case where the relaying user in a cooperative NOMA user and does SIC before forwarding the message to the end-user. The results show that the outage performance increases due to the absence of interference from the other NOMA user. This model shows that there is a trade-off as the end-user performance increases, but the lack of a relaying link lowers the relaying NOMA user performance.

In Chapter 4 it is shown that the outage probability decreases as the interference SNR/ maximum available transmit power increases until error floors occur for Fig. 4.2 and 4.3, respectively. The results also showed that when we experience some error in the SIC, the outage probability of the NOMA user that performs SIC will increase (U_2 in this case). Fig. 4.4 shows the improvement that comes with incorporating a set of DF relays in the model. The critical contribution shown is that in as much as introducing multiple relays improves outage performance, SIC error will increase outage probability. Fig. 4.6 show that as the SIC error increases outage probability increases as well. The results also show that outage performance becomes independent of interference power for high values which verifies the asymptotic outage analysis. Fig. 4.7 shows the outage probability against maximum allowable transmit power. The outage performance decreases as the SIC error increases. At high maximum allowable transmit power, error floors exist since outage performance is now independent of the maximum allowable transmit power which validates the asymptotic analysis.

The outcome in Fig. 5.3 and 5.4 of Chapter 5 reveal that outage performance improves until a specific outage floor value determined by interference constraint and maximum allowable transmit power of the system, respectively. This model differs from Chapter 3 and 4 in that it employs AF relaying. However in Fig. 5.4 a comparison of the performance of the DF versus the AF relaying is made. Both schemes improve as the number of relays increases but it’s evident that DF relaying outperforms AF relaying. The main reason is that the models assume perfect SIC, which subtracts interference for the destination SINR compared to the AF model, which amplifies and forwards the signal inclusive of the interference.

6.2 Contributions

The work done in this write-up focus on the implementation of NOMA integrated with cognitive radio network and cooperative relaying to enhance spectrum optimization. The contributions below were made:

i. In this model, we consider a network was the secondary source transmit to two NOMA users through a set of DF relays. The analytical expressions of the outage probabilities of both destination nodes are derived in closed-form, and they differ from [21] in that, interference from the stronger NOMA user is considered, and the relayed signal is transmitted without successive interference cancellation (SIC). Capitalizing on the offered results, we provide useful insights on the impact of the number of available relays in the networks and the interfering signals from the primary transmissions on the underlying performance metric. Monte Carlo simulations demonstrate the correctness of the proposed analytical framework.

ii. Motivated by the work in Chapter 3 in Chapter 4, we propose a more realistic and practical model that takes into account the effect of SIC error. This model also incorporates both the direct link and the relaying link to increase reliability and overall throughput of the system. Novel analytical expressions for outage probabilities of both destinations are derived in closed-form. Using the offered results, we provide insightful discussions on the impact of imperfect SIC in the overall system performance. To simplify the derived expressions of the outage probabilities, the asymptotic analysis of the performance mentioned in the above metric is obtained under two scenarios: a) the maximum allowable transmit power grows sufficiently large; b) the interference power constraint grows infinitely large. Monte Carlo simulations are provided for some scenarios (without loss of generality) to verify the accuracy of our proposed analytical.

iii. Chapter 5 presented the model used in chapter 3 but employing AF relaying. Monte Carlo simulations from this model were compared to the DF model from chapter 3. The DF model had better outage performance since we assumed perfect decoding. However, in practical scenarios, DF relaying is complicated and results in substantial re-encoding errors which degrade the performance and increase outage probability. AF outage performance results showed a significant improvement for both users with an increase in the number of relays from one to two. However, we conclude from the implementation three relays that the improvement is quite insignificant, and for a NOMA AF model, it would be optimal to use two relays. Results in fig. 5.3 also revealed that for a fixed maximum allowable transmit, and the outage probability decreases as the interference power increases, with error floors existing which are dependent on the maximum allowable transmit power.

6.3 Future Works

The main concept addressed in this dissertation is the incorporation of NOMA in an underlay CR network with cooperative relaying. The idea of NOMA being a promising solution for spectrum optimization through reuse is still open for further studying to come up with an integrated solution that performs well. Specific concepts that we recommend for future exploration are as below:

i. Relay selection criterion - The relay selection implementation in chapter 3 considered the highest SNR link between any of the relay node and the two destinations, being selected for transmission. However, it is worth mentioning that this selection is not optimal for both relays. It can be the best for one destination but not necessarily for the other destination. An optimal relay selection in the context of both destination nodes will be the subject of future works.

ii. Number of NOMA users - The work covered focused on two NOMA users; however, future studies can implement multiple users higher than two. This will mean users going through multiple SIC and work can be done to determine the maximally admissible NOMA users in the models that we have studied in this write-up.

iii. SIC error - We assume that the SIC error follows a Gaussian distribution and future work can consider cases in which the error follows other distributions. Future work can consider determining an approximate probability of error instead of just taking any residual interference levels greater than or equal to zero but less than or equal to one

iv. Outdated channel state information (CSI) - It is important to note that the relay with the best channel state information at the time of selection is not necessarily the relay that will be having the best channel state information during transmission. Future research will study the impact of outdated CSI on partial relay selection in an underlay NOMA cognitive network.

References

[1] Zanella, A., Bui, N., Castellani, A., Vangelista, L. and Zorzi, M., 2014. Internet of things for smart cities. *IEEE Internet of Things Journal*, *1*(1), pp.22-32.

[2] Carrie Lynch Springer., September 2018. https://news.wisc.edu/foxconn-competition-seeks-ideas-for-smart- *Presentation in the Smart Futures Summit, UW-Madison.*

[3] Haci, H., 2015. *Non-orthogonal multiple access (NOMA) with asynchronous interference cancellation* (Doctoral dissertation, University of Kent,).

[4] Soldani, D., 2013. On the Advanced 5G Network Infrastructure for the Future Internet. *Presentation in IEEE ICC*, pp.1-15.

[5] Y. Saito, Y. Kishiyama, A. Benjebbour, T. Nakamura, A. Li, and K. Higuchi, "Non-orthogonal multiple access (NOMA) for cellular future radio access," in *Proc. of IEEE 77th Vehicular Technol. Conf. (VTC Spring)*, Dresden, Germany, Jun. 2013, pp. 1–5.

[6] Li, A., Lan, Y., Chen, X. and Jiang, H., 2015. Non-orthogonal multiple access (NOMA) for future downlink radio access of 5G. *China Communications*, *12*(Supplement), pp.28-37.

[7] Li, A., Harada, A. and Kayama, H., 2014. Investigation of low complexity power assignment method and performance gain of non-orthogonal multiple access systems. *IEICE Trans. Fundamentals*, *97*(1).

[8] Higuchi, K. and Kishiyama, Y., 2013, September. Non-orthogonal access with random beamforming and intra-beam SIC for cellular MIMO downlink. In *2013 IEEE 78th Vehicular Technology Conference (VTC Fall)* (pp. 1-5).

[9] Umehara, J., Kishiyama, Y. and Higuchi, K., 2012, November. Enhancing user fairness in non-orthogonal access with successive interference cancellation for cellular downlink. In *2012 IEEE International Conference on Communication Systems (ICCS)* (pp. 324-328).

[10] Zhu, H., 2012. Radio resource allocation for OFDMA systems in high-speed environments. *IEEE Journal on Selected Areas in Communications*, *30*(4), pp.748-759.

[11] Endo, Y., Kishiyama, Y. and Higuchi, K., 2012, August. Uplink non-orthogonal access with MMSE-SIC in the presence of inter-cell interference. In *2012 international symposium on wireless communication systems (ISWCS)* (pp. 261-265).

[12] Zhu, H. and Wang, J., 2009. Chunk-based resource allocation in OFDMA systems-part I: chunk allocation. *IEEE Transactions on Communications*, *57*(9), pp.2734-2744.

[13] Ali, M.S., 2017. Non-orthogonal multiple access (NOMA) for cellular wireless communications.

[14] Liu, Y., Ding, Z., Elkashlan, M., *et al.*: 'Non-orthogonal multiple access in large-scale underlay cognitive radio networks', *IEEE Trans. Veh. Technol.*, 2016, **65**, (12), pp. 10152–10157

[15] Dhungana, Y. and Tellambura, C., 2014, December. Outage probability of underlay cognitive relay networks with spatially random nodes. In *2014 IEEE Global Communications Conference* (pp. 3597-3602).

[16] Lv, L., Ni, Q., and Ding Z.: 'Application of non-orthogonal multiple access in cooperative spectrum-sharing networks over Nakagami-*m* fading channels', *IEEE Trans. Veh. Technol.*, 2017, **66**, (6), pp. 5506–5511

[17] Ding, Z., Fan, P. and Poor, H.V., 2015. Impact of user pairing on 5G nonorthogonal multiple-access downlink transmissions. *IEEE Transactions on Vehicular Technology*, *65*(8), pp.6010-6023.

[18] Kim, J.-B., Lee, I.-H.: 'Capacity analysis of cooperative relaying systems using non-orthogonal multiple access', *IEEE Commun. Lett,* 2015, **19**, (11), pp. 1949–1952

[19] Lee, S., da Costa, D.B., and Duong T.Q.: 'Non-orthogonal multiple access with partial relay selection'. Proc. IEEE Personal, Indoor, Mobile Radio Communications (PIMRC), Valencia, Spain, 2016, pp. 1–6

[20]Men, J. and Ge, J., 2015. Performance analysis of non-orthogonal multiple access in downlink cooperative network. *IET Communications*, *9*(18), pp.2267-2273.

[21] Sunyoung Lee, Trung Q. Duong, Daniel Benevides da Costa, Dac-Binh Ha, Sang Quang Nguyen, "Underlay cognitive radio networks with cooperative non-

orthogonal multiple access”, 15th February 2018 doi: 10.1049/iet-com.2017.0559 www.ietdl.org

[22] Kader, M.F., Shahab, M.B. and Shin, S.Y., 2017. Exploiting non-orthogonal multiple access in cooperative relay sharing. *IEEE Communications Letters*, *21*(5), pp.1159-1162.

[23] Im, G. and Lee, J.H., 2019. Outage probability for cooperative NOMA systems with imperfect SIC in cognitive radio networks. *IEEE Communications Letters*, *23*(4), pp.692-695.

[24] Ranta, P.A., Hottinen, A. and Honkasalo, Z.C., 1995, June. Co-channel interference cancelling receiver for TDMA mobile systems. In *Proceedings IEEE International Conference on Communications ICC'95* (Vol. 1, pp. 17-21).

[25] Jia, Y. and Vosoughi, A., 2009, June. A novel selective relaying protocol for wireless networks. In *2009 IEEE 10th Workshop on Signal Processing Advances in Wireless Communications* (pp. 489-493).

[26]Chu, S.I., 2013. Outage probability and DMT performance of underlay cognitive networks with incremental DF and AF relaying over Nakagami-m fading channels. *IEEE Communications Letters*, *18*(1), pp.62-65.

[27] Hwang, K.S., Ko, Y.C. and Alouini, M.S., 2009. Performance analysis of incremental opportunistic relaying over identically and non-identically distributed cooperative paths. *IEEE Transactions on Wireless Communications*, *8*(4), pp.1953-1961.

[28] Ikki, S.S. and Ahmed, M.H., 2011. Performance analysis of incremental-relaying cooperative-diversity networks over Rayleigh fading channels. *IET Communications*, *5*(3), pp.337-349.

[29] Ding, Z., Ratnarajah, T. and Cowan, C.F., 2009. Spectrally efficient cooperative diversity protocol for uplink wireless transmission. *IET signal processing*, *3*(5), pp.368-380.

[30] Ikki, S.S. and Ahmed, M.H., 2008. Performance of multiple-relay cooperative diversity systems with best relay selection over Rayleigh fading channels. *EURASIP Journal on Advances in Signal Processing*, *2008*, pp.1-7.

[31] Bletsas, A., Khisti, A., Reed, D.P. and Lippman, A., 2006. A simple cooperative diversity method based on network path selection. *IEEE Journal on Selected Areas in Communications*, *24*(3), pp.659-672.

[32] Médard, M. and Gallager, R.G., 2002. Bandwidth scaling for fading multipath channels. *IEEE Transactions on Information Theory*, *48*(4), pp.840-852.

[33] Xia, M. and Aïssa, S., 2015. Fundamental relations between reactive and proactive relay-selection strategies. *IEEE Communications Letters*, *19*(7), pp.1249-1252.

[34] Bletsas, A., Shin, H., Win, M.Z. and Lippman, A., 2006, April. Cooperative diversity with opportunistic relaying. In *IEEE Wireless Communications and Networking Conference, 2006. WCNC 2006.* (Vol. 2, pp. 1034-1039).

[35] De, C.K. and Kundu, S., 2016. Proactive and reactive DF relaying for a cognitive network with multiple primary users. *Radioengineering*, *25*(3), p.475.

[36] Liu, S., Jin, S., Zhu, H. and Wong, K.K., 2014. On the impact of relay placement for energy-efficient cooperative networks. *IET Communications*, *8*(1), pp.140-151.

[37] Ibrahim, A.S., Sadek, A.K., Su, W. and Liu, K.R., 2008. Cooperative communications with relay-selection: when to cooperate and whom to cooperate with? *IEEE Transactions on Wireless Communications*, *7*(7), pp.2814-2827.

[38] Asghari, V., Affes, S. and Ghrayeb, A., 2012, April. Reactive relay selection in cooperative spectrum-sharing systems. In *2012 IEEE Wireless Communications and Networking Conference (WCNC)* (pp. 1098-1102).

[39] Atapattu, S., Jing, Y., Jiang, H. and Tellambura, C., 2013. Relay selection schemes and performance analysis approximations for two-way networks. *IEEE Transactions on Communications*, *61*(3), pp.987-998.

[40] Ikhlef, A., Michalopoulos, D.S. and Schober, R., 2012. Max-max relay selection for relays with buffers. *IEEE Transactions on Wireless Communications*, *11*(3), pp.1124-1135.

[41] Levin, G. and Loyka, S., 2012. Amplify-and-forward versus decode-and-forward relaying: Which is better? In the *22nd International Zurich seminar on communications (IZS)*. Eidgenössische Technische Hochschule Zürich.

[42] Souryal, M.R. and Vojcic, B.R., 2006, May. Performance of amplify-and-forward and decode-and-forward relaying in Rayleigh fading with turbo codes. In *2006 IEEE International Conference on Acoustics Speech and Signal Processing Proceedings* (Vol. 4, pp. IV-IV).

[43] Wahyu Adhi Prasetyo, "Relay Selection and Resource Allocation in Cooperative Wireless Communication Networks"

[44] P. Anghel and M. Kaveh, "Analysis of two-hop transmission over Rayleigh fading channels," in *Proc. IEEE Int. Symp. Advances in Wireless Communications*, Victoria, BC, Canada, Sept. 2002, pp. 155–156

[45] Farhadi, G. and Beaulieu, N.C., 2008. On the performance of amplify-and-forward cooperative systems with fixed gain relays. *IEEE Transactions on Wireless Communications*, *7*(5), pp.1851-1856.

[46] Patteti, K., Tipparti, A.K., Kalitkar, K.R., Kanapala, S. and Prasanna, N.M., 2016, July. Performance analysis of dual-hop relaying over rayleigh fading channels. In *2016 Thirteenth International Conference on Wireless and Optical Communications Networks (WOCN)* (pp. 1-5).

[47] Yang, C.Y., Lin, Y.S. and Hwang, M.S., 2013, July. Downlink relay selection algorithm for amplify-and-forward cooperative communication systems. In *2013 Seventh International Conference on Complex, Intelligent, and Software Intensive Systems* (pp. 331-334).

[48] J. N. Laneman and G. W. Wornell, "Energy efficient antenna sharing and relaying for wireless networks," in *Proc. IEEE Wireless Communications Networking Conf.*, Chicago, IL, Oct. 2000, pp. 7–12.

[49] Siriwongpairat, W.P., Himsoon, T., Su, W. and Liu, K.R., 2006, April. Optimum threshold-selection relaying for decode-and-forward cooperation protocol. In *IEEE Wireless Communications and Networking Conference, 2006. WCNC 2006.* (Vol. 2, pp. 1015-1020).

[50] Celik, Y., Odabasioglu, N. and Uysal, M., 2016, May. Adaptive relay selection method for asynchronous amplify and forward cooperative communications. In *2016 23rd International Conference on Telecommunications (ICT)* (pp. 1-4).

[51] Gao, R., Ji, X., Li, Y. and Bao, Z., 2018, August. Performance of Adaptive Link Selection with Buffer-Aided Denoise-and-Forward Relays. In *2018 IEEE/CIC International Conference on Communications in China (ICCC)* (pp. 163-167).

[52] Phadke, A.G. and Horowitz, S.H., 1990. Adaptive relaying. *IEEE Computer Applications in Power*, *3*(3), pp.47-51.

[53] Peiyao, Y., Hai, L., Shujuan, H. and Liuqing, Y., 2020. BER-based relay selection strategy for cooperative communication. *Journal of Systems Engineering and Electronics*, (99), pp.1-7.

[54] Baucke, S., Sachs, J. and Wiemann, H., Telefonaktiebolaget LM Ericsson AB, 2011. *Allocation of Resources to Shared Spectrum Operators*. U.S. Patent Application 12/746,074.

[55] A. Benjebbour, Y. Saito, Y. Kishiyama, A. Li, A. Harada, and T. Nakamura, “Concept and practical considerations of non-orthogonal multiple access (noma) for future radio access," in Intelligent Signal Processing and Communications Systems (ISPACS), 2013 International Symposium on. IEEE, 2013, pp. 770-774.

[56] A. Benjebbour, A. Li, Y. Saito, Y. Kishiyama, A. Harada, and T. Nakamura, “System-level performance of downlink noma for future lte enhancements," in Globecom Workshops (GC Workshops), 2013 IEEE. IEEE, 2013, pp. 66-70.

[57] A. Benjebbour, K. Saito, A. Li, Y. Kishiyama, and T. Nakamura, “Non-orthogonal multiple access (noma): Concept, performance evaluation and experimental trials," in Wireless Networks and Mobile Communications (WINCOM), 2015 International Conference on. IEEE, 2015, pp. 1-6.

[58] Ali_Md Shipon,”Non-Orthogonal Multiple Access (NOMA) for Cellular Wireless Communications,” Thesis University of Manitoba,Winnipeg, 2017

[59] Al-Imari, M., Xiao, P., Imran, M.A. and Tafazolli, R., 2014, August. Uplink non-orthogonal multiple access for 5G wireless networks. In *2014 11th international symposium on wireless communications systems (ISWCS)* (pp. 781-785).

[60]Islam, S.R., Avazov, N., Dobre, O.A. and Kwak, K.S., 2016. Power-domain non-orthogonal multiple access (NOMA) in 5G systems: Potentials and challenges. *IEEE Communications Surveys & Tutorials*, *19*(2), pp.721-742.

[61] A. Sendonaris, E. Erkip, and B. Aazhang, “User cooperation diversity - part I: system description,” *IEEE Trans. Commun.*, vol. 51, no. 11, pp. 1927–1938, Nov. 2003.

[62] P. A. Anghel and M. Kaveh, “Exact symbol error probability of a cooperative network in a Rayleigh-fading environment,” *IEEE Trans. Wireless Commun.*, vol. 3, no. 5, pp. 1416- 1421, Sep. 2004.

[63] Y. Liu, Z. Ding, M. Elkashlan, and H. V. Poor, “Cooperative non-orthogonal multiple access with simultaneous wireless information and power transfer,” *IEEE J. Sel. Areas Commun.*, vol. 34, no. 4, pp. 938–953, Apr. 2016.

[64] Z. Ding, M. Peng, and H. V. Poor, “Cooperative non-orthogonal multiple access in 5G systems,” *IEEE Commun. Lett.*, vol. 19, no. 8, pp. 1462–1465, Aug. 2015.

[65] Liang, X., Wu, Y., Ng, D.W.K., Zuo, Y., Jin, S. and Zhu, H., 2017. Outage performance for cooperative NOMA transmission with an AF relay. *IEEE Communications Letters*, *21*(11), pp.2428-2431.

[66] Kim, J.B. and Lee, I.H., 2015. Non-orthogonal multiple access in coordinated direct and relay transmission. *IEEE Communications Letters*, *19*(11), pp.2037-2040.

[67] Z. Ding, H. Dai, and H. V. Poor, “Relay selection for cooperative NOMA,” *IEEE Commun. Lett.*, vol. 5, no. 4, pp. 416–419, Aug. 2016.

[68] J. Men and J. Ge, “Non-orthogonal multiple access for multiple-antenna relaying networks,” *IEEE Commun. Lett.*, vol. 19, no. 10, pp. 1686–1689, Oct. 2015.

[69] Dan Deng, Lisheng Fan, Xianfu Lei, Weiqiang Tan, and Dongqing Xie, “Joint User and Relay Selection for Cooperative NOMA Networks” IEEE Access October 25, 2017.

[70] Abbasi, O., Ebrahimi, A. and Mokari, N., 2018. NOMA inspired cooperative relaying system using an AF relay. *IEEE Wireless Communications Letters*, *8*(1), pp.261-264.

[71] Jameel, F., Wyne, S., Nawaz, S.J., Chang, Z. and Ristaniemi, T., 2018, December. Outage Analysis of Relay-Aided Non-Orthogonal Multiple Access with

Partial Relay Selection. In *2018 IEEE Globecom Workshops (GC Wkshps)* (pp. 1-6).

[72] Fıdan, E. and Kucur, O., 2019, April. On Relay Selection for NOMA Based Cooperative Networks. In *2019 27th Signal Processing and Communications Applications Conference (SIU)* (pp. 1-4).

[73] Lv, L., Chen, J. and Ni, Q., 2016. Cooperative non-orthogonal multiple access in cognitive radio. *IEEE Communications Letters*, *20*(10), pp.2059-2062.

[74] Manglayev, T., Kizilirmak, R.C. and Kho, Y.H., 2016, October. Optimum power allocation for non-orthogonal multiple access (NOMA). In *2016 IEEE 10th International Conference on Application of Information and Communication Technologies (AICT)* (pp. 1-4).

[75] Andrews, J.G. and Meng, T.H., 2003. Optimum power control for successive interference cancellation with imperfect channel estimation. *IEEE Transactions on Wireless Communications*, *2*(2), pp.375-383.

[76] Manglayev, T., Kizilirmak, R.C., Kho, Y.H., Bazhayev, N. and Lebedev, I., 2017, July. NOMA with imperfect SIC implementation. In *IEEE EUROCON 2017-17th International Conference on Smart Technologies* (pp. 22-25).

[77] Bazhayev, N., Lebedev, I., Krivtsova, I., Sukhoparov, M., Salakhutdinova, K., Davydov, A. and Shaparenko, Y., 2016, October. Evaluation of the available wireless remote devices subject to the information impact. In *2016 IEEE 10th International Conference on Application of Information and Communication Technologies (AICT)* (pp. 1-6).

[78]Bazhayev, N., Lebedev, I., Korzhuk, V. and Zikratov, I., 2015, October. Monitoring of the information security of wireless remote devices. In *2015 9th International Conference on Application of Information and Communication Technologies (AICT)* (pp. 233-236).

[79] Xu, M., Ji, F., Wen, M. and Duan, W., 2016. Novel receiver design for the cooperative relaying system with non-orthogonal multiple access. *IEEE Communications Letters*, *20*(8), pp.1679-1682.

[80] Goldsmith, A.J., Jafar, S.A., Maric, I. and Srinivasa, S., 2009. Breaking spectrum gridlock with cognitive radios: An information theoretic perspective. *Proceedings of the IEEE*, *97*(5), pp.894-914.

[81] Mitola, J.I., 2002. Cognitive radio. An integrated agent architecture for software defined radio.

[82] Chung, G., Sridharan, S., Vishwanath, S. and Hwang, C.S., 2012. On the capacity of overlay cognitive radios with partial cognition. *IEEE transactions on information theory*, *58*(5), pp.2935-2949.

[83] Spectrum Efficiency Working Group, 2002. Report of the spectrum efficiency working group. *Federal Communications Commission, Tech. Rep*. http://www.fcc.gov/sptf/files/SEWGFinalReport 1.pdf.

[84] Agrawal, G. and Banerjee, A., 2013, April. Stable throughput of an interweave cognitive radio system employing SR-ARQ protocol. In *European Wireless 2013; 19th European Wireless Conference* (pp. 1-5). VDE.

[85] Moualeu, J.M., Hamouda, W. and Takawira, F., 2016. Cognitive coded cooperation in underlay spectrum-sharing networks under interference power constraints. *IEEE Transactions on Vehicular Technology*, *66*(3), pp.2099-2113.

[86] Zhong, B., Zhang, Z., Zhang, X., Wang, J. and Long, K., 2013. Partial relay selection with fixed-gain relays and outdated CSI in underlay cognitive networks. *IEEE Transactions on Vehicular Technology*, *62*(9), pp.4696-4701.

[87] da Costa, D.B., Ding, H. and Ge, J., 2011. Interference-limited relaying transmissions in dual-hop cooperative networks over Nakagami-m fading. *IEEE Communications Letters*, *15*(5), pp.503-505.

[88] Zhong, C., Ratnarajah, T. and Wong, K.K., 2011. Outage analysis of decode-and-forward cognitive dual-hop systems with the interference constraint in Nakagami-m fading channels. *IEEE Transactions on Vehicular Technology*, *60*(6), pp.2875-2879.

[89] Krikidis, I., Thompson, J.S., McLaughlin, S. and Goertz, N., 2009. Max-min relay selection for legacy amplify-and-forward systems with interference. *IEEE Transactions on Wireless Communications*, *8*(6), pp.3016-3027.

[90] Huang, H., Li, Z., Si, J. and Gao, R., 2013. Outage analysis of underlay cognitive multiple relays networks with a direct link. *IEEE Communications Letters*, *17*(8), pp.1600-1603.

[91] Cain, J.B., Billhartz, T., Foore, L., Althouse, E. and Schlorff, J., 2003, October. A link scheduling and ad hoc networking approach using directional antennas.

In *IEEE Military Communications Conference, 2003. MILCOM 2003.* (Vol. 1, pp. 643-648).

Appendix A

A.1 Derivation of SINR in first phase

After substituting (3.4) in (3.1) and performing some manipulations as shown below, the received instantaneous SINR R_k to receive the signal x_1 is as given below

$$\gamma_{SD_1} = \frac{a_1|h_{SD_1}|^2 P_S}{a_1|h_{SD_1}|^2 P_S + P_P|h_{UD_1}|^2 + \delta^2} \quad \text{(A1.1)}$$

Now dividing all terms in (A1.1) by δ^2 we get

$$\gamma_{SD_1} = \frac{a_1|h_{SD_1}|^2 \frac{P_S}{\delta^2}}{a_2|h_{SD_1}|^2 \frac{P_S}{\delta^2} + \frac{P_P}{\delta^2}|h_{UD_1}|^2 + 1}$$

$$\gamma_{SD_1} = \frac{a_1|h_{SD_1}|^2 \gamma_0}{a_2|h_{SD_1}|^2 \gamma_0 + \gamma_2|h_{UD_1}|^2 + 1} \quad \text{(A1.2)}$$

The result in (A1.2) reduces to give equation (3.9) in chapter 3 where $X_1 = \gamma_0|h_{SD_1}|^2$ and $B_{D_1} = \gamma_2|h_{UD_1}|^2$. Using the approach mentioned above, the received SNR at D_2 used to detect $x_1$is given by

$$\gamma_{SD_{12}} = \frac{a_1|h_{SD_2}|^2 \frac{P_S}{\delta^2}}{a_2|h_{SD_2}|^2 \frac{P_S}{\delta^2} + \frac{P_P}{\delta^2}|h_{UD_1}|^2 + 1}$$

$$\gamma_{SD_{12}} = \frac{a_1|h_{SD_2}|^2 \gamma_0}{a_2|h_{SD_2}|^2 \gamma_0 + \gamma_2|h_{UD_2}|^2 + 1} \quad \text{(A1.3)}$$

The result in (A1.3) reduces to give equation (3.10) in chapter 3 where $X_2 = \gamma_0|h_{SD_2}|^2$ and $B_{D_2} = \gamma_2|h_{UD_2}|^2$. After substituting (3.4) in (3.1) and performing some manipulations as shown below, the received instantaneous SINR R_k to receive the signal x_1 is as given below

$$\gamma_{SD_2} = \frac{a_2 |h_{SD_2}|^2 P_S}{P_P |h_{UD_2}|^2 + \delta^2} \tag{A1.4}$$

Now dividing all terms in (A1.4) by δ^2 we get

$$\gamma_{SD_2} = \frac{a_2 |h_{SD_2}|^2 \frac{P_S}{\delta^2}}{\frac{P_P}{\delta^2} |h_{UD_2}|^2 + 1}$$

$$\gamma_{SD_2} = \frac{a_2 |h_{SD_2}|^2 \gamma_0}{\gamma_2 |h_{UD_2}|^2 + 1} \tag{A1.5}$$

The result in (A1.5) reduces to give equation (3.11) in chapter 3 where $X_1 = \gamma_0 |h_{SD_1}|^2$ and $B_{D_1} = \gamma_2 |h_{UD_1}|^2$.

A.2 Derivation of SINR in second phase

In the second phase, using equation (3.7), the instantaneous SINR at D_1 is derived as shown below

$$\gamma_{R_k D_1} = \frac{|h_{R_k D_1}|^2 d_1 P_{R_k}}{|h_{R_k D_1}|^2 d_2 P_{R_k} + |h_{UD_1}|^2 P_P + \delta^2} \tag{A2.1}$$

Now dividing all terms in (A2.1) by δ^2 we get

$$\gamma_{R_k D_1} = \frac{|h_{R_k D_1}|^2 d_1 \frac{P_{R_k}}{\delta^2}}{|h_{R_k D_1}|^2 d_2 \frac{P_{R_k}}{\delta^2} + |h_{UD_1}|^2 \frac{P_P}{\delta^2} + 1}$$

$$\gamma_{R_k D_1} = \frac{\gamma_1 |h_{R_k D_1}|^2 d_1}{\gamma_1 |h_{R_k D_1}|^2 d_2 + \gamma_2 |h_{UD_1}|^2 + 1} \tag{A2.2}$$

The result in (A2.2) reduces to give equation (3.12) in chapter 3 where $Z_{1_k} = \gamma_1 |h_{R_k D_1}|^2$ with $\gamma_1 = \min\left(\gamma_P\ , \frac{\gamma_I}{|h_{R_k V}|^2}\right)$. Now using equation (3.8), the received instantaneous SINR used for D_2 to detect x_1 is given by

$$\gamma_{R_kD_{12}} = \frac{\left|h_{R_kD_2}\right|^2 d_1 P_{R_k}}{\left|h_{R_kD_2}\right|^2 d_2 P_{R_k} + \left|h_{UD_2}\right|^2 P_P + \delta^2} \quad \text{(A2.3)}$$

Now dividing all terms in (A2.3) by δ^2 we get

$$\gamma_{R_kD_{12}} = \frac{\left|h_{R_kD_2}\right|^2 d_1 \frac{P_{R_k}}{\delta^2}}{\left|h_{R_kD_2}\right|^2 d_2 \frac{P_{R_k}}{\delta^2} + \left|h_{UD_2}\right|^2 \frac{P_P}{\delta^2} + 1}$$

$$\gamma_{R_kD_{12}} = \frac{\gamma_1 \left|h_{R_kD_2}\right|^2 d_1}{\gamma_1 \left|h_{R_kD_2}\right|^2 d_2 + \gamma_2 \left|h_{UD_2}\right|^2 + 1} \quad \text{(A2.4)}$$

The result in (A2.4) reduces to give equation (3.13) in chapter 3 where $Z_{2_k} = \gamma_1 \left|h_{R_kD_2}\right|^2$. Also we note that after SIC the instantaneous SINR used for D_2 to detect x_2 is given by

$$\gamma_{R_kD_2} = \frac{\left|h_{R_kD_2}\right|^2 d_2 P_{R_k}}{\left|h_{UD_2}\right|^2 P_P + \delta^2} \quad \text{(A2.5)}$$

Now dividing all terms in (A2.5) by δ^2 we get

$$\gamma_{R_kD_2} = \frac{\left|h_{R_kD_2}\right|^2 d_2 \frac{P_{R_k}}{\delta^2}}{\left|h_{UD_2}\right|^2 \frac{P_P}{\delta^2} + 1}$$

$$\gamma_{R_kD_2} = \frac{\gamma_1 \left|h_{R_kD_2}\right|^2 d_2}{\gamma_2 \left|h_{UD_2}\right|^2 + 1} \quad \text{(A2.6)}$$

The result in (A2.6) reduces to give equation (3.14) in chapter 3

Appendix B

B.1 Derivation of CDF $F_{\gamma_{SD_1}}(\gamma_{th})$

This section shows a detailed derivation of the CDF $F_{\gamma_{SD_1}}(\gamma_{\text{th}})$ from equation (3.22) in chapter 3. This is important to give proof of equation (3.26).

$$F_{\gamma_{SD_1}}(\gamma_{th}) = \Pr\left(\gamma_{SD_1} \leq \gamma_{th}\right) \tag{B1.1}$$

$$F_{\gamma_{SD_1}}(\gamma_{th}) = \Pr\left(\frac{a_1 X_1}{a_2 X_1 + B_{D_1} + 1} \leq \gamma_{th}\right) \tag{B1.2}$$

Now equation (B1.2) can be rewritten as below

$$F_{\gamma_{SD_1}}(\gamma_{th}) = \Pr\left(\frac{a_1 \frac{\gamma_I}{|h_{SV}|^2}\left|h_{SD_1}\right|^2}{a_2 \frac{\gamma_I}{|h_{SV}|^2}\left|h_{SD_1}\right|^2 + \left|h_{UD_1}\right|^2 \frac{P_P}{\mathcal{N}_0} + 1} \leq \gamma_{th}, \frac{\gamma_I}{|h_{SV}|^2} \leq \gamma_P\right)$$
$$+\Pr\left(\frac{\left|h_{SD_1}\right|^2 a_1 \gamma_P}{\left|h_{SD_1}\right|^2 a_2 \gamma_P + \left|h_{UD_1}\right|^2 \frac{P_P}{\mathcal{N}_0} + 1} \leq \gamma_{th}, \frac{\gamma_I}{|h_{SV}|^2} \geq \gamma_P\right) \tag{B1.3}$$

Now lets consider

$$I_1 = \Pr\left(\frac{a_1 \frac{\gamma_I}{|h_{SV}|^2}\left|h_{SD_1}\right|^2}{a_2 \frac{\gamma_I}{|h_{SV}|^2}\left|h_{SD_1}\right|^2 + \left|h_{UD_1}\right|^2 \frac{P_P}{\mathcal{N}_0} + 1} \leq \gamma_{th}, \frac{\gamma_I}{|h_{SV}|^2} \leq \gamma_P\right) \tag{B1.4}$$

Taking $\mu_1 = a_1\gamma_I$, and $\mu_2 = a_2\gamma_I$ we have

$$I_1 = \Pr\left(\frac{\frac{\mu_1}{|h_{SV}|^2}\left|h_{SD_1}\right|^2}{\frac{\mu_2}{|h_{SV}|^2}\left|h_{SD_1}\right|^2 + \left|h_{UD_1}\right|^2 \gamma_2 + 1} \leq \gamma_{th}, \frac{\gamma_I}{|h_{SV}|^2} \leq \gamma_P\right) \tag{B1.5}$$

Equation (B1.5) can be written as

$$I_1 = Pr\left(\frac{1}{|h_{SV}|^2}\left(\mu_1 - \mu_2\gamma_{th}\right)\left|h_{SD_1}\right|^2 \le \gamma_2\left|h_{UD_1}\right|^2\gamma_{th} + \gamma_{th}\right)Pr\left(\left|h_{h_{SV}}\right|^2 \ge \frac{\gamma_I}{\gamma_P}\right)$$

$$I_1 = Pr\left(\left|h_{SD_1}\right|^2 \le \left(\frac{\gamma_{th}}{\left(\mu_1 - \mu_2\gamma_{th}\right)}\right)\left(\gamma_2\left|h_{UD_1}\right|^2 + 1\right)|h_{SV}|^2\right)Pr\left(|h_{SV}|^2 \ge \frac{\gamma_I}{\gamma_P}\right)$$

(B1.6)

Now taking $(\mu_1 - \mu_2\gamma_{th}) = \emptyset$ we get

$$I_1 = Pr\left(\left|h_{SD_1}\right|^2 \le \left(\frac{\gamma_{th}}{\emptyset}\right)\left(\gamma_2\left|h_{UD_1}\right|^2 + 1\right)|h_{SV}|^2\right)Pr\left(|h_{SV}|^2 \ge \frac{\gamma_I}{\gamma_P}\right)$$

(B1.7)

This can be further expressed as

$$I_1 = Pr\left(\left|\left|h_{SD_1}\right|\right|^2 \le \mathcal{g}_1\right)Pr\left(|h_{SV}|^2 \ge \frac{\gamma_I}{\gamma_P}\right)$$

(B1.8)

Where $\mathcal{g}_1 = \left(\frac{\gamma_{th}}{\emptyset}\right)\left(\gamma_2\left|h_{UD_1}\right|^2 + 1\right)|h_{SV}|^2$

$$I_1 = \left[1 - exp\left(-\frac{\mathcal{g}_1}{\Omega_{SD_1}}\right)\right]\left(e^{-\frac{\gamma_I}{\gamma_P\Omega_{SV}}}\right)$$

(B1.9)

$$I_1 = \left[1 - \mathbb{E}_{|h_{SV}|^2,\left|h_{UD_1}\right|^2}\left[exp\left(\frac{-\gamma_{th}\gamma_2\left|h_{UD_1}\right|^2|h_{SV}|^2}{\Omega_{SD_1}\emptyset} + \frac{-\gamma_{th}|h_{SV}|^2}{\Omega_{SD_1}\emptyset}\right)\right]\right]\left(e^{-\frac{\gamma_I}{\gamma_P\Omega_{SV}}}\right)$$

$$I_1 = \left[1 - \mathbb{E}_{|h_{SV}|^2,\left|h_{UD_1}\right|^2}\left[exp\left(\frac{-\gamma_{th}\gamma_2\left|h_{UD_1}\right|^2|h_{SV}|^2}{\Omega_{SD_1}\emptyset}\right) \times exp\left(\frac{-\gamma_{th}|h_{SV}|^2}{\Omega_{SD_1}\emptyset}\right)\right]\right]\left(e^{-\frac{\gamma_I}{\gamma_P\Omega_{SV}}}\right)$$

(B1.10)

Now considering that

$$I_1 = \left[1 - \mathbb{E}_{|h_{UD_1}|^2}\left[\mathbb{E}_{|h_{SV}|^2} exp\left(\frac{-\gamma_{th}\gamma_2|h_{UD_1}|^2|h_{SV}|^2}{\Omega_{SD_1}\emptyset}\right)\mathbb{E}_{|h_{SV}|^2}\, exp\left(\frac{-\gamma_{th}|h_{SV}|^2}{\Omega_{SD_1}\emptyset}\right)\right]\right] \times \left(e^{-\frac{\gamma_I}{\gamma_P\Omega_{SV}}}\right)$$

(B1.11)

This can be expressed as below

$$I_1 = \left[1 - \mathbb{E}_{|h_{UD_1}|^2}\left[\mathcal{M}_{|h_{SV}|^2}\left(-\frac{\gamma_{th}\gamma_2\Omega_{UD_1}}{\emptyset\Omega_{SD_1}}\right)\mathcal{M}_{|h_{SV}|^2}\left(-\frac{\gamma_{th}}{\emptyset\Omega_{SD_1}}\right)\right]\right]\left(e^{-\frac{\gamma_I}{\gamma_P\Omega_{SV}}}\right)$$

(B1.12)

The solution in (A1.12) can then be approximated after applying Jensen's inequality as,

$$I_1 \cong \left[1 - \left[\left(1 + \frac{\gamma_{th}\gamma_2\Omega_{h_{SV}}\Omega_{UD_1}}{\emptyset\Omega_{SD_1}}\right)^{-1}\left(1 + \frac{\gamma_{th}\Omega_{h_{SV}}}{\emptyset\Omega_{SD_1}}\right)^{-1}\right]\right]\left(e^{-\frac{\gamma_I}{\gamma_P\Omega_{h_{SV}}}}\right)$$

The above results in the solution used in equation (3.26)

Appendix C

C.1 Derivation of SINR at U_1 to detect v_1 ($\gamma_{R_jU_1}^{v_1}$)

In this section, we find the instantaneous SINR $y_{R_jU_1}$ from the received signal

$$y_{R_jU_1} = h_{U_1}\widetilde{v_{R_J}} + \sqrt{P_P}g_{U_1}v'' + n_{U_1}^{R_j} \tag{C1.1}$$

But since $\widetilde{v_{R_J}} = G_j y_{R_j}$

$$y_{R_jU_1} = h_{U_1}t_{R_j}G_j\sqrt{\delta_1 P_S}v_1 + h_{U_1}t_{R_j}G_j\sqrt{\delta_2 P_S}v_2 + t_{R_j}G_j\sqrt{P_P}g_{R_j}v'$$

$$+ n_{R_j}t_{R_j}G_j + \sqrt{P_P}g_{U_1}v' + n_{U_1}^{R_j} \tag{C1.2}$$

Using equation (C1.2) the SINR to detect v_1 can then be initially expressed as $\gamma_{R_jU_1}^{v_1}$

$$\gamma_{R_jU_1}^{v_1} = \frac{|h_{U_1}|^2|t_{R_j}|^2\delta_1 P_S {G_j}^2}{|h_{U_1}|^2|t_{R_j}|^2\delta_2 P_S {G_j}^2 + |h_{U_1}|^2|g_{R_j}|^2 P_P {G_j}^2 + |h_{U_1}|^2 {G_j}^2\delta^2 + |g_{U_1}|^2 P_P + \delta^2} \tag{C1.3}$$

Divide all terms on the right of the equation by ${G_j}^2$

$$\gamma_{R_jU_1}^{v_1} = \frac{|h_{U_1}|^2|t_{R_j}|^2\delta_1 P_S}{|h_{U_1}|^2|t_{R_j}|^2\delta_2 P_S + |h_{U_1}|^2|g_{R_j}|^2 P_P + |h_{U_1}|^2\delta^2 + \frac{|g_{U_1}|^2 P_P + \delta^2}{{G_j}^2}} \tag{C1.4}$$

But we know

$${G_j}^2 = \frac{P_{R_j}}{P_S|t_{R_j}|^2 + P_P|g_{R_j}|^2 + \mathcal{N}_0}$$

Such that

$$\frac{\left|g_{U_1}\right|^2 P_P + \delta^2}{{G_j}^2} = \frac{\left(\left|g_{U_1}\right|^2 P_P + \delta^2\right)\left(P_S\left|t_{R_j}\right|^2 + P_P\left|g_{R_j}\right|^2 + \delta^2\right)}{P_{R_j}}$$

(C1.5)

$$\gamma_{R_jU_1}^{v_1} = \frac{\left|h_{U_1}\right|^2\left|t_{R_j}\right|^2 \delta_1 P_S P_{R_j}}{\left|h_{U_1}\right|^2\left|t_{R_j}\right|^2 \delta_1 P_S P_{R_j}\left|h_{U_1}\right|^2\left|g_{R_j}\right|^2 P_P P_{R_j} + \left|h_{U_1}\right|^2 \delta^2 P_{R_j} + \forall}$$

(C1.6)

Where, $\forall = \left(\left|g_{U_1}\right|^2 P_P + \delta^2\right)\left(P_S\left|t_{R_j}\right|^2 + P_P\left|g_{R_j}\right|^2 + \delta^2\right)$ and after expansion and simplification we get (C1.7)

$$\forall = \left|g_{U_1}\right|^2 P_P P_S\left|t_{R_j}\right|^2 + \left|g_{U_1}\right|^2 P_P P_P\left|g_{R_j}\right|^2 + \delta^2\left|g_{U_1}\right|^2 P_P + P_S\left|t_{R_j}\right|^2 \delta^2 + P_P\left|g_{R_j}\right|^2 \delta^2 + \delta^2\delta^2$$

(C1.7)

Now when we divide each element of (C1.7) with $\delta^2\delta^2$ we get

$$\mathbb{Z} = \frac{P_P}{\delta^2}\left|g_{U_1}\right|^2 \frac{P_S}{\delta^2}\left|t_{R_j}\right|^2 + \frac{P_P}{\delta^2}\left|g_{U_1}\right|^2 \frac{P_P}{\delta^2}\left|g_{R_j}\right|^2 + \frac{P_P}{\delta^2}\left|g_{U_1}\right|^2 + \frac{P_S}{\delta^2}\left|t_{R_j}\right|^2 + \frac{P_P}{\delta^2}\left|g_{R_j}\right|^2 + 1$$

Which reduces to

$$\mathbb{Z} = \gamma_4\gamma_1 + \gamma_4\gamma_2 + \gamma_4 + \gamma_1 + \gamma_2 + 1$$

(C1.8)

Now the complete expression in (C1.6) reduces to the equation below

$$\gamma_{R_jU_1}^{v_1} = \frac{\left|h_{U_1}\right|^2 \frac{P_{R_j}}{\delta^2}\left|t_{R_j}\right|^2 \delta_1 \frac{P_S}{\delta^2}}{\left|h_{U_1}\right|^2 \frac{P_{R_j}}{\delta^2}\left|t_{R_j}\right|^2 \delta_1 \frac{P_S}{\delta^2} + \left|h_{U_1}\right|^2 \frac{P_{R_j}}{\delta^2}\left|g_{R_j}\right|^2 \frac{P_P}{\delta^2} + \left|h_{U_1}\right|^2 \frac{P_{R_j}}{\delta^2} + \mathbb{Z}}$$

(C1.10)

The expression in (C1.10) gives the SINR at U_1 for detecting v_1

$$\gamma_{R_jU_1}^{v_1} = \frac{\delta_1\gamma_7\gamma_1}{\delta_2\gamma_7\gamma_1 + \gamma_7\gamma_2 + \gamma_7 + \gamma_4\gamma_1 + \gamma_4\gamma_2 + \gamma_4 + \gamma_1 + \gamma_2 + 1}$$

(C1.11)

This derivation results in equation (5.12) in chapter 5